CELL WALL CHANGES AND THE ROLE OF C*x*-CELLULASE DURING AVOCADO FRUIT RIPENING

By

ERIN MARGARET O'DONOGHUE

A DISSERTATION PRESENTED TO THE GRADUATE SCHOOL
OF THE UNIVERSITY OF FLORIDA IN PARTIAL FULFILLMENT
OF THE REQUIREMENTS FOR THE DEGREE OF
DOCTOR OF PHILOSOPHY

UNIVERSITY OF FLORIDA

1992

ACKNOWLEDGMENTS

I would like to thank Don Huber for his willingness to teach me the fundamentals of cell wall research, and for passing on his own fascination for plant biochemistry. He has given me plenty of space to develop my own research direction while also keeping me within the bounds of reality! I am also grateful to Jeff Brecht, Greg Erdos, Paul Klein and Steve Sargent who have all given me timely advice, and to Judy Timpa for allowing me to work with her wonderful HPLC. I also appreciate the technical advice and moral support of the biologists in both the Electron Microscopy and Hybridoma Laboratories.

A very big Thank You goes to the faculty, staff and graduate students of the Post harvest group--my family many miles from home! Somehow, they all created a happy, warm and relaxed atmosphere conducive to both research and friendship. My special thanks go to lab-mates Abd.-Shukor Abd. Rahman and Pedro Gallego, and biologists James Lee, Kathy Bergsma and Judy Zoellner, who have all put up with my lab habits, given encouragement at the right times and laughed with me (and at me!) on many, many occasions. It has been a real pleasure to work with them--I am glad our paths crossed.

This dissertation is dedicated with gratitude and love to those who taught me to read: Daniel and Margaret O'Donoghue--my parents, my sister Maree Catherine O'Donoghue and my first schoolteacher, Sister Mary Josephine Farrell.

TABLE OF CONTENTS

LIST OF ABBREVIATIONS

BP	buffered phenol
CDTA	1,2-cyclohexylenedinitrilotetraacetic acid
CMC	carboxymethylcellulose
CWG	cell wall ghosts
DMAC	dimethylacetamide
DP	degree of polymerization
EIS	ethanol-insoluble solids
HEPES	N-2-hydroxylethylpiperazine-N'-2-ethane sulfonic acid
HST	high-salt Tween
M_r	molecular weight
MWCO	molecular weight cut-off
PAW	phenol/acetic acid/water
PBS	phosphate-buffered saline
PEG	polyethylene glycol
PG	polygalacturonase
PME	pectinmethylesterase
Pt/C	platinum/carbon
RS	ripening stage
XG	xyloglucan

Abstract of Dissertation Presented to the Graduate School
of the University of Florida in Partial Fulfillment of the
Requirements for the Degree of
Doctor of Philosophy

CELL WALL CHANGES AND THE ROLE OF C*x*-CELLULASE DURING AVOCADO FRUIT RIPENING

By

Erin Margaret O'Donoghue

December 1992

Chairman: Dr. D.J. Huber
Major Department: Horticultural Science

Experiments were designed to characterize the compositional and structural changes in the cell walls of ripening avocado fruit. During ripening, cellulose levels decreased while total pectin and chelator-soluble pectins increased (on a fresh weight basis). Hemicelluloses, a comparatively minor component of the cell wall, showed little quantitative change during ripening.

Gel permeation chromatography of cell wall fractions indicated changes in polymer structure during avocado softening. There was an increase in low molecular weight pectic fragments and an almost complete loss of large-sized pectic polymers as the fruit progressed from hard to edibly soft. Hemicelluloses, of which xyloglucan was a major component, shifted slightly to a lower average molecular weight, but there was no production of small-sized fragments.

Electron microscopy following platinum/carbon shadowing of cell walls from ripening fruit revealed the changing physical state of cellulose microfibrils from being

compact and strongly associated with cell wall material to dispersed and filamentous, with microfibril substructure becoming apparent.

Xyloglucan, a putative substrate for C*x*-cellulase in avocados, was resistant to the endo-hydrolytic activity of the purified enzyme. Treatment of cell walls from unripe avocados with C*x*-cellulase caused a loss of large molecular weight cellulose chains and the microfibrils appeared to be unraveled and dispersed--similar to those seen in ripe fruit. The cell wall crystallinity also increased following enzyme treatment. C*x*-cellulase caused physical disorganization of micro-crystalline Avicel, and an increase in average molecular weight indicating a loss of lower molecular weight cellulose.

It is concluded that C*x*-cellulase attacks the amorphous regions of cellulose microfibrils leading to a loss of cohesiveness within the fibril structure and an alteration in the binding of associated cell wall matrix polysaccharides. It is proposed that the C*x*-cellulase causes disruption of the cellulose network and constitutes the initial step in avocado mesocarp softening.

CHAPTER 1
INTRODUCTION

The flesh of avocado fruit acquires a distinctively soft, buttery texture during ripening. Accompanying softening is extensive synthesis and accumulation of the enzyme C*x*-cellulase. In avocado fruit, this enzyme is active at levels far exceeding those recorded in other fruit studied such as tomato and peach (Lewis et al., 1974), and has been immunolocalized in the cell walls of the ripening mesocarp (Dallman et al., 1989). While numerous studies have focused on the identification of the cellulase gene and its control of expression (Christofferson et al., 1982, 1984; Tucker and Laties, 1984; Bennett and Christofferson, 1986), there has been less attention directed at defining its physiological role in ripening-associated cell wall hydrolysis. Only one report (Hatfield and Nevins, 1986) has addressed this specific issue in relation to avocado fruit. These workers identified the bond preferences of the avocado cellulase, characterizing the enzyme as a β-1,4-glucanase. Nevertheless, Hatfield and Nevins (1986) were unable to find solubilization products expressly related to this type of hydrolysis when the enzyme was incubated with cell walls from unripe avocado fruit.

The objectives of the research described herein were to examine the activity of avocado C*x*-cellulase in relation to specific cell wall polysaccharides and to identify the physiological role of the enzyme in ripening fruit. As an adjunct to this, characterization of the status of cell wall components, particularly cellulose, during avocado ripening was also undertaken to define the biochemical environment for cellulase activity. Specialized experimental techniques such as gel permeation chromatography for high molecular weight polymers (e.g., cellulose), x-ray diffraction and electron microscopy were used to

investigate special properties of cellulose and other cell wall polysaccharides in relation to C*x*-cellulase activity.

CHAPTER 2
LITERATURE REVIEW

Introduction

General

The avocado (*Persea americana* Mill.) is a member of the Lauraceae family. Three strains of avocados are known: Mexican (with high oil content and cold-hardy trees), West Indian (the most cold sensitive fruit with generally the lowest oil content) and Guatemalan, which has properties midway between the other two (Ryall and Pentzer, 1982).

Estimates from the Food and Agricultural Organization (1991) identify the major avocado producing regions as Central and South America (65% combined), whereas the United States supplied approximately 12% of the total world production. Total United States production for the 1990-91 year was 144,600 metric tons (USDA, 1992), primarily from California and Florida.

Development

A number of comprehensive reviews are available regarding the physiology of the avocado fruit (Valmayor, 1967; Biale and Young, 1971; Lewis, 1978; Bower and Cutting, 1988). The fruit are classified as berries, containing one carpel and a single seed (Cummings and Schroeder, 1942). The flowers of the avocado tree are dichogamous (Nirody, 1922; Stout, 1923), resulting in two very distinct periods of anthesis, the first for the gynoecium to receive pollen, and the next (a day later) for the stamens to shed pollen. In this way self-pollination is largely avoided, but it can be induced by factors such as insects or low temperatures. The fruit continues cell division throughout development (Schroeder, 1953), and the attainment of full size does not appear to be reliant on cell

expansion so much as increasing cell number. An unusual feature of the avocado is the absence of ripening while the fruit are attached to the tree, even though full horticultural maturity may have been reached (Biale et al., 1954). The precise nature of this ripening inhibition has not been identified although the most prevalent viewpoint has been that an inhibitory substance is transmitted from the tree to the fruit. Once the fruit was detached the effect of such an inhibitor would gradually wear off (Burg and Burg, 1964). Tree girdling experiments (Tingwa and Young, 1975) eliminated avocado leaves as the inhibitor source and indicated that the peduncle and stem may be providing the inhibitor since ripening occurred faster in detached fruit when the peduncle was removed. Tingwa and Young (1975) suggested that auxin may be involved. This issue has not been resolved to date.

Avocado fruit display climacteric characteristics during ripening, such as enhanced respiration (Biale, 1941) and associated ethylene evolution (Biale et al., 1954). The respiratory climacteric can be induced without a lag phase when mature avocados are treated with 10 ppm exogenous ethylene (Biale, 1960), although there is also some evidence that avocado fruit are physiologically unresponsive to added ethylene in the first 24 hours after harvest (Eaks, 1980; Starrett and Laties, 1991). Sitrit et al. (1986) suggested that the presence of 1-aminocyclopropane-1-carboxylic acid-synthase is the limiting factor for ethylene production in preclimacteric avocados. It appears that the high respiration rate attained during the ripening phase of avocado fruit is achieved without the contribution of cyanide-resistant respiration, although the fruit does have the capacity to engage the alternate pathway in ripening mesocarp discs (Theologis and Laties, 1978).

Plant Cell Walls

General

The plant cell wall is chemically and structurally heterogeneous. It is composed of polysaccharides, proteins and water, and may contain unique sugar residues and linkages.

The general organization within the cell wall is well established: crystalline cellulose microfibrils embedded in a matrix of hemicelluloses, pectins and structural proteins (McNeil et al., 1984). While this basic arrangement remains constant throughout plant tissues, the nature and relative quantities of each constituent may vary considerably in each plant part as necessary for the maintenance of specific form and function.

The cell wall structure of fruit tissues has long been a subject of interest, primarily since the change in cell wall composition and rigidity greatly affects the firmness of the fruit as a whole. Such organizational changes are an integral part of the endogeneously controlled fruit ripening process and ultimately translate into market and consumer acceptance parameters.

Cellulose Structure and Properties

The cellulose polymer is a linear chain of β-1,4-linked glucose residues. Alternate glucose residues are rotated 180^{o} so that the repeating unit of cellulose is actually cellobiose. There is strong hydrogen bonding within the chains of the polymer, particularly through the substituents of C-3 and C-6. The individual chains strongly associate with each other through interchain hydrogen bonds along the long axes. This leads to the general organization of cellulose in the form of microfibrils which have a central core of rigidly held chains (highly crystalline in nature) and zones of less perfectly aligned chains (amorphous), particularly in central areas where there is chain overlap and on the microfibril periphery. The crystalline nature of the microfibrils can be quantified by x-ray diffraction (Segal et al., 1959) and is a feature which distinguishes cellulose from other cell wall polysaccharides. The irregularity of the amorphous portion of the microfibril gives rise to inner and outer surfaces (Ladisch et al., 1983). Both crystallinity and surface area are important features when considering the susceptibility of cellulose to enzymic attack. While the structural relationship between crystalline and amorphous regions along the length of the cellulose microfibril remains the subject of speculation

(Nevell and Zeronian, 1985), the microfibrillar network is an important factor in the protection of the cell and the stability of the cell wall (Fry, 1988).

Pectin Structure and Properties

Pectin is one of the matrix components of the cell wall, and is particularly predominant in the middle lamella region of the mature cell wall (Moore et al., 1986; Moore and Staehelin, 1988). Pectic polymers can be chemically separated from the other cell wall carbohydrates by solubility in hot water or chelator solutions. Pectins are composed of a backbone of α-1,4-linked galacturonic acid units, with occasional rhamnose residues found in conjunction with specific areas of branching (Jarvis, 1984; BeMiller, 1986; de Vries et al., 1986). The main chain galacturonic acid units may be methyl-esterified at C-6 and may also be acetylated at C-2 and C-3 (McNeil et al., 1984). Side-chains, composed primarily of arabinose and galactose, are usually found attached to the rhamnose units of the main chain (Jarvis, 1984; McNeil et al., 1984; de Vries et al., 1986). It is often difficult to identify individual pectic polymers due to the difficulty of distinguishing whether the side-chains (often of considerable length) are substituents of the pectin itself or are actually hemicelluloses which have been crosslinked to the pectin.

Pectins are considered to be 'block co-polymers' (Jarvis, 1984) with 'hairy' (branched) zones interspersed with smooth regions. Broadly speaking, there are three basic pectin classifications: homogalacturonan, rhamnogalacturonan I and rhamnogalacturonan II.

Unbranched pectins. Homogalacturonan ('smooth' pectin) is unbranched and has variable degrees of methyl esterification. The backbone is composed of α-1,4-galacturonan, and while homogalacturonan is found in continuous regions, it may often be interrupted by the presence of rhamnose, which may introduce a conformational kink in the linear chain. The esterification of this polymer is thought to occur in blocks, which may be delineated by the rhamnose units (Jarvis, 1984). Areas that are not esterified are negatively charged at normal cell wall pH and may participate in ionic interactions with

cell wall calcium (Grant et al., 1973). The divalent calcium serves as a junction between two charged regions in one chain or between separate chains (Grant et al., 1973).

Rhamnogalacturonans. Rhamnogalacturonan I is composed of alternating galacturonic acid and rhamnose units with side-chains of galactose and arabinose (McNeil et al., 1980, 1984). This type of pectin may be found interrupting the unsubstituted homogalacturonan. Rhamnogalacturonan II is a relatively small polymer and is one of the most complex polysaccharides known. The linear α-1,4-galacturonic acid backbone has a number of branch points with rhamnose, galactose, arabinose (both pyranose and furanose forms), fucose, glucuronic acid, 2-O-methylfucose, 2-O-methylxylose, apiose, aceric acid, 3-deoxy-D-manno-2-octulosonic acid and 3-deoxy-D-lyxo-2-heptulsaric acid organized as sidechains (Darvill et al., 1978: Stevenson et al., 1988). Due to the complexity of the polymer, rhamnogalacturonan II has been studied in only a few plant tissues, but the less complex homogalacturonan and rhamnogalacturonan I are readily distinguished by solubilities and sugar identification. Because of the extensive branching found in these polymers, rhamnogalacturonans I and II are considered to comprise the 'hairy' fraction of pectin.

Hemicellulose Structure and Properties

Hemicelluloses are defined as those cell wall polysaccharides that are insoluble in water or chelator, but are readily soluble in strong alkali (Fry, 1988). A disparate group of polymers is included in this category including xylans, glucomannans, galactomannans, β-1,3-,β-1,4-glucans, arabinogalactans, callose and xyloglucans (XG). Depending on the plant source, some of these hemicellulosic polymers are more predominantly featured in the cell wall than others. Xyloglucan, however, appears to be rather ubiquitously distributed, and is usually always found in close association with cellulose microfibrils.

Xyloglucan. The structure of the XG polymer has been reviewed by Fry (1989) and Hayashi (1989). The backbone is identical to that of cellulose (repeating cellobiose units). Three of every four glucose residues have xylose substituents at the C-6 position.

These xylose units have galactose or galactose/fucose substituents at regularly placed intervals in the cell walls of dicots (Bauer et al., 1973; Hayashi and Maclachlan, 1984). The presence of fucose in XG of monocot cell walls is much less common (Hayashi, 1989). The physical form of XG has been studied by Ogawa et al. (1990). Most notable is the strong resemblance of the conformation of its glucan backbone to that of cellulose and indeed it is able to form extremely tight interactions with cellulose microfibrils via hydrogen bonds (Bauer et al., 1973; Hayashi and Maclachlan, 1984; Hayashi et al., 1987). This bonding appears to arise during microfibril formation and is able to prevent the fasciation of cellulose and stabilize the extra-cellular cellulose network. It has also been shown that heptasaccharide and nonasaccharide fragments derived from enzymic hydrolysis of XG may have both a moderating influence on auxin-stimulated extension growth (York et al., 1984; McDougall and Fry, 1988; Hoson et al., 1991), and at higher concentrations may also stimulate the activity of endogenous cellulase (Fry, 1986; Farkas and Maclachlan, 1988; McDougall and Fry, 1990; Maclachlan and Brady, 1992).

Structural Proteins

Currently, three distinct structural proteins have been identified in the cell wall. Hydroxyproline-rich glycoproteins (extensin) are extensively glycosylated (ca 50%) and contain hydroxyproline as well as valine, serine, threonine, lysine and tyrosine (Cassab and Varner, 1988). Extensin is linked to itself and possibly to other cell wall constituents through isodityrosine bonds. Glycine-rich proteins are found particularly associated with vascular tissue (Keller et al., 1988) and have glycine at alternate positions in the primary protein sequence (Varner and Cassab, 1986). Arabinogalactan proteins have a polypeptide structure that is rich in hydroxyproline, serine and alanine. Long arabinose/galactose sidechains and much shorter oligoarabinose sidechains may be attached to hydroxyproline residues (Strahm et al., 1989; Fincher et al., 1983; Bacic et al., 1987).

Polysaccharide Organization Within the Cell Wall

The bonding association between cellulose microfibrils and XG is well documented and has been demonstrated by both biochemical and ultrastructural methods (Bauer et al., 1973; Hayashi and Maclachlan, 1984; Hayashi et al., 1987) as well as by conformation studies (Ogawa et al., 1990).

Until recently, the interaction of pectins and hemicelluloses was thought to be due to covalent bonds such as ester and glycosidic cross-linkages (Bauer et al., 1973; Keegstra et al., 1973; Talmadge et al., 1973). Direct evidence for these bonds has been absent, however. Talbott and Ray (1992) have questioned this principle of covalent interaction and instead suggest that pectic/hemicellulosic interactions are via noncovalent associations and may also involve intertwining and overlap mechanisms that provide cohesive strength. The opinion of these authors is based on fractionation studies of pea cell wall polysaccharides and is supported by direct visualization techniques (McCann et al., 1990) and studies on polysaccharide fractionation of potato (Jarvis et al., 1981) and runner bean (O'Neill and Selvendran, 1983). It seems likely that a major cause of the differences now being discussed in the literature is the inherent differences in the source of cell wall samples, such as fresh tissue (Talbott and Ray, 1992) and sycamore suspension-cultures (Bauer et al., 1973). Talbott and Ray (1992) also classified arabinogalactans as hemicelluloses rather than as pectin side chains due to the amount of arabinogalactan solubilized with alkali compared to that removed by a previous chelator treatment.

Changes in Fruit Cell Walls During Ripening

During ripening, fruit acquire a number of characteristics such as aroma and flavor, undergo changes in sugar and acid content, and exhibit change in texture and color. The attainment of ripeness is largely consumer-determined according to the commodity, while fruit ripening in the physiological sense is considered to be a phase of plant organ senescence (Huber, 1987).

Fruit textural changes are due to the modification of various cell wall components. The cell wall undergoes modifications that can be either catabolic or anabolic in nature, and are usually enzyme mediated. Although there are some unifying factors in ripening-associated cell wall breakdown, many fruit have unique characteristics which in turn determine the eventual texture at their ripe state.

During ripening a number of qualitatively new proteins are synthesized, some of which are cell wall-directed hydrolytic enzymes. Hydrolases temporally associated with fruit ripening and textural changes include polygalacturonases (E.C. 3.2.1.15), pectinmethylesterases (E.C. 3.2.1.11) and C*x*-cellulase (E.C. 3.2.1.4). C*x*-cellulases will be discussed later in the literature review.

Polygalacturonase. The polygalacturonase (PG) enzymes (particularly the endo form) have been the subject of the majority of studies focused on the enzymology of fruit softening, and experiments have been aided by a knowledge of its particular substrate and hydrolysis site. Endo-PG attacks α-1,4-linked galacturonosyl residues and is involved in pectin degradation. The contribution of endo-PG activity to fruit softening (particularly tomato) has been recently questioned even though PG mRNA, PG protein and the activity of the PG increase dramatically with tomato fruit ripening (Hobson, 1964; Tucker et al., 1980; Brady et al., 1982; DellaPenna et al., 1986; Biggs and Handa, 1988). While PG is well known to degrade cell wall pectin *in vitro* in a manner similar to that observed in softening fruit (Huber and Lee, 1988), and pectin degradation is associated with increases in tomato PG (Gross and Wallner, 1979; Huber, 1983a; Seymour et al., 1987), the enzyme is not a requirement for softening in some fruit types including strawberry (Barnes and Patchett, 1976) and apple (Bartley, 1978). Insertion of a gene construct coding for antisense PG mRNA did not prevent softening or polyuronide depolymerization seen during normal tomato fruit ripening (Sheehy et al., 1988; Smith et al., 1988). Moreover, insertion of a promoter and the gene coding for PG into the *rin* tomato mutant (which does not normally soften) caused the fruit to undergo polyuronide solubilization and

depolymerization, but not softening (Giovannoni et al., 1989). Kramer et al. (1992) have recently reported that ripe tomato fruit containing the antisense transcript for PG are firmer than normal tomato fruit. This finding is in direct contrast to earlier work published from this group (Sheehy et al., 1988) and the results of Smith et al. (1988). It is clear that there is still much to be clarified regarding the role of PG in textural changes and softening during fruit ripening.

Pectinmethylesterase. Pectinmethylesterase (PME) is able to remove the methoxyl groups of esterified pectins and has been implicated in cell wall softening events even though their contribution to the process is not entirely clear (Huber, 1983b). The capacity of PG to attack pectin is enhanced by prior de-esterification by PME (Pressey and Avants, 1982). During tomato fruit ripening, pectin esterification decreases from approximately 90% to 35% between the breaker and pink stages (Koch and Nevins, 1989). PME activity increases during tomato ripening (Hobson, 1963; Tucker et al., 1982), even though mRNA coding for the enzyme decreases over this period (Ray et al., 1988; Harriman et al., 1991). A cDNA clone for PME mRNA has been used to indicate that the *rin* tomato mutation reduces the expression of PME (Harriman et al., 1991). There is substantial PME activity in normal mature but unripe tomato fruit (Pressey and Avants, 1982; Tucker et al., 1982), and the activity of the enzyme may decline with the onset of avocado ripening (Zauberman and Schiffmann-Nadel, 1972; Awad and Young, 1980).

Turnover. The turnover of cell wall polysaccharides is an important factor in the ripening and softening of fruit (Labavitch, 1981). It is likely that during fruit ripening the anabolic reactions may not keep pace with the catabolic series, and might cease prior to the attainment of full fruit ripeness. Knee et al. (1977) found that radiolabelled carbon was incorporated into the cell wall of developing strawberry fruit, but that this decreased (particularly with respect to galactose residues) during cell expansion and ripening. Other radiolabelling experiments (Mitcham et al., 1989, 1991) have shown there is cell wall synthesis in tomato fruit right up to and beyond the attainment of the red-ripe stage. In

the *rin* and *nor* tomato ripening mutants there is an alteration in the amount and timing of label incorporation. Tong and Gross (1988) found evidence of new types of glycosyl linkages in the hemicellulose fraction of cell walls during tomato fruit ripening.

Ripening-Induced Compositional Changes

Cell wall polymer alterations during fruit ripening determine the final texture of the ripe fruit. While a quantitative change in a particular cell wall component may have an effect on cell wall cohesion, even limited endo-hydrolysis may be sufficient to change polymer interactions and loosen the cell wall structure. An increase in soluble polyuronides has been reported during the ripening of tomato (Huber, 1983a; Seymour et al., 1987), apple (Knee, 1973; Bartley, 1978), pear (Ahmed and Labavitch, 1980; Bartley et al., 1982; Wang et al., 1985), mango (Roe and Bruemmer, 1981), strawberry (Knee et al., 1977; Huber, 1984) and muskmelon (McCollum et al., 1989) fruit. Gross (1986) found that while total amounts of water-soluble polyuronide increased during normal tomato ripening, there was no change in the quantity solubilized in *rin* and *nor* ripening mutants of similar chronological age.

Typically, the molecular weight (M_r) of the chelator-soluble polyuronides decreases during ripening. Exceptions have been noted with apple (Knee, 1978) and strawberry (Huber, 1984). Neither of these fruit contain active endo-PG. While changes in the total amount of extractable hemicelluloses are not usually seen, ripening is often characterized by a lowering of the M_r of this polymer (Huber, 1984; Huber and Lee, 1986; Tong and Gross, 1988; McCollum et al., 1989; Redgwell et al., 1991). Cellulose has been reported to decrease during the ripening of avocados (Colinas-Leon and Young, 1982) and peaches (Nightingale, 1930). The cellulose content of tomato increases in the pericarp during ripening but declines in the locule gel (Huber, 1985). Pear fruit cellulose content decreases (Jermyn and Isherwood, 1956) or remains unchanged (Ahmed and Labavitch, 1980) during ripening.

Another facet of cell wall degradation during fruit ripening is the loss of non-cellulosic neutral sugars, presumably solubilized by the action of cell wall glycosidases or exohydrolases. Gross and Sams (1984) investigated the change in neutral sugar composition of alcohol-insoluble solids during the ripening of a number of fruit types and found that the most predominant feature was the loss of galactose, arabinose and/or xylose. This work is supported by a number of other studies which have documented a loss of neutral sugars during ripening (Knee, 1973; Knee et al., 1977; Gross and Wallner, 1979; Yamaki et al., 1979; Ahmed and Labavitch, 1980; Huber, 1984; Wang et al., 1985; Huber and Lee, 1986; McCollum et al., 1989).

Cx-cellulase

General

Cx-cellulase is formally described as β-1,4-glucan-4-glucanohydrolase (E.C. 3.2.1.4) and may also be referred to as endoglucanase. Despite an inferred activity against cellulose, plant-derived Cx-cellulase has not been shown to hydrolyze pure crystalline cellulose and has been traditionally identified by its ability to reduce the viscosity of carboxymethylcellulose (CMC). While CMC is a synthetic substrate and is likely to be hydrolyzed by other cell wall enzymes it does serve to distinguish various properties of the Cx-cellulase enzyme including the ability to attack a β-1,4-glucan backbone, tolerance for some degree of substitution along this backbone, and a propensity for endohydrolysis. Although Cx-cellulase does not hydrolyze cellulose directly, the enzyme has some ability to bind to this polymer, a feature which has been used to assist in purifying the protein (Awad and Lewis, 1980; Bennett and Christofferson, 1984; Durbin and Lewis, 1988). Even so, quantitative recovery is often low (Bennett and Christofferson, 1984).

Cx-cellulases have been identified in several aspects of plant development, including abscission, tissue expansion growth and fruit ripening, as well as in cellulose-degrading enzyme complexes of bacteria and fungi.

The Cellulase Complexes of Bacterial and Fungal Systems

Bacterial and fungal systems contain C*x*-cellulase, although it is usually associated with an enzyme complex that has the capacity to completely hydrolyze crystalline cellulose. Three types of enzymes have been associated with cellulose-degrading ability in bacterial and fungal systems: endoglucanases (endo-1,4-β-glucanases, 1,4-β-D-glucan 4-glucanohydrolases or C*x*-cellulases, E.C. 3.2.1.4), cellobiohydrolases (exo-1,4-β-glucanases or 1,4-β-glucan cellobiohydrolases, E.C. 3.2.1.91) and cellobiases (β-glucosidases or β-D-glucoside glucohydrolases, E.C. 3.2.1.21) (Klyosov, 1990; Walker and Wilson, 1991). There are a number of isoforms of each type of enzyme and the manifestation of the different characteristics of these isozymes tends to be influenced by the nature of the other enzymes present (Kylosov, 1990; Walker and Wilson, 1991). Wood and McCrae (1979) have suggested that the role of endoglucanase is to hydrolyze the amorphous domains of cellulose microfibrils, since the enzyme has little ability to solubilize cotton or Avicel (microcrystalline wood cellulose) but is able to rapidly degrade CMC and acid-swollen cellulose. Cellobiohydrolase, identified in the early literature as 'C_1-cellulase', can degrade highly crystalline cellulose over a period of time (Walker and Wilson, 1991). Cellobiose can act as a feedback inhibitor of cellulose hydrolysis which may explain the presence of the glucosidase enzyme in most cellulase complexes of fungal/bacterial origin (Wood, 1985).

There is a great deal of synergism between cellobiohydrolase and endoglucanase, and the activity of these two enzyme types accounts for the majority of cellulose hydrolysis. So-called 'full value' cellulase complexes are thought to be able to hydrolyze both crystalline and amorphous cellulose since they contain an endoglucanase (with the ability to bind tightly onto cellulose) and cellobiohydrolase. Conversely, other cellulase systems ('low value') attack only amorphous cellulose, maybe because of the particular isoform of cellobiohydrolase present, the absence of cellobiohydrolase in the cellulase complex, or the binding properties of the endoglucanase (Kylosov, 1990).

Mode of attack. Cellulose hydrolysis by fungal and bacterial cellulase complexes involves a more complex combination of chemical events than those encountered during hydrolysis of soluble substrates. Walker and Wilson (1991) have summarized the basic mechanism of cellulose degradation as '(1) transfer of enzymes from the bulk aqueous phase to the surface of the cellulose particles, (2) adsorption of the enzymes and formation of enzyme-substrate complexes, (3) hydrolysis of cellulose, (4) transfer of the cellodextrins, glucose and cellobiose from the surface of the cellulosic particles to the bulk aqueous phase, and (5) hydrolysis of cellodextrins and cellobiose into glucose in the aqueous phase'. The biophysical state of the cellulose has a great influence on the formation of enzyme:substrate complexes, particularly the surface area and crystallinity properties. The crystalline regions of cellulose microfibrils are less accessible and therefore more difficult to degrade than the amorphous areas (Ladisch et al., 1983). The cellulose substrate is porous and has both internal and external surfaces (Ladisch et al., 1983). It has been found that pretreatments to increase the surface area enhance the adsorption of cellulase enzymes to the cellulose substrate, but the effectiveness of cellulose hydrolysis is reliant on the initial crystallinity values (Lee and Fan, 1982). A reduction in the crystallinity of the cellulose also aids hydrolysis (Bertran and Dale, 1985), perhaps by improving the enzyme binding capacity (Ooshima et al., 1983).

Specific roles for the endoglucanase component of the cellulase complex have been studied. Endoglucanase from *Cellulomonas fimi* bacteria has been found to contain both a binding and a catalytic domain (Ong et al., 1989). These two domains have been synthesized individually in *Escherichia coli* and their separate effects on cotton cellulose have been examined using scanning electron microscopy and confocal microscopy (Din et al., 1991). The binding domain does not act in a hydrolytic fashion but burrows into the interior of the microfibril, causing mechanical disruption of the crystalline structure and resulting in the sloughing of small particles. The catalytic domain appears to attach to the exterior of the cellulose fiber and 'polishes' the outer surface of the microfibril. In doing

so it releases reducing sugars and small fibers. It appears that the individual activity of the two domains of endoglucanase are complementary; nevertheless, the activity of each domain within the native molecule maybe modified by physical constraints.

The mechanism of cellulose breakdown by endoglucanase has been examined ultrastructurally by Sprey and Bochem (1991) who found that treatment of *Sinapis alba* seed slime cellulose with purified endoglucanase from *Trichoderma reesei* resulted in the erosion of the tight fibril orientation and the development of extremely frayed subfibrils. Complete breakage of the subfibrils from the primary microfibril was not seen. This tends to support the idea that endoglucanase (C*x*-cellulase) acts to disrupt the microfibril organization rather than to cause large-scale hydrolysis. However, it seems that the strong tendency towards synergism with cellobiohydrolase could enable endoglucanase to be effective at hydrolysis of the main cellulose chains.

Abscission Zone C*x*-cellulase

Typically, senescence of many vegetative, floral and fruit organs is accompanied by the abscission of the affected plant part. The cell walls in a restricted band of cells in the abscission zone are particularly responsive to ethylene and become weakened, resulting in a decrease in the force (breakstrength) required to remove the abscising element (Osborne, 1989). A primary event in the course of abscission is the appearance of C*x*-cellulase (Horton and Osborne, 1967). Using labelled amino acids and isopycnic equilibrium sedimentation, Lewis and Varner (1970) showed that the appearance and increase in C*x*-cellulase of bean abscission zones was due to the synthesis of qualitatively new protein. They also found evidence for two forms of C*x*-cellulase (i.e., CMC viscosity-reducing activity), distinguishable on the basis of isoelectric points. The abscission zone-specific enzyme is basic with a pI of 9.5, while the second isozyme has a pI of 4.5 and appears to be unrelated to abscission events, being distributed throughout the plant (Durbin et al., 1981; Lewis et al., 1970). Immunoblot (del Campillo et al., 1988) and radioimmunoassay (Koehler et al., 1981) analyses showed that the two isozymes are

not crossreactive and may therefore result from different genes (del Campillo et al., 1988). This finding highlights the difficulty in assigning particular characteristics to an enzyme based on its activity against a nonspecific, synthetic substrate. Prior to the induction of abscission, only 1% of the C*x*-cellulase in the abscission zone is of the 9.5 form (Lewis et al., 1974) and, following the induction of abscission, the relative amounts of this form increase while the presence of the 4.5 form declines (Durbin et al., 1981). On the basis of vacuum infiltration and solubility experiments, Reid et al. (1974) speculated that the 9.5 cellulase is extracellular and wall bound, while the 4.5 cellulase is located within the cell. A cDNA clone for the 9.5 abscission-zone cellulase has been sequenced (Tucker et al., 1988; Tucker and Milligan, 1991) and codes for a 51 kDa. protein. This probe has been used to confirm earlier work establishing the 9.5 C*x*-cellulase as being synthesized *de novo* following an abscission stimulus.

Although the synthesis of C*x*-cellulase is temporally correlated with abscission, the precise function of the enzyme has yet to be determined. To date, detailed cell wall compositional studies have not yet been undertaken, no doubt due to the technical difficulties in obtaining ample abscission-zone tissue samples. Electron micrographs have revealed that the middle lamella is the first region to exhibit breakdown. Swelling of the primary wall follows, associated with changes in the orientation and organization of cellulose microfibrils (Addicott and Wiatr, 1977; Osborne, 1989).

Lieberman et al. (1982) utilized a copper marker to localize C*x*-cellulase in tobacco flower abscission zones. After incubation of tissue segments with CMC, a copper precipitate was used to visualize reducing groups released by the enzyme. Electron micrographs of thin sections from this treated tissue showed the that majority of C*x*-cellulase activity was associated with fibrillar components of the middle lamella. A small amount of precipitate was also found in the primary and secondary wall. No interpretation of these data was offered. Immunolocalization and tissue printing experiments have revealed the presence of the C*x*-cellulase protein in both the proximal and distal abscission

zones and associated vascular structures of bean tissue (Sexton et al., 1981; del Campillo et al., 1990). *In situ* and tissue hybridization techniques have shown the distribution of mRNA to be localized in a very distinct layer of cells (irrespective of cell type) on both sides of the fracture zone. There is also specific accumulation of the message around the vascular tissue of the abscission zone (Tucker et al., 1991).

There has been some dispute over the importance of C*x*-cellulase in breakstrength reduction of stem tissue during abscission. Data from time-course studies focusing on the relationship between the appearance of 9.5 cellulase and breakstrength in bean tissue argued against an initiative role for the enzyme in abscission (Reid et al., 1974); however, these workers did propose that the enzyme may play an important role in the final separation process. Conversely, Durbin et al (1981), using radioimmunoassays, observed a high correlation between the appearance of 9.5 C*x*-cellulase and breakstrength decline in bean tissue. Sexton et al. (1980) showed that polyclonal cellulase antibodies, when injected into the stem-petiole abscission zone of bean leaves, prevented the loss of breakstrength. Preimmune serum had no such effect. These studies provided strong evidence for a participatory role for C*x*-cellulase in abscission metabolism.

Cellulases of Vegetative Expansion Zones

C*x*-cellulases are strongly implicated in the mechanism of directional growth. The enzyme is present in the growing regions of pea epicotyls (Maclachlan and Perrault, 1964), and increases dramatically after the application of auxin (Fan and Maclachlan, 1966; Byrne et al., 1975; Verma et al., 1975). Two forms of cellulase from pea epicotyls have been isolated and characterized (Byrne et al., 1975). Both are non-glycosylated endo-hydrolases and accumulate to the same extent in response to auxin. One isozyme (M_r of 21 kDa., pI of 5.2) is solubilized by dilute phosphate buffer whereas the second (M_r of 70 kDa., pI of 6.9) is solubilized by buffers of high ionic strength (Byrne et al., 1975). Bal et al. (1976) used pea tissue treated with ferritin-conjugated antibodies and electron microscopy to establish that the buffer-soluble cellulase isozyme resides in the

endoplasmic reticulum, whereas the salt-soluble form is found on the inner surface of the cell wall, close to fibrillar material. Both cellulase isozymes exhibited similar kinetic characteristics when hydrolyzing internal linkages of soluble β-1,4-glucans; however, they are not immunologically cross-reactive and have very different amino acid compositions (Byrne et al., 1975). Nevertheless, kinetic data were interpreted as indicating the two enzymes had identical or similar active sites (Byrne et al., 1975). This apparent contradiction may be due to the ability of all C*x*-cellulases to hydrolyze CMC which, while identifying the presence of a cellulase, may not describe their true activity.

Verma et al. (1975) examined the *in vitro* translation products of isolated polysomal mRNA from auxin-treated pea epicotyls and found that only the smaller, buffer-soluble cellulase was present. This has led to speculation (Wong et al., 1977) that the larger, buffer-insoluble C*x*-cellulase might be derived from the membrane-associated, buffer-soluble form through modifications occurring during cell wall secretion. However, this appears to be in contradiction with the amino acid compositions and immuno-reactivity differences recorded by Byrne et al. (1975).

A great deal of attention has been directed toward the physiological role of the expansion zone-associated C*x*-cellulase, perhaps aided by interest in the hormonal control of this developmental phenomenon. The association of C*x*-cellulase activity and XG degradation is apparent from studies on excised pea epicotyls (Hayashi et al., 1984) and azuki bean (Nishitani and Masuda, 1983) and soybean hypocotyls (Koyama et al., 1981, 1983). Soluble XG was recovered in tissue homogenates within 15 minutes of treating etiolated pea seedlings with auxin (Labavitch and Ray, 1974). This observation indicated that auxin could either facilitate a loss of tightly bound, alkali-soluble XG or conversely, enhance the synthesis of new XG. Evidence for the former mechanism was provided by Nishitani and Masuda (1983) who found that auxin treatment of azuki bean epicotyl tissue led to a decrease in both the amount and M_r of alkali-soluble XG. Koyama et al (1981)

demonstrated that a cell-free preparation of wall-bound protein (containing C*x*-cellulase activity) from soybean hypocotyl tissue could degrade native XG.

Hayashi et al. (1984) provided more direct evidence regarding the association of C*x*-cellulase activity and loss of XG by demonstrating that C*x*-cellulase (semi-purified by ion-exchange and gel filtration chromatography) degraded isolated pea XG. In addition, cell wall 'ghosts' (cell walls retaining only cellulose and XG after preferential pectin extraction) treated with the C*x*-cellulase preparation showed a selective loss of XG as measured by a loss of fluorescence from fluorescein-lectin labeled XG and liberation of reducing groups from radioactive labeled XG (Hayashi and Maclachlan, 1984; Hayashi et al., 1984). Solubilization of cellulose in these preparations was negligible. It was proposed that since C*x*-cellulase has the capacity to disrupt the integrity of XG, a consequence of its action could be to cause loosening of the cellulose microfibrils, allowing expansion following the auxin stimulus (Hayashi et al., 1984).

C*x*-cellulases and Fruit Ripening

The presence of C*x*-cellulase has been documented in numerous fruit types including tomato (Hall, 1963; Hobson, 1968; Pharr and Dickinson, 1973; Sobotka and Stelzig, 1974; Huber, 1985; Maclachlan and Brady, 1992), peach (Hinton and Pressey, 1974), pear (Ben Aire et al., 1979), strawberry (Barnes and Patchett, 1976; Abeles and Takeda, 1990), blackberry (Abeles and Takeda, 1989), date (Hasegawa and Smolensky, 1971), apple (Abeles and Takeda, 1990; Abeles and Biles, 1991) and avocado (Awad, 1977; Pesis et al., 1978; Awad and Young, 1979) fruit.

In tomato fruit, C*x*-cellulase activity increases during ripening and is found in higher levels in the locular gel than in the pericarp (Hall, 1963; Hobson, 1968; Huber, 1985). Preliminary work (Lashbrook et al., 1991) has identified at least two members of the tomato cellulase gene family while Maclachlan and Brady (1992) found multiple C*x*-cellulase activities in ripening fruit. The enzyme is also present and increases with physiological maturity in the *rin* tomato mutant (Buescher and Tigchelaar, 1975). The *rin*

fruit do not ripen, and soften exceedingly slowly (Gonzalez and Brecht, 1978). Sobtoka and Stelzig (1974) reported the presence of a cellulose degrading 'cellulase enzyme complex' in tomato fruit, similar to the complement of cellulases found in fungal and bacterial organisms. The members of this complex found in tomato included a non-specific β-glucosidase, an exo-β-1,4-cellulase and two endocellulases. These enzymes were distinguished only by differential solubility in ammonium sulfate and were not tested against tomato cell wall polymers. Pharr and Dickinson (1973) provided evidence for C*x*-cellulase and cellobiase activity in extracts of tomato pericarp but did not find any indication of a cellobiohydrolase-type enzyme. Significantly, the presence of a cellulase complex in tomato fruit has not been confirmed.

Hinton and Pressey (1974) suggested that the cellulase was involved in the initiation of peach softening rather than contributing directly to the textural changes since the activity of the enzyme decreased prior to a significant loss of flesh firmness. Barnes and Patchett (1976) speculated that C*x*-cellulase was involved in degrading a non-cellulosic glucan during strawberry ripening but stopped short of identifying such a polysaccharide or suggesting its contribution to the ripening process. Most information about C*x*-cellulase from fruit tissues has been derived from the study of avocado mesocarp, although this work has focused on the synthesis and physical characteristics of the protein rather than its role in cell wall metabolism in general or fruit textural changes in particular.

Avocado C*x*-cellulase

The ripening of avocado fruit is distinguished by the accumulation of copious quantities of C*x*-cellulase in association with mesocarp softening. The enzyme activity level is low or absent in firm, unripe tissue (Awad, 1977; Pesis et al., 1978; Awad and Young, 1979) but increases dramatically as the fruit soften, reaching levels 150x that of ripe peaches and 700x that of ripe tomatoes (Lewis et al., 1974). Awad and Young (1979) reported that C*x*-cellulase begins to increase simultaneously with mesocarp

softening and its activity was followed about three days later by the increase in activity of polygalacturonase. Activity of both enzymes continues to increase for approximately two days after the fruit have become edibly soft.

Analysis of poly(A)$^+$mRNAs from ripening avocado tissue demonstrated that among the qualitatively new mRNAs synthesized during ripening were a set corresponding specifically for C*x*-cellulase. Identification was made on the basis of immunoprecipitation of antibodies for avocado C*x*-cellulase (Christofferson et al., 1982; Tucker and Laties, 1984). Since these mRNAs were absent in preclimacteric avocado tissue, the enzyme is believed to be synthesized *de novo* at the onset of ripening and softening. A specific ripening clone for C*x*-cellulase was selected from a cDNA library and showed definitively that the ripening-induced enzyme increase was due to the appearance of mRNAs coding for C*x*-cellulase rather than translational control or enzyme activation (Christofferson et al., 1984). In addition, the sequence of the avocado C*x*-cellulase protein has been determined, and it is thought that cellulase may be coded for by a small gene family (Tucker et al., 1987). At least two separate genes coding for the enzyme have been cloned, one of which is inactive (Cass et al., 1990). Although auxin is important in the induction of C*x*-cellulase in abscission zones and elongating tissue, the factors controlling C*x*-cellulase transcription in ripening avocado fruit are currently unknown although ethylene appears to play a critical role (Tucker and Laties, 1984).

Bennett and Christofferson (1986) traced the synthesis and post-translational modification of avocado C*x*-cellulase. The C*x*-cellulase mRNA is translated initially into a 54 kDa. pre-protein followed by removal of a signal sequence. The pre-secretory protein also contains carbohydrates enriched in mannose which are trimmed to achieve the mature form of the protein (54.2 kDa.). Although not experimentally verified in avocado tissue, the site of synthesis and glycosylation is presumed to be the endoplasmic reticulum, while carbohydrate trimming probably takes place in the Golgi apparatus (Bennett and Christofferson, 1986).

While there is a high nucleotide sequence similarity between the bean abscission-zone, tomato and avocado-ripening cellulase clones (Tucker et al., 1988; Lashbrook et al., 1991; Tucker and Milligan, 1991), there was no evidence of a cellulase isozyme with a pI of 9.5 in avocado fruit, as is the case in bean abscission zones (Lewis et al., 1974). Hatfield and Nevins (1986) found two isozymes in ripe avocado tissues having slightly different pIs (5.1 and 5.2), similar activities against CMC, and similar M_r (45 kDa.).

Ultrastructural analysis of ripe avocado tissue shows the disappearance of the middle lamella and some loss of microfibrillar material. Microfibrils of hard fruit are tightly packed while those of soft fruit are less dense and assume a diagonal orientation (Pesis et al., 1978; Platt Aloia et al., 1980). C*x*-cellulase has been immunolocalized in the mesocarp of ripening avocado fruit (Dallman et al., 1989). The enzyme is associated with the endoplasmic reticulum during the early stages of ripening and, as ripening progresses, it is also found throughout the cell wall. Cell fractionation studies have located C*x*-cellulase in the Golgi complexes (Dallman et al., 1989). A proliferation of endoplasmic reticulum was seen in ripening avocado mesocarp (Platt Aloia and Thomson, 1981) and this, along with the association of cellulase with plasmodesmata in the cell wall (Dallman et al., 1989) suggest a packaging/secretion scenario for the enzyme.

Recent work has defined some of the catalytic characteristics of C*x*-cellulase in avocado (Hatfield and Nevins, 1986) and there appears to be some mechanistic similarities to the vegetative expansion-associated cellulases studied in pea (Wong et al., 1977). The enzyme is an endohydrolase and is specific for β-1,4-linked glucans. In addition, it will attack these linkages only if they are adjacent to other β-1,4-linkages. Avocado C*x*-cellulase will preferentially hydrolyze oligosaccharides with a degree of polymerization of ≥ 5. Its action against derivatized glucans is dependent on the extent of substitution along the polymer chain, being more effective against less substituted glucans. Avocado cellulase does not produce reducing groups related to cellulose degradation following incubation with isolated cell walls of unripe or ripe avocado tissue. Hatfield and Nevins

(1986) suggested the possibility that this cellulase may have a role in degrading specific regions of XG or cellulose microfibrils leading to disruption of hydrogen bonding between these two cell wall polymers. Their assays of cellulase with soybean XG did not produce significant quantities of reducing groups however, unlike similar experiments performed with pea cellulase and XG (Hayashi et al., 1984).

CHAPTER 3
CHARACTERIZATION OF THE AVOCADO CELL WALL

Introduction

Fruit ripening involves a series of coordinated biochemical events which result in characteristic changes in fruit flavor, color and texture. Softening of fruit tissue involves changes in the structure of the cell wall, and there is evidence that both hydrolysis and synthesis are involved (Huber, 1983a, 1984; Tong and Gross, 1988; Mitcham et al., 1991). Much emphasis has been placed on the role of pectin metabolism and particularly the part polygalacturonase activity may play in fruit softening. Although recent work has challenged the central role of polygalacturonase in cell wall degradation during fruit softening (Sheehy et al., 1988; Smith et al., 1988), a compelling number of studies show that pectin alterations, either by solubilization, side-chain modification or enzyme-induced depolymerization (e.g., Gross and Wallner, 1979; Bartley et al., 1982; Huber, 1983a; Huber and Lee, 1988), are at least temporally associated with fruit firmness reductions.

To date, the avocado cell wall has not been the subject of major study. This is particularly intriguing since this fruit is the focus of much of the work in the molecular and genetic control of the cell wall enzyme C*x*-cellulase. The function of this enzyme in the cell wall has also not been disclosed--in avocado or in any other fruit. The avocado fruit is an attractive commodity to study cell wall changes in relation to textural changes. The fruit softens extensively, and developmental changes in association with the respiratory climacteric are relatively clear. The homogeneity of the avocado mesocarp is an advantage in comparison to the more widely studied tomato fruit, which possesses a

number of distinct tissues, thereby introducing some confounding factors in relating absolute cell wall changes to the loss of whole fruit firmness.

The objective of this work was to characterize the cell wall components during avocado ripening, particularly with respect to the dramatic loss of mesocarp firmness and the onset of C*x*-cellulase and polygalacturonase activity.

Materials and Methods

Plant Material

Fruit source. Avocado fruit (*Persea americana* Mill., cv. Lula) were obtained in November, 1989 from the IFAS Tropical Research and Education Center at Homestead, Florida, and in November, 1990 from J.R. Brooks and Sons, Inc., Homestead, Florida. The Lula cultivar is a Mexican/Guatemalan hybrid. Fruit were transported to Gainesville 1 to 2 days after picking and were surface-sterilized in commercial (5% Na hypochlorite) bleach solution diluted 1 in 20 with water, rinsed, dried and ripened at 20°C (1989) or 25°C (1990).

Fruit ripening stages. Fruit were classified into developmental stages according to ethylene production and respiration rates. Individual fruit were sealed in 2 L jars and gas samples removed via rubber septa fittings after 1 h. Respiration was measured using a Gas Partitioner Model 1200 (Fisher Scientific, Pittsburgh, PA) and expressed in units of ml CO_2 $kg^{-1}h^{-1}$, while ethylene production was measured on a Photovac 10A10 portable photoionization gas chromatograph (Photovac Inc., Thornhill, Ontario, Canada) and expressed as µl ethylene kg^{-1} h^{-1}. Ripening stages (RS) were

RS1: hard, preclimacteric fruit

RS2: preclimacteric, but in ripening environment at least 24 h

RS3: at the climacteric peak of ethylene production

RS4: post-climacteric and fully ripe.

Respiration and ethylene values used to characterize each RS were the average of 12 individual fruit measurements. Ripening stages from both years were equivalent.

Firmness determinations. The firmness of individual fruit in each RS was measured using an Instron Textural Measurement Instrument Model 1132 (Instron Corp., Canton, MA). Fruit were prepared for firmness measurements by removal of the exocarp at two sites in the equatorial region. A 500 kg load cell was used for the firmness determinations of fruit of RS1, RS2 and RS3, while fruit at RS4 were measured with a 50 kg load cell. Crosshead speed was 20 cm min^{-1}. A 1.27 cm diameter flat-end probe was used to penetrate the mesocarp to a depth of 0.85 cm. Firmness data (in Newtons) were recorded and expressed as the average of the 12 fruit in each RS.

Mesocarp preparation. Following firmness determinations, avocado fruit in each RS were prepared for further analysis by removing the remaining exocarp and the seed. The mesocarp of the equatorial region was sectioned and stored at -20°C.

Cell Wall Preparations

Both ethanol-insoluble material (which includes polysaccharides with a degree of polymerization [DP] of ≥ 2) and true cell walls (buffer-insoluble material) were prepared. Buffered-phenol (BP) or phenol/acetic acid/water (PAW) were used to inactivate co-extracted enzymes.

Buffered-phenol treated ethanol-insoluble solids. Approximately 100 g of partially thawed avocado mesocarp from each RS was homogenized in 400 ml of cold 100% ethanol over ice, for 3 min at speed setting #7 in a Polytron. The homogenate was incubated for 1 h at 1°C, then filtered through miracloth (Calbiochem Corp., La Jolla, CA) and the insoluble material transferred to 250 ml of BP (Huber, 1991). The suspension was stirred at room temperature for 30 min, then reprecipitated in 1 L of 100% ethanol for 1.5 h at -20°C. The ethanol-insoluble solids (EIS) were filtered through miracloth and washed sequentially with 1 L cold 80% ethanol, 1 L cold 80% acetone and 1 L cold 100% acetone. Residual phenol was removed by a 30 min incubation of the EIS in

chloroform/methanol (1:1, v/v). The EIS were then filtered under vacuum through a Whatman GF 934-AH filter and washed with 1 to 2 L of room temperature acetone. These BP-EIS samples were dried and stored with desiccant at room temperature.

Buffered-phenol treated cell walls. Approximately 100 g of partially thawed mesocarp from each RS were homogenized for 2 min in 400 ml of 40 mM N-2-hydroxyethylpiperazine-N'-2-ethane sulfonic acid (HEPES), pH 7.0 using a Polytron. The isolate was filtered through miracloth, washed with 1.6 L of the buffer and then suspended in 250 ml of BP (Huber, 1991) for 30 min at room temperature with stirring. The cell walls were then washed over miracloth with 4 L cold deionized water, 2 L of cold 80% ethanol and 2 L cold acetone. To remove residual phenol, the sample was stirred in chloroform/methanol (1:1, v/v) for 30 min at room temperature. The cell walls were filtered over a vacuum (using a Whatman GF 934-AH filter) and washed with 2 L of 100% acetone, then air dried and stored with dessicant at room temperature.

The buffer homogenates of RS4 mesocarp were very slow to drain through miracloth. Since the tissue was still enzymically active at this point, the filtration process was hastened by gentle squeezing, or by centrifugation at 3830 x *g* in a Beckman JA14 rotor at 4°C for 15 min. This centrifugation process was repeated 3 times with resuspension of the pellets in fresh buffer. The BP treatment and all subsequent filtration steps were carried out as outlined above.

Removal of starch. Where necessary, cell walls were destarched, either by overnight extraction in dimethylsulfoxide (Fry, 1988), or by incubation with α-amylase. Cell wall material was incubated overnight with 40 mM HEPES, pH 7.6 (wall to buffer ratio of 1:20 w/v) including 1 unit/ml of porcine α-amylase (Sigma Chemical Co., St Louis, MO) and 0.02% NaN_3. The walls were washed with deionized water (until a phenol-sulfuric acid assay performed on the washings was negative), 80% ethanol and 100% acetone, then air-dried. To check that starch removal was complete, aqueous wall suspensions were heated at 100°C for 10 min, cooled and then incubated for 30 min at

34°C with amylase from *Bacillus subtilis* (Sigma). Reducing sugars produced were quantified using the Nelson (1944) procedure.

Phenol/acetic acid/water cell walls. Mesocarp tissue from all RS was prepared essentially as for BP cell walls with the exception that the Tris-buffered phenol was replaced by PAW (2:1:1, v/v/v, Selvendran, 1975).

Cx-cellulase Activity Determination

Buffer-soluble protein was prepared from mesocarp of each RS by homogenizing 10 g of partially thawed mesocarp in 20 ml of 100 mM NaOAc, pH 5.0, containing 1.8 M NaCl, for 1 min. The samples were maintained at 2.5°C for 30 min, centrifuged (30 000 x *g* for 30 min) and the supernatant was analyzed for C*x*-cellulase activity by viscometric assay. A 100 µl aliquot of protein extract was added to 1.5 ml of a 2.5% solution of carboxymethylcellulose (CMC.7HSP; Fisher, Fair Lawn, NJ) in 40 mM NaOAc, pH 5.0, with 0.02% NaN_3 and the mixture was incubated at room temperature for 30 min. The time taken for the solution to pass through a calibrated portion of a 1-ml pipette was recorded and the specific viscometric activity of each protein extract was calculated as units (% viscosity reduction after 30 min incubation) mg^{-1} protein. Protein content of the extracts was measured according to the method of Smith et al. (1985) with bovine serum albumin used as a standard. Results were the average of four separate extractions from each RS.

Polygalacturonase Activity Determination

Buffer-soluble protein was prepared as for the C*x*-cellulase assay above. Polygalacturonase activity was assayed reductometrically by incubating an aliquot of the protein extract with a substrate of partially-deesterified citrus pectin (Sigma) dissolved in 30 mM NaOAc, pH 4.5, containing 150 mM NaCl. Incubation was at 37°C for 30 min. Reducing groups specifically from terminal uronic acids were measured using the method of Milner and Avigad (1967). Results are the average of four separate extractions from

each RS, and are expressed in units (μmol galacturonic acid equivalents produced during the 30 min incubation) mg^{-1} protein.

Cell Wall Characterization

Cellulose content. Approximately 30 mg of de-starched BP-treated cell wall material from each RS was analyzed for cellulose content using modifications to the method of Updegraff (1967). The cell wall samples were suspended in 3 ml of acetic acid/water/nitric acid reagent (8:2:1, v/v/v) and heated for 30 min in a boiling water bath. Following centrifugation (10 min at 3800 x *g*) the supernatant was removed by vacuum aspiration and the remaining material was washed and centrifuged with 4 ml of water (3 x) and 2 ml ethanol. The dried cellulose was dissolved in 67% H_2SO_4 (2 ml), and the hexose sugar content quantified using the anthrone assay (Dische, 1953). Results are the average of 6 extractions and are expressed as mg g^{-1} mesocarp fresh weight.

Hemicellulose content. Hemicelluloses were isolated using the method of Huber and Nevins (1981) as modified by de Vetten and Huber (1990). Cell wall material was extracted in 4 M NaOH including 26 mM $NaBH_4$. Cell wall to extractant volume ratio was 10 mg ml^{-1} and extraction time was 4 h. The suspension was filtered through miracloth and a Whatman 934-AH glass fiber filter. The solution was neutralized over ice with glacial acetic acid and then dialyzed (molecular weight cut-off [MWCO] of 2000 Da.) overnight against running deionized water followed by 10% methanol (2 x 4 L, 24 h total) and deionized water (2 x 4 L, 24 h total). Co-extracted acidic polymers were removed by passing each sample through a column (2.5 cm wide, 18 cm high) of DEAE-Sephadex (Sigma) in 10 mM Na phosphate, pH 6.8, containing 20 mM NaCl. The non-binding fraction contained the hemicelluloses and these were quantified by the phenol-sulfuric acid method (Dubois et al., 1956) and expressed as mg g^{-1} mesocarp fresh weight (the average of 7 separate extractions from PAW- and BP-treated cell walls).

Total pectin extraction. The method of Ahmed and Labavitch (1977) was used to extract and quantify total pectins from BP-EIS of each avocado RS. Approximately 5 mg

of the wall material was treated with 2.5 ml of cold concentrated H_2SO_4 and stirred on ice for 10 min. The volume was slowly made up to 50 ml with cold deionized water and the suspension was filtered through miracloth and Whatman GF/C. Total uronic acids in the solution were determined as mg g^{-1} avocado fresh weight from four separate extractions, using the *m*-hydroxydiphenyl method of Blumenkrantz and Asboe-Hansen (1973).

Chelator-soluble pectin extraction. Soluble pectins were extracted from 50 mg BP-EIS with 20 ml of 50 mM NaOAc, pH 6.5, containing 50 mM 1,2-cyclohexylenedinitrilotetraacetic acid (CDTA; Jarvis, 1982). Extractions were carried out at 25°C for a 6 h duration and quantified in terms of uronic acid content (Blumenkrantz and Asboe-Hansen, 1973). Four separate extractions were performed and results were expressed in mg g^{-1} avocado mesocarp fresh weight.

Compositional Analysis of Cell Walls and Hemicellulose Fractions

The hemicellulosic neutral-sugar composition of destarched, BP-treated cell walls and the 4 M alkali-extractable hemicelluloses was analyzed by hydrolysis and alditol acetate derivatization (Albersheim et al., 1967). An internal standard of 200 µg myo-inositol was dried down with approximately 1 mg of sample and hydrolyzed with 1 ml of 2 M trifluoroacetic acid for 2 h at 120°C. The sample was cooled and the acid removed by volatilization. The hydrolyzed sugars were then reduced with 1 ml of 0.66 M $NaBH_4$ in 1 M NH_4OH overnight at room temperature. The samples were neutralized with Dowex-50W cation exchange resin, filtered, dried and then derivatized with 200 µl each of acetic anhydride and pyridine for 1 h at 100°C. After drying, the alditol acetates were dissolved in methylene chloride and separated by gas chromatography (Hewlett Packard, Model 5710A, Atlanta, GA) on a column of 3% SP-2340 on 100-120 mesh Supelcoport (Supelco, Inc., Bellafonte, PA) at 225°C with flame ionization detection. Composite sugars were identified and quantified in relation to standard quantities of derivatized rhamnose, fucose, arabinose, xylose, mannose, galactose and glucose.

Hemicellulose Glycosyl Linkage Analysis

Glycosyl linkages of component sugars in the hemicellulose fractions of each RS were identified using the method detailed in de Vetten et al., (1991) and references therein. Briefly, 1 mg samples were methylated, and then hydrolyzed with trifluoroacetic acid. The free hydroxyl groups that had been involved in linkages in the whole polymer were reduced and acetylated, creating a means for identifying the different molecular species by mass spectroscopy. Gas chromatography with mass spectrometric detection was carried out at the USDA Horticultural Crops Quality Laboratory of Dr. K.C. Gross, at Beltsville, MD.

Molecular Weight Distribution of Chelator-Soluble Pectins

The chelator-soluble pectin extracted from BP-EIS from each RS was flash-evaporated to attain a final uronic acid concentration of approximately 500 $\mu g\ ml^{-1}$. Aliquots (2 ml) were passed through a Sepharose CL 4B-200 (Sigma) gel filtration column (1.5 cm wide and 28 cm high) operated in 30 mM NaOAc at pH 6.5 and containing 10 mM EDTA and 20 mM NaCl. Fractions (2 ml) were collected and assayed for uronic acids (Blumenkrantz and Asboe-Hansen, 1973). The column void and total volumes were identified by the elution positions of Blue Dextran (2000 kDa.) and glucose, respectively.

To determine the presence of oligosaccharides in the pectin preparation from RS4, a sample from the low molecular weight end of the 4B-200 column polymer distribution was concentrated to 1 ml and applied to a Bio-Gel P-2 column (1.5 cm wide and 33 cm high; Bio-Rad, Richmond, CA) operating in 25 mM NaOAc, pH 4.5, containing 50 mM NaCl and 3 mM EDTA. Fractions (1 ml) were collected and assayed for uronic acid content. The void and total volumes of the P-2 column were identified by the elution positions of a CDTA-soluble pectin extract from BP-EIS of unripe tomato fruit and galacturonic acid respectively. The CDTA extract had been previously shown to void on

Sepharose CL 4B-200 and therefore exceeded the nominal 2000 Da. fractionation limit for the Bio-Gel P-2.

Results and Discussion

General

Avocados ripened at 25°C showed a loss of firmness temporally aligned with the climacteric evolution of ethylene and the increase in CO_2 production (Table 3-1). Avocado fruit have very little ability to resist pressure and no elasticity when they approach the edibly soft stage. In the light of general ripening work on other fleshy fruits, this dramatic loss of textural integrity points to rapid cell wall modification. Mesocarp firmness was unchanged between RS1 and RS2, but decreased by approximately 52% between RS2 and RS3, while the firmness of RS4 fruit was reduced to only 4% of the previous stage (Table 3-1).

Even though there was no change in firmness over the first 36 h in ripening conditions there was a significant increase in the activity of C*x*-cellulase, and this activity continued to increase throughout the ripening period (Table 3-1). In comparison, only a trace of polygalacturonase activity was found at RS3, with a major increase seen when the fruit were edibly soft at RS4. The low levels of C*x*-cellulase activity in preripe fruit have been noted previously (Pesis et al., 1978; Awad and Young, 1979). It has been shown that avocado ripening is accompanied by synthesis of qualitatively new mRNAs, one of which codes for C*x*-cellulase (Christofferson et al., 1984; Tucker and Laties, 1984) so the apparent activity toward CMC exhibited by protein derived from preripe fruit may be due to the presence of other enzymes (e.g., β-glucosidase, exo-cellulase) capable of acting on this substrate.

Table 3-1. Respiration, ethylene production, firmness of individual avocado fruit (n = 12) at each RS, and C*x*-cellulase and polygalacturonase activities (n = 4) of combined mesocarp samples at each RS. Data from 1990 material; ± SE.

Ripeness Stages	RS1	RS2	RS3	RS4
Hours at 25°C	0	36	56	117
Respiration (ml CO_2 $kg^{-1}h^{-1}$)	23.02 (0.97)	64.33 (2.12)	116.11 (4.19)	82.73 (4.12)
Ethylene (µl $kg^{-1}h^{-1}$)	0.37 (0.02)	18.92 (3.18)	141.23 (6.00)	17.89 (1.35)
Firmness (Newtons)	497 (6)	510 (13)	267 (36)	12 (1)
C*x*-cellulase (units mg^{-1} protein)	10.09 (4.51)	52.56 (6.35)	94.98 (6.13)	123.52 (10.08)
Polygalacturonase (units mg^{-1} protein)	ND	ND	0.10 (0.07)	1.93 (0.02)

ND = not detected

Table 3-2. Yield of cell wall material from each RS (mg g^{-1} mesocarp fresh weight).

Ripening Stages	RS1	RS2	RS3	RS4
BP-EIS	48.2	54.3	59.7	61.1
BP Cell Walls	47.5	42.2	36.0	20.9
PAW Cell Walls	43.5	48.4	29.6	23.2

Cell Wall Composition

The quantity of cell wall material declined during avocado fruit ripening regardless of the method (BP or PAW) used for endogenous enzyme deactivation (Table 3-2). Ethanol-insoluble solids did increase however, indicating an accumulation of wall components during ripening. Colinas-Leon and Young (1981) reported a decrease in avocado cell wall material (expressed on a mg g^{-1} mesocarp dry weight basis), and Huber (1984) described an increase in strawberry EIS per fruit which was masked by an increase in fruit weight throughout development. There is minimal change in water content during avocado ripening so the changes recorded in cell wall material are absolute in this case.

Table 3-3. Non-cellulosic neutral sugar composition of de-starched BP-cell walls of avocado fruit at each RS. Results are expressed as mole % and are the average of two separate derivatizations.

Ripening Stages	RS1	RS2	RS3	RS4
Rhamnose	4.1	4.8	3.8	1.6
Fucose	2.8	2.4	3.0	4.5
Arabinose	36.7	37.5	46.8	25.6
Xylose	20.0	20.3	22.2	37.9
Mannose	4.5	5.6	3.8	8.5
Galactose	25.2	21.2	15.9	13.3
Glucose	6.8	8.3	4.6	8.6

Non-cellulosic neutral sugar analysis of the avocado cell wall showed that while there was a loss of water-soluble polysaccharides during ripening, the composition of the remaining wall material was also changing (Table 3-3). The major non-cellulosic neutral sugars were arabinose, galactose and xylose, collectively comprising 82% and 77% of the

neutral sugars in cell walls of unripe and ripe fruit respectively. Fucose, mannose, rhamnose and non-cellulosic glucose were also detected. During ripening there was an overall loss of galactose and an increase of xylose. The quantity of arabinose peaked at RS3 but declined at RS4, to a value lower than in that seen prior to ripening. In their extensive species survey of non-cellulosic neutral sugar changes, Gross and Sams (1984) noted that the cell wall sugars affected most by ripening were galactose, arabinose and xylose. In particular, net losses of galactose and/or arabinose occurred during ripening in the majority of the fruit commodities studied and this appears to be the case for avocado fruit also.

Cellulose

Changes in cellulose levels during fruit ripening have not been thoroughly examined in terms of contributions to the loss of cell wall integrity. In a number of instances the quantity of cellulose is identified only as the residual material following comprehensive extraction of pectins and hemicelluloses. In this manner, kiwifruit cellulose has been shown to increase on a percent dry tissue weight basis (Redgwell et al., 1990), pear cellulose declines slightly per fruit (Jermyn and Isherwood, 1956) and cellulose levels decrease as Japanese pears overripen (Yamaki et al., 1979). Alternatively, the Updegraff (1969) procedure for cellulose determination employs an acid digestion step to remove other cell wall components, and the remaining cell wall material, consisting largely of cellulose, is solubilized in stronger sulfuric acid. This method does not rely on the adequacy of sequential extraction techniques and is therefore a more reliable indicator of cellulose content. This approach has been used to show a decline in the cellulose content of the locular gel and an increase in the pericarp tissue cellulose during tomato fruit ripening (Huber, 1985). The cellulose content of pear (Ahmed and Labavitch, 1980) and muskmelon (Lester and Dunlap, 1985) did not change during fruit ripening while avocado cellulose declined on a mg g^{-1} dry weight basis (Colinas-Leon and Young, 1981), a trend similar to that reported in Table 3-4 for fresh mesocarp.

Table 3-4. Cellulose (n = 6), hemicellulose (n = 7), total pectin (n = 4) and chelator-soluble pectin (n = 4) content of cell walls from avocado fruit at each RS (mg g^{-1} mesocarp fresh weight $\pm$ SE).

Ripening Stages	RS1	RS2	RS3	RS4
Cellulose	13.01 (0.64)	12.57 (0.16)	12.51 (0.17)	10.59 (0.47)
Hemicellulose	1.67 (0.16)	1.56 (0.06)	1.94 (0.18)	1.64 (0.13)
Total Pectin	9.91 (0.18)	10.75 (0.19)	11.41 (0.10)	12.27 (0.11)
Chelator-Soluble Pectin	1.37 (0.08)	2.16 (0.30)	3.70 (0.05)	10.23 (0.07)

The loss of cellulose in avocado fruit does not appear to be correlated with fruit firmness, as the major decrease in this wall polymer occurs between RS3 and RS4, well after the onset of fruit softening (Table 3-4). Cell walls at RS4 formed very viscous suspensions with buffer and were slow to filter, therefore preparative conditions may be a factor in the cellulose decline. Although the target of C*x*-cellulase activity has not been experimentally determined it has, in the past, been aligned with cellulose hydrolysis. From a quantitative point of view, there is substantial C*x*-cellulase activity (Table 3-1) prior to any detectable change in cellulose levels on a fresh weight basis (Table 3-4). It should be borne in mind that the avocado is undergoing continual cell division, so that any appreciable cellulose degradation may be masked by cellulose synthesis. While evidence to support ongoing cellulose synthesis has not been addressed in this study, the quantity of cellulose in BP-treated cell walls from the first three stages of ripening remains constant while the levels of cell wall material is steadily decreasing (data not shown). At RS4 the proportion of cellulose in the buffer-soluble cell walls increases dramatically, presumably

due to the loss of other components during ripening. This indicates that conditions exist whereby an overall loss of cellulose could go undetected. However, assigning cellulose hydrolysis to C*x*-cellulase activity simply on the basis of this data is correlative at best.

Table 3-5. Compositional analysis of 4 M alkali-soluble hemicellulose extracts from avocado fruit at each RS. Results are expressed as mole % and are the average of two separate derivatizations.

Ripening Stage	RS1	RS2	RS3	RS4
Rhamnose	ND	0.3	ND	ND
Fucose	4.6	4.3	4.5	5.9
Arabinose	3.1	4.4	2.9	2.2
Xylose	27.8	22.2	23.5	27.3
Mannose	18.9	23.5	21.2	11.9
Galactose	10.7	10.9	11.7	12.2
Glucose	34.9	34.4	36.2	40.6

ND = none detected

Hemicellulose

Hemicelluloses (4 M alkali-soluble) are present in avocado cell walls in low quantities compared to either cellulose or pectins and there appears to be no quantitative change in this fraction during ripening (Table 3-4). Hemicelluloses, particularly xyloglucan (XG), are involved in tenacious hydrogen bonding around and between cellulose microfibrils. Previous studies have shown that there are major changes in the composition of hemicelluloses during ripening. This indicates a preferential loss of certain glycosyl residues associated with particular hemicellulosic polymers, but also the likelihood of cell wall synthesis during an overall catabolic phase along with the possibility that the physiological role of the hemicellulosic polysaccharides may be changing.

Analyses revealed that the hemicelluloses of avocado fruit are composed of polymers containing glucose, xylose and mannose with smaller quantities of galactose, fucose and arabinose (Table 3-5). Only trace levels of rhamnose were found at RS2. During ripening there is an overall increase in glucose (mole % basis) and galactose. Mannose levels increase at RS2 but decline through the climacteric and tissue softening. Conversely, the xylose levels decreased at RS2 and then increased back to original values by RS4.

Table 3-6. Glycosyl-linkage composition of hemicelluloses from each RS. Results are expressed as mole % and are the average of two separate derivatizations.

Ripening Stages	RS1	RS2	RS3	RS4
t-Arabinose	ND	1.3	1.9	ND
t-Xylose	21.7	21.5	19.7	22.7
2 & 4-Xylose	13.7	15.2	16.0	16.6
t-Mannose	6.4	5.5	7.0	8.9
4-Mannose	13.7	15.5	13.1	12.8
t-Galactose	6.2	6.3	6.2	6.5
2-Galactose	4.6	4.3	4.4	2.8
t-Glucose	1.5	ND	ND	1.7
4-Glucose	13.1	12.9	12.5	11.2
4,6-Glucose	19.4	17.8	19.3	17.2

t = terminal

ND = not detected.

Other fruits also display similar changes in hemicellulose content during ripening. Glucose and galactose decreased and xylose increased during ripening of muskmelon

(McCollum et al, 1989), while there were major losses of galactose and increases in glucose and xylose content during kiwifruit ripening (Redgwell et al., 1990, 1991). In tomato fruit, glycosyl-linkage analysis of hemicelluloses has indicated the presence of qualitatively new hemicellulose polymers by identifying new types of linkages during ripening (Tong and Gross, 1988). Senescing carnation petals undergo similar cell wall changes as ripening fruit (de Vetten and Huber, 1990; de Vetten et al., 1991). In contrast to the situation in tomato, the glycosyl linkage characteristics of carnation hemicellulose did not change during senescence (de Vetten et al., 1991).

During avocado fruit ripening there were only subtle changes in the types of linkages within the hemicellulose fraction (Table 3-6). Terminal arabinose groups were seen only at RS2 and RS3, while terminal glucose residues were seen only at RS1 and RS4. Fucose was identified as a constituent of the hemicellulose fraction by alditol acetate derivatization, but it, as well as arabinose at RS1 and RS4, was not identified by linkage analysis. There is a substantial amount of glucose linked at the C-4 position, accompanied by glucose both linked at C-4 and substituted at C-6. In accounting for the linked and terminal mannose and xylose, it would appear that the glucose is involved in both XG and glucomannan. The terminal and C-4-linked galactose residues are likely to be involved in the XG structure, but the presence of arabinogalactans cannot be ruled out. While arabinose is absent in the linkage analysis, it is present in roughly equal amounts with the galactose in the normal compositional analysis. From the compositional and linkage analyses, there is no strong indication that qualitatively new hemicelluloses are being synthesized during ripening. Two scenarios are suggested to explain the fate of hemicelluloses during avocado fruit ripening. Either the hemicelluloses of the avocado cell wall are in a state of metabolic equilibrium i.e., synthesis equaling degradation, and also remain unchanged qualitatively during fruit ripening, or the nature and quantity of hemicelluloses are totally unaffected by ripening. Given that the total quantity of hemicellulose does not change during ripening, the second proposal seems more likely.

Hatfield and Nevins (1986) suggested that a possible role for C*x*-cellulase of avocado fruit could be to hydrolyze XG. Given the relatively low quantities of hemicellulose in the cell wall, and the absence of quantitative change during ripening, it would seem that the onset of C*x*-cellulase activity has no influence on these polymers. However, as in the case of cellulose, polymer synthesis (or lack of) can only be surmised from the data here and equally, the role of C*x*-cellulase cannot be determined solely on the basis of quantitative changes.

Pectic Polysaccharides

In a number of fruit types, the increase in the amount of soluble polyuronides is accompanied by a reduction in the amount of large-sized polymers and an increase in much smaller fractions. In 'Galia' muskmelon tissue, which softens extensively but contains no polygalacturonase, there is a progressive decline in total pectin and an increase in soluble pectin (on a mg^{-1} EIS basis, [McCollum et al., 1989]), although for 'Perlita' muskmelon tissue there was little change in total cell wall pectin as the fruit aged (Lester and Dunlap, 1985). In Japanese pear, there is an increase in the quantity of both total pectin and chelator-soluble pectins (Yamaki et al., 1979). There is continual synthesis of polyuronides during strawberry fruit ripening--as indicated by the increase in both EIS and polyuronide content over the ripening period (Huber, 1984). The proportion of chelator-soluble pectin in the EIS increased as the strawberry fruit progressed from green to red. This polyuronide did not show significant molecular weight (M_r) alteration during ripening, which seems to be consistent with the absence of polygalacturonase activity in strawberry fruit. There are obviously other factors apart from size reduction involved in the conversion of insoluble pectin to soluble pectins. Chelator-soluble pectin decreased during ethylene-induced ripening of kiwifruit (Redgwell et al., 1992), but the M_r distribution was altered dramatically to become composed of predominantly smaller polymers. Tomato fruit pectins are arguably the most comprehensively studied group of pectins. With the advent of techniques such as PAW (Selvendran, 1975) and BP (Huber,

1991) to deactivate wall-associated hydrolytic enzymes the true quantity of chelator-soluble pectin has been shown to increase during ripening (Huber, 1983a; Seymour et al., 1987). The average M_r of this pectin was lowered during ripening (Huber, 1983a; Huber and Lee, 1986; Seymour et al., 1987) but while soluble pectins in the locular gel increased in quantity during ripening they were not altered in terms of M_r (Huber and Lee, 1986).

There is an increase in total pectin (g^{-1} fruit fresh weight) extracted from EIS (Table 3-4) during avocado fruit ripening, as well as an increase in the amount of EIS itself (Table 3-2). As in the case of strawberries (Huber, 1984), this is an indication of continual synthesis of pectin throughout the ripening process. Dolendo et al. (1966) also detected an increase in water-soluble pectin extracted from avocado EIS, while Colinas-Leon and Young (1981) reported a loss of total uronic acid expressed in terms of mesocarp dry weight. Prior to obvious signs of softening (between RS1 and RS2) and when softening is initiated (between RS2 and RS3) there are low but significant increases in the amount of pectin associated through chelation with calcium. However, there is almost a 3-fold increase in chelator-soluble pectin between RS3 and RS4--a developmental stage that sees a 96% reduction in mesocarp firmness.

The M_r characteristics of the CDTA-soluble avocado pectin was examined at each RS. The chelator-soluble polyuronides from RS1 to RS3 (Figure 3-1A, B and C) were large enough to be eluted at the void volume of the Sepharose CL 4B-200. However, by RS4 (Figure 3-1D) this large-sized pectin had virtually disappeared and was replaced by polymers that eluted close to the total volume of the column. Since the 4B-200 column fractionation cutoff is approximately 30 kDa. as determined with linear dextrans, this limit is only an approximation for branched and/or charged polymers such as pectins. Notwithstanding, the M_r properties of chelator-soluble pectins clearly change, especially at the latter stages of avocado ripening, and while the direction of change is similar to that seen for tomato (Huber, 1983a; Huber and Lee, 1986; Seymour et al., 1987) and muskmelon (McCollum et al., 1989) the loss of large M_r polymers appears much more

complete. The M_r distribution of CDTA-soluble polyuronides from ripening kiwifruit (Redgwell et al., 1992) appears to be the most similar in form to the situation in ripening avocado, even though the comparison must be tempered due to the different permeation columns used.

To investigate the possibility that such a dramatic decrease in the M_r of CDTA-soluble pectins could involve the production of pectic oligomers, the RS4 polysaccharide eluting from 52-68 ml (the low M_r end of the peak in Figure 3-1D) was rechromatographed on Bio-Gel P-2. Pectic fragments of DP $\leq$ 8 were identified as multiple peaks between the void and the total volumes (Figure 3-2). The presence of pectic oligomers originating from enzymically-inactive cell wall material has not been reported before, although gel permeation studies of kiwifruit (Redgwell et al., 1992) and tomato pericarp (Huber and Lee, 1986) CDTA-soluble pectins have shown a large proportion of the pectin in the ripe fruit to be eluting very close to the inclusion limits of fractionation media with a much broader Mr distribution range than P-2.

The presence of monomer in the avocado pectin extracts raised concerns that the EIS were not washed sufficiently during preparation, or that the EIS were not completely enzymically inactive and the oligomers were released by enzyme activity during pectin extraction. In order to address the first of these considerations, EIS from RS4 (edibly soft fruit) were washed repetitively with ethanol to solubilize any monomer or dimer present in the powder. The ethanol extracts were pooled, concentrated and exchanged with buffer, then fractionated through the Bio-Gel P-2 column using the same buffer conditions as for the Sepharose CL 4B-200. The remaining EIS were extracted with CDTA and also examined on P-2. Quantitatively, the amount of carbohydrate (and in particular the oligosaccharides) removed by additional ethanol washings was minimal compared to that solubilized by CDTA. The quantities of polyuronide solubilized from EIS by CDTA with and without an ethanol pretreatment were 9.77 ± 0.16 mg g^{-1} fruit fresh weight and 9.53 ± 0.15 mg g^{-1} fruit fresh weight respectively. The profile of the ethanol-soluble wash

(Figure 3-3A) shows minimal amounts of monomer, plus trace amounts of a fractionated oligosaccharide and a larger polymer (possibly due to inadequate sample filtration). In contrast, CDTA extracts from ethanol-washed BP-EIS (Figure 3-3B) contained substantial amounts of oligosaccharides, and the elution pattern was similar to that of CDTA-solubilized material without the ethanol wash (Figure 3-3C). Pectic oligomers, but not monomers, therefore, appear to be a genuine component of the cell wall pectin fraction.

To address the second concern, namely that the EIS contained active enzymes, BP-EIS of RS4 was extracted as normal with CDTA and then washed thoroughly with water to remove all the solubilized material. This depectinated EIS was then incubated (6 h at room temperature) with exogenous polyuronide extracted from BP-EIS of RS1 (an enzymically inactive developmental stage). Incubated alongside this treatment were controls of (a) the depectinated RS4 BP-EIS without the RS1 polyuronide, and (b) the RS1 polyuronide alone. Following incubation, the pectin released in each case was examined on Sepharose CL 4B-200. When RS4 BP-EIS was incubated with the large-M_r polyuronides from RS1 there was no sign of degradation (Figure 3-4C) confirming the absence of active cell wall hydrolases in the BP-EIS of RS4, and supporting the notion that the pectic oligomers seen at RS4 were generated during ripening. There was minimal release of polyuronide from either of the controls--depectinated RS4 EIS incubated in buffer only (Figure 3-4A) or CDTA-soluble polyuronide from RS1 incubated in buffer alone (Figure 3-4B).

To investigate whether the pectin M_r changes during avocado fruit ripening were due to endogenous enzyme activity, 20 mg samples BP-EIS from RS1 (in a buffer of 40 mM NaOAc, pH 5.0, including 100 mM NaCl and 10 mM CDTA) were incubated for 24 h with 200 mg of crude active or denatured enzyme extract from fully ripened avocado fruit (RS4). The addition of the enzyme extract solubilized approximately twice as many uronic acid equivalents as a similar EIS sample incubated with heat-denatured enzyme.

The presence of CDTA resulted in some background solubilization of pectin. The Sepharose CL 4B-200 distribution of the solubilized polyuronide showed that the heated enzyme controls contained some material small enough to elute near the inclusion volume of the column, but by far the majority of control polyuronide was of large molecular size and eluted at the void volume (Figure 3-5A). The pectin solubilized by the active enzyme extract was polydisperse, containing a relatively small amount of the large M_r pectin and a broad distribution of lower M_r material, including polymers small enough to elute close to the total column volume (Figure 3-5B). Although this profile does not resemble that of pectic extracts from ripe fruit (Figure 3-1D), there is evidence that depolymerization is occurring. It may be that prolonged exposure to a variety of cell wall enzymes and a longer incubation time under these same conditions could have produced a higher proportion of the smaller uronides. Sampling avocados at regular intervals following the climacteric and well into the overripe stage could answer this question.

The contribution of polygalacturonase to the alteration of pectin M_r is the subject of speculation. Profiles similar to that of Figure 3-5B were found following incubation of pectin from RS1 with semi-purified polygalacturonase from tomato fruit. Levels of polygalacturonase activity do not appear until RS3 (Table 3-1) and even at this point the activity is low enough to indicate that polygalacturonase induction has only just begun. The principal stage of chelator-soluble pectin production and the radical M_r changes (RS4) correlates well with the phase of major polygalacturonase activity. Given the ability of polygalacturonase to hydrolyze pectin one must assume there is polygalacturonase involvement in the pectin M_r changes seen here during avocado fruit ripening. Equally, other enzymes, such as galactosidase and pectinmethylesterase are probably involved, and there is a strong likelihood of a synergistic relationship between all these enzyme systems.

Summary

During the ripening of avocado fruit there are significant changes in the composition and structure of cell wall polysaccharides. While the fruit weight does not change during ripening, there is an increase in EIS over this period, indicating there is still significant cell wall production. Although this is not unusual in ripening fruit (e.g., strawberry, tomato) the avocado has the added feature of still undergoing cell division during maturation and ripening, which implies an added requirement for cell wall production. In this light, the alterations in pectin solubility and M_r are all the more remarkable. Most of the biochemical changes occur between RS3 and RS4, after the climacteric surge of ethylene and CO_2 production. Arabinose content of the cell wall increases up to RS3, then declines rapidly in the ripe fruit (RS4). Galactose levels decline especially during the early stages of ripening (RS1 to RS3) and xylose levels increase, particularly between RS3 and RS4. On the basis of linkage analysis, there is no evidence of qualitatively new hemicelluloses being produced during ripening, although this has been shown to be the case in tomato fruit (Tong and Gross, 1988; Greve and Labavitch, 1991). Yields of total hemicelluloses (those polysaccharides solubilized by 4 M NaOH) did not change during ripening, and the most notable features of the compositional changes over this period were an increase in glucose and a loss of mannose on a mole % basis.

Avocado fruit lose firmness rapidly and dramatically. While attention may be paid to the state of texture in the mesocarp of fully ripe avocado, the full extent of the softening process is only appreciated when the firmness values of the unripe fruit are considered. The change from 497 N to 12 N in a little under 5 days at 25°C is quite remarkable. Ultrastructural studies comparing unripe and ripe avocado fruit (Platt Aloia et al., 1980) have provided physical evidence of considerable cell wall disruption, particularly in the middle lamella region. Pectins are the major components of the middle lamella and the experiments documented here show that during avocado ripening there is an increase in chelator-soluble pectin with an accompanying and substantial decrease in pectin M_r. Total

pectin also increases during ripening. This may indicate that the increase in soluble pectin is due to endogenous synthesis of polymers with this characteristic, but likewise the solubility may be the result of enzyme-mediated modifications. That the latter contributes in some way to the production of low M_r was shown by incubation of unripe EIS with crude enzyme extracts from ripe avocados, although degradation did not occur to the same extent as seen in pectins from RS4. The possibility of other factors influencing the solubility of pectin during ripening, such as synthesis, calcium availability or esterification cannot be ruled out.

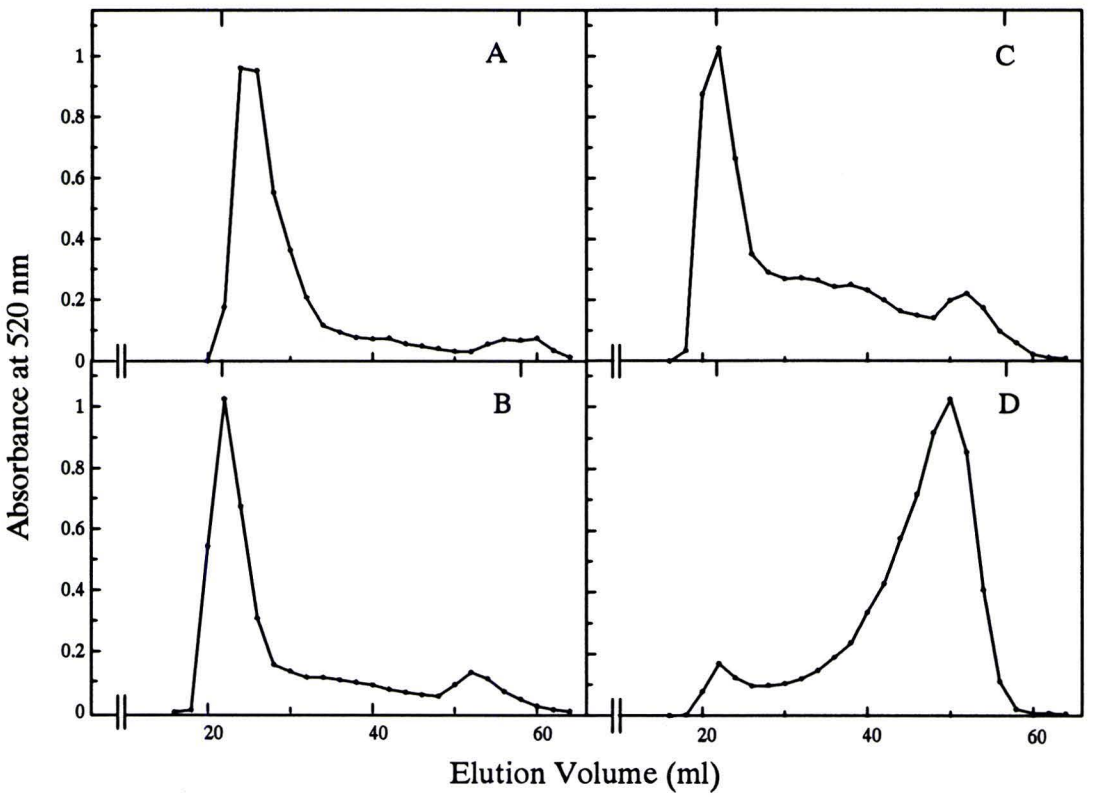

Figure 3-1. Sepharose CL 4B-200 profiles of CDTA-soluble pectins from EIS derived from avocado fruit at (A) RS1, (B) RS2, (C) RS3 and (D) RS4. Vertical ticks at the top of each profile indicate the elution positions of Blue Dextran (2000 kDa.) and glucose, respectively. Absorbance at 520 nm: colorimetric determination of galacturonic acid equivalents.

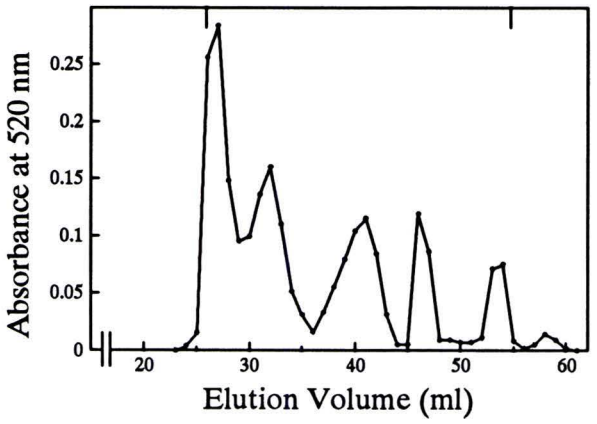

Figure 3-2. Bio-Gel P-2 profile of pectins from Figure 3-1D (eluting at 52-68 ml on Sepharose CL 4B-200). Vertical ticks at the top of the profile indicate the elution position of excluded polymers of tomato pectin, and galacturonic acid, respectively. Absorbance at 520 nm: colorimetric determination of galacturonic acid equivalents.

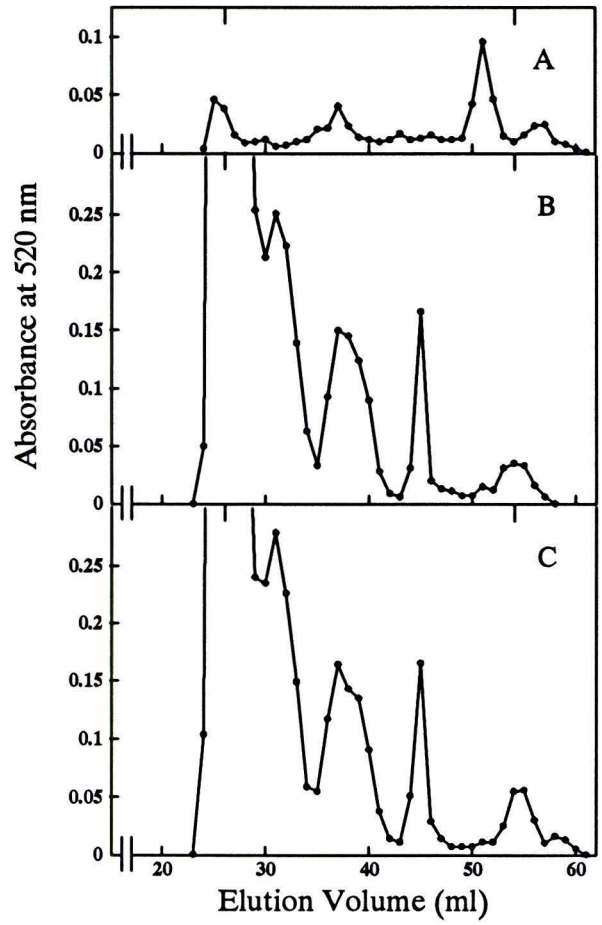

Figure 3-3. Bio-Gel P-2 profiles of (A) pectic oligomers solubilized during an ethanol pretreatment of BP-EIS, (B) polyuronides solubilized from BP-EIS by CDTA following the ethanol pretreatment and (C) polyuronides solubilized from BP-EIS by chelator without the ethanol pretreatment. Marks at the top of each profile denote the elution positions of excluded polymers of tomato pectin and galacturonic acid, respectively. Absorbance at 520 nm: colorimetric determination of galacturonic acid equivalents.

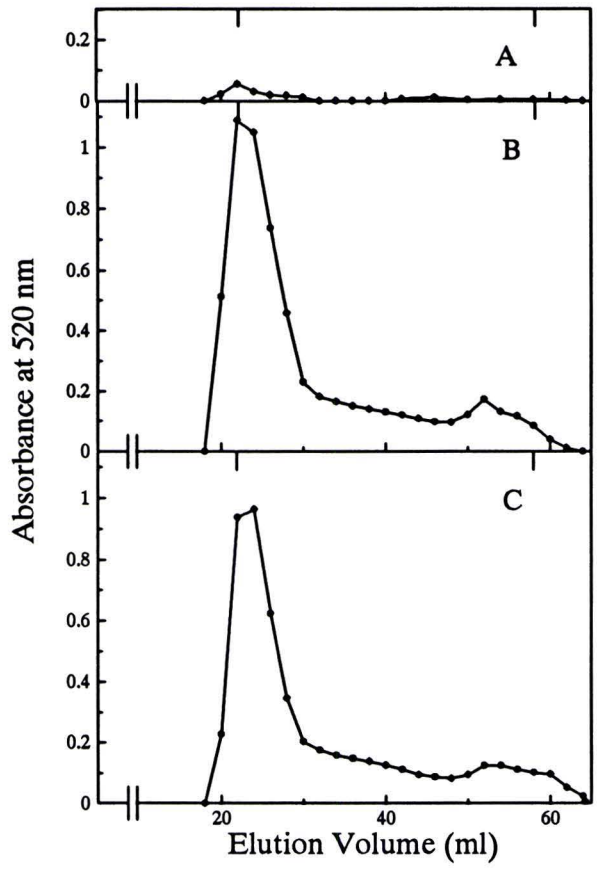

Figure 3-4. Sepharose CL 4B-200 profiles of CDTA-soluble polyuronides of (A) RS4 BP-EIS previously extracted with CDTA, (B) RS1 BP-EIS and (C) RS1 BP-EIS with CDTA-treated RS4 BP-EIS. Incubations were for 6 h at room temperature. Vertical ticks at the top of each profile denote the elution positions of Blue Dextran (2000 kDa.) and glucose, respectively. Absorbance at 520 nm: colorimetric determination of galacturonic acid equivalents.

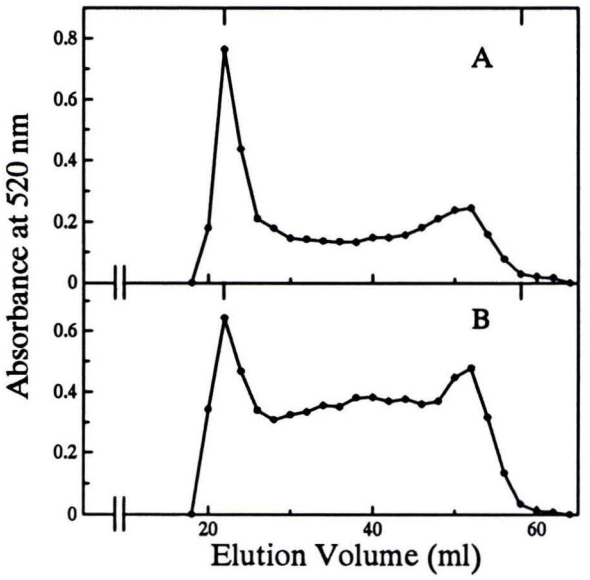

Figure 3-5. Sepharose CL 4B-200 profiles of CDTA-soluble pectin of RS1 following a 24 h incubation with a heat-denatured (A) or active (B) crude enzyme extract from RS4 avocado mesocarp. Marks at the top of each profile denote the elution positions of Blue Dextran (2000 kDa.) and glucose, respectively. Absorbance at 520 nm: colorimetric determination of galacturonic acid equivalents.

CHAPTER 4
HEMICELLULOSE MODIFICATION DURING AVOCADO FRUIT RIPENING: AN ASSESSMENT OF THE ROLE OF C*x*-CELLULASE

Introduction

The hemicellulose fraction of the plant cell wall is composed of a variety of polysaccharides, all of which are insoluble in aqueous chelator solutions and soluble in strong alkali (Fry, 1988). Hemicelluloses have been shown to change in molecular weight (M_r) distribution during the ripening of all fruit examined including tomato (Huber, 1983a; Tong and Gross, 1988), strawberry (Huber, 1984), mango (Mitcham and McDonald, 1992), kiwifruit (Redgwell et al., 1991) and muskmelon (McCollum et al., 1989). To date, the cause of these molecular weight changes is unknown, but it seems likely that enzyme-mediated hydrolysis is involved to some degree. Even though hemicellulose modifications are found in concert with the loss of fruit firmness, the extent to which cell wall strength is controlled by hemicellulose integrity is unknown.

Endo β-1,4-glucanase (C*x*-cellulase) is known to increase during the ripening and softening of numerous climacteric and nonclimacteric fruit types. In the case of avocado, this enzyme has been localized in the cell wall during fruit softening (Dallman et al., 1989). While its particular role in the fruit cell wall has not been fully investigated, a C*x*-cellulase-type enzyme has been implicated in xyloglucan (XG) metabolism of expanding vegetative tissues (Hayashi et al., 1984, Koyama et al., 1981) and it is also frequently associated with the cell wall degeneration of abscission zones (Durbin et al., 1981, Sexton et al., 1980), although in this case the target of cellulase activity is still unclear. The preference of the avocado C*x*-cellulase for β-1,4-linked glucans, but the inability of the enzyme to hydrolyze crystalline cellulose led to the suggestion by Hatfield and Nevins (1986) that the enzyme

may have a role in the hydrolysis of hemicelluloses, in particular the degradation of XG. This hypothesis seems appropriate, since in one instance at least an apparent M_r decrease and eventual disappearance of XG accompanied fruit ripening (Huber and Lee, 1986). The following experiments were conducted to investigate the effect of mesocarp softening on the M_r characteristics of avocado hemicelluloses including XG and to examine the response of these polymers to avocado-derived C*x*-cellulase. Fruit of three distinctly different firmness values (ripening stages [RS] 1, 3 and 4; Chapter 3) were used for these studies.

Materials and Methods

Hemicellulose Preparation

Hemicelluloses were extracted from cell wall preparations of RS1, RS3 and RS4 using the procedure outlined in Chapter 3. Following the removal of co-extracted pectins by ion exchange chromatography, each sample was dialyzed (2000 Da. molecular weight cut off [MWCO] tubing) for a total of 16 h (2 x 4 L) against water and concentrated by flash evaporation to approximately 1 mg ml^{-1}. For the most part, cell walls inactivated with phenol:acetic acid:water (PAW; 2:1:1 v/v/v; Chapter 3) were used for hemicellulose extraction; other cell wall types were also employed and are noted where appropriate in the Results and Discussion.

Xyloglucan Preparation

Xyloglucan was extracted using a modification of the method of Hayashi and Delmer (1988). Avocado mesocarp (150 g) from RS1 fruit was homogenized in 400 ml of 40 mM N-2-Hydroxyethylpiperazine-N'-2-ethane sulfonic acid (HEPES), pH 7.0, the suspension filtered through miracloth and the retained material washed with 1.6 L of the same buffer. The retained material was sequentially extracted with hot (85-90°C) 40 mM HEPES, pH 7.0, for 1 h, 1 M NaOH with 26 mM $NaBH_4$ (2 x 2 h), and 6 M NaOH with 26 mM $NaBH_4$ (2 x 2 h). The extraction volumes were 500 ml in each case. The

homogenate was filtered and washed briefly with water between each extraction. The 6 M NaOH extract (containing solubilized XG) was neutralized with glacial acetic acid, adjusted to 80% ethanol and maintained at 1°C for 16 h. The precipitate was collected by slow vacuum filtration (Whatman 934-AH filter), redissolved in deionized water and then dialyzed (MWCO 6-8000 Da.) sequentially against running tap water (overnight), 10% methanol (2 x 4 L, 24 h total) and deionized water (2 x 4 L, 24 h total). The extract was passed through a DEAE-Sephadex column as described for the hemicellulose preparation (Chapter 3) and the unretained carbohydrates were dialyzed against deionized water (2 x 4 L, 24 h total), then concentrated by flash evaporation to 37 ml. Solid $CaCl_2$ was added to make a final concentration of 1 M and the solution was cooled to 4°C. To precipitate the XG, approximately 12.5 ml of a 3% I_2:4% KI solution was slowly added and the sample left for 16 h at 4°C. The precipitate was collected by centrifugation at 30 000 x *g* for 45 min, then redissolved in deionized water over a boiling water bath and decolorized with a drop of 2 M $Na_2S_2O_3$. Following dialysis (MWCO 6-8000 Da.) against deionized water (2 x 4 L, 16 h total) the solution, containing approximately 428 mg carbohydrate, was stored at -20°C.

Preparation of Cell Wall Ghosts

Cell wall ghosts (CWG) were prepared from partially thawed mesocarp from RS1 (CWG1) and RS4 (CWG4) following the method of Hayashi et al. (1984) with some modifications. Initial steps in the isolation were similar to that for XG (above) up to the point of 1 M NaOH extraction. The insoluble material from this step was washed with deionized water until the washings were of neutral pH, then treated with 50 mM NaOAc, pH 6.0 containing 50 mM EDTA (2 x 500 ml) for a total of 16 h. The CWG were washed with deionized water and freeze-dried.

Neutral Sugar Composition

The neutral sugar composition of the XG-enriched sample and CWG were examined by derivatizing the component sugars to their alditol acetates and using gas

chromatography for separation and identification. Details of this procedure are described in Chapter 3.

Gel Permeation Chromatography of Hemicelluloses

A 1.5 mg sample of each hemicellulose solution (at approximately 1 mg ml^{-1}) was heated for 5 min in a boiling water bath (to disperse aggregates) before being applied to a column (1.5 cm wide, 70 cm high) of Sephacryl Superfine S-300 (Pharmacia LKB Technology, Uppsala, Sweden) operated in 40 mM NaOAc, pH 5.0 buffer containing 0.02% NaN_3, at room temperature. Fractions of 2 ml were collected and aliquots were separately assayed for total sugars (Dubois et al., 1956) and XG (Kooiman, 1960). The column was calibrated with dextran standards of 5-40 x 10^3 kDa., 70 kDa., 40 kDa., 10.5 kDa. (Sigma, St. Louis, MO) and glucose.

A Sepharose 4B-200 (Pharmacia) column (1.5 cm wide, 28 cm high) was also used for gel permeation for hemicelluloses. The operating buffer and calibration conditions, fraction size and assay methods were the same as for the Sephacryl S-300 column.

Isolation of Crude Enzyme Extract

Fresh avocado mesocarp from fruit of RS4 was homogenized in 100 mM NaOAc, pH 5.0 buffer containing 1.8 M NaCl (tissue to buffer ratio 1:2, w/v), and then maintained at 1°C for 1 h. The homogenate was centrifuged at 12 400 x *g* for 30 min and the supernatant filtered through miracloth to remove flocculent material. The precipitate recovered in a 20-50% ammonium sulfate cut of the supernatant was collected by centrifugation at 12 400 x *g*. Protein derived from this procedure is referred to as a 'crude' enzyme preparation and was dissolved in and dialyzed (MWCO 6-8000 Da.) against 40 mM NaOAc, pH 5.0 (2 x 4 L, 16 h total).

Purification of C*x*-cellulase

To purify C*x*-cellulase to homogeneity, protein was extracted and precipitated by ammonium sulfate as detailed above. This 20-50% ammonium sulfate precipitate was then dissolved and dialyzed in 50 mM NaOAc, pH 6.2 (2 x 4 L, 16 h total) and passed through

a CM-Sephadex (Sigma) ion-exchange column (2.5 cm wide, 18 cm high, operated at 4ºC) equilibrated in the same buffer. C*x*-cellulase did not bind under these conditions but the procedure removed up to 60% of the added protein including all detectable polygalacturonase activity. The protein eluting from the CM-Sephadex column, including C*x*-cellulase, was dialyzed against 40 mM NaOAc, pH 5.0 (2 x 4 L, 24 h total), and applied to a bed (2.2 cm wide, 11 cm high) of phosphoric acid-swollen cellulose in the NaOAc buffer at 4ºC. The column packing was prepared from Avicel (wood-based crystalline cellulose, Sigma) using a procedure described by Wood (1971). The bound protein was released with 100 mM Tris, pH 8.0.

Final purification was accomplished using a column (1.5 cm wide, 10 cm high) of Concanavalin A-Sepharose (Sigma) operated at 4ºC in 50 mM NaOAc, pH 6.0, containing 500 mM NaCl, 1 mM $MnSO_4$ and 1 mM $Ca(OAc)_2$. Protein binding to this matrix (including C*x*-cellulase) was removed by elution with the same buffer containing 10 mM methyl mannopyranoside (Sigma). Fractions containing C*x*-cellulase activity were pooled and dialyzed against 40 mM NaOAc, pH 5.0.

The purity of the final extract was analyzed using SDS-PAGE. Sample aliquots (7 µg protein) and molecular weight standards (Bio-Rad, Richmond, CA) were applied to lanes of 7.5% polyacrylamide mini-gel which was then run at constant voltage (100 V) for approximately 1.5 h (Mini-Protean II equipment, Bio-Rad). Nondiamine silver (Merril, 1990) was used to stain the gel. Results confirmed the presence of one protein band at approximately 50 kDa. (Figure 4-1). The presence of C*x*-cellulase was confirmed in column fractions by viscometric assay against carboxymethylcellulose (CMC), according to the method outlined in Chapter 3.

Preparation of C*x*-cellulase-Depleted Enzyme Extract

Protein from RS4 avocado mesocarp was extracted in 100 mM NaOAc, pH 5.0 containing 1.2 M NaCl as detailed above. Following dialysis against 40 mM NaOAc, pH 5.0 (2 x 4 L, 16 h total), the extract was passed through an acid-swollen cellulose column

(conditions as detailed above). The non-retained protein was found to have no C*x*-cellulase activity over the standard assay time; long-term viscometric assays (24 h) did disclose some loss of CMC viscosity. Western blots of these protein extracts, using enzyme detection via polyclonal antibodies for C*x*-cellulase indicated that the extract was truly C*x*-cellulase depleted (Figure 4-2). Clearly, there are low levels of other enzymes with the ability to hydrolyze CMC--this has been noted previously with respect to the ability of protein extracts from unripe avocado fruit to exhibit low levels of CMCase activity (Chapter 3).

Activity of Enzyme Extracts Toward Native Hemicelluloses and Purified Xyloglucan

Samples of hemicellulose or XG (2 mg glucose equivalents) in 40 mM NaOAc, pH 5.0, containing 0.02% NaN_3, were incubated with 4 µg pure C*x*-cellulase, 20 µg cellulase-depleted extract or 80 µg crude enzyme (total volume of 2.42 ml) for 24 h at 37°C. Reactions were terminated by heating the samples in a boiling water bath. Enzyme-mediated M_r changes were assessed by Sephacryl S-300 chromatography. Column specifications and operating conditions were as described above for hemicellulose analysis. Fractions of 2 ml were collected and assayed for total sugars and XG.

Activity of Enzyme Extracts Toward Cell Wall Ghosts

Approximately 10 mg of CWG from RS1 were incubated with 20 µg purified C*x*-cellulase in 40 mM NaOAc, pH 5.0 containing 0.02% NaN_3 (total volume of 1.1 ml). Heated-denatured enzyme or buffer replaced the active enzyme in incubation controls. Incubations were for 72 h at 34°C. The reactions were terminated by heating in a boiling water bath and then centrifuged for 10 min at 16 000 x *g*. The aqueous supernatants were removed and were assayed for reducing sugars using the arsenomolybdate method (Nelson, 1944). The residual CWG following enzyme treatment was then extracted with 0.1 M NaOH containing 26 mM $NaBH_4$ (2 x 1 ml, 4 h each) to extract any weakly bound hemicelluloses, followed by a similar extraction procedure using stronger alkali (6 M NaOH). The 0.1 M NaOH extracts were assayed for total sugars (Dubois et al., 1956).

The presence of XG in this fraction was assessed visually using the iodine binding assay (Kooiman, 1960). The hemicelluloses solubilized by the 6 M NaOH were precipitated in 80% ethanol overnight at -20°C and centrifuged (3080 x *g*). The pellets were washed in ethanol, re-centrifuged and then suspended in water. The M_r distribution of these hemicelluloses were measured by elution behavior of the aqueous solutions through a Sephacryl S-300 gel permeation column. Fractions (2 ml) were assayed for total sugars and XG.

Results and Discussion

Molecular Weight Distribution of Avocado Hemicelluloses

Hemicelluloses of tomato (Huber, 1983a; Tong and Gross, 1988), strawberry (Huber, 1984) and muskmelon (McCollum et al., 1989) fruit fractionate on gel permeation columns into two M_r groups. During ripening there is a reduction in large-sized polymers and a proportional increase in those of lower M_r. Molecular weight distributions and changes similar to those of the above fruit types have been noted for hemicelluloses derived from senescing carnation petals (de Vetten and Huber, 1990, de Vetten et al., 1991). Hemicelluloses from mango also display two size populations of polymers as the fruit ripens, although there does appear to be some varietal differences in this behavior (Mitcham and McDonald, 1992). Redgwell et al. (1991) have reported three distinct M_r classes of hemicellulose from kiwifruit, with a proportional increase in the smaller polymers as the fruit ripens.

Hemicelluloses from avocado fruit at ripening stages representative of decreasing firmness were fractionated on Sephacryl S-300. The characteristic pattern of M_r changes in these 4 M alkali-soluble polysaccharides is unlike that observed for hemicelluloses from other fruit fractionated on similar gel permeation matrices. Avocado fruit exhibit a broad range of hemicellulose M_r sizes which undergo a collective shift to a lower average M_r during ripening (Figure 4-3). These ripening-related changes do not appear to be derived

from selective modification of specific hemicelluloses but appear to represent a general reduction in size across the range of polymer types present. Hemicelluloses from RS1 were polydisperse and included some components excluded from the gel (Figure 4-3A). The subsequent stages of fruit softening were depleted of the majority of these excluded polymers and there was a general shift to a lower average M_r. The M_r distributions of RS3 and RS4 hemicelluloses were similar (Figure 4-3B, C). While the firmness values of fruit at these three ripening stages are extremely different (from 497 N [RS1] to 12 N [RS4]), alterations in the hemicellulose M_r characteristics at corresponding stages seem to be relatively limited, especially when compared to the extent of modification found in the other fruits. On the basis of these data it does not appear that hemicellulose degradation contributes in a critical way to the softening of avocado mesocarp.

To determine the magnitude of the disparity in M_r between the polymers excluded from Sephacryl S-300 as compared to those polymers retained by the gel, 4 M alkali-soluble hemicelluloses (extracted from hydrated, buffered phenol-treated cell walls) were examined using Sepharose 4B-200, a permeation matrix with a higher M_r exclusion limit for dextrans than S-300. Hemicelluloses eluted as one polydisperse peak on the 4B-200 column, with a slight decrease in average M_r from approximately 54 kDa. in RS1 to 43 kDa. for RS4 (Figure 4-4). Approximate M_r values were calculated using the logarithmic relationship between the K_{av} and M_r of the standard dextrans. K_{av} is a partition coefficient based on the elution volume of each standard dextran in relation to the available volume of the gel media. While the average M_r decreased only slightly during fruit softening the polymer distribution sharpened markedly to a narrower M_r range (Figure 4-4B, C)

Tong and Gross (1988) did not observe dramatic M_r changes in 4 M NaOH-soluble polymers from tomato fruit but did demonstrate changes in polymers subsequently extracted in stronger alkali (8 M). Edelmann and Fry (1992) have recently found that a 6 M alkali extraction of cell walls, followed by water washing, released more XG than two

successive alkali treatments. This finding places the quantitative efficacy of a second 8 M NaOH extraction in doubt. A subsequent treatment of avocado cell walls from each RS with 8 M NaOH (following the normal 4 M extraction) solubilized an average 14.3% additional carbohydrate as measured by the phenol-sulfuric acid assay; however, the M_r distributions of the 8 M-extracted hemicelluloses were not consistent with a different class of hemicelluloses being solubilized by this treatment (data not shown). Inconsistencies of quantity and M_r distribution between duplicate extractions using the 8 M NaOH indicates that this stronger alkali does not solubilize a separate size class of hemicellulose but acts to supplement the original extract.

The limited changes in hemicellulose M_r during ripening raises the question of whether water-soluble hemicellulose-derived fragments were lost during cell wall preparation. This possibility was examined by extracting hemicelluloses from buffered phenol-treated ethanol-insoluble solids (EIS), which were prepared according to the procedure in Chapter 3. The EIS contain cell wall polymers with a degree of polymerization of ≥ 2. The M_r profiles of hemicelluloses, including XG, extracted from these preparations (Figure 4-5) were similar to those of cell wall-derived hemicelluloses (Figure 4-3), confirming that freely soluble, low M_r hemicelluloses are not generated during ripening, and highlighting the difference between the hemicelluloses of avocado and the other fruit studied.

Molecular Weight Distribution of Avocado Xyloglucan

The XG component of the avocado hemicellulose was identified by the iodine-binding assay of Kooiman (1960). The M_r of XG closely followed that of the total hemicelluloses whether this polymer was fractionated on Sephacryl S-300 or Sepharose 4B-200 (Figures 4-3 and 4-4, dashed lines). There was a loss in large M_r XG between RS1 and RS3, and a gradual decrease to lower average M_r at RS4. Talbott and Ray (1992) found substantial iodine binding with XG chains of ≤ 20 kDa. derived from pea epicotyl segments, confirming that the assay for XG is adequate for detecting low M_r

fragments if they are indeed present. Xyloglucan M_r changes have been observed for ripening tomato pericarp and locule tissues (Huber and Lee, 1986). In this fruit however, the XG component remained associated with the larger M_r polymers and did not closely follow the M_r distribution of total hemicelluloses.

Susceptibility of Avocado Hemicelluloses to Enzymic Hydrolysis

Evidence is accumulating to support the idea that cell wall synthesis and degradation occur simultaneously during plant senescence in general, and fruit ripening in particular. Tong and Gross (1988) found a changing glycosyl-linkage composition in the hemicellulose fraction of cell walls from ripening tomato fruit. Moreover, incorporation of radiolabelled sucrose into cell wall carbohydrates continued throughout tomato ripening (Mitcham et al., 1989, 1991; Greve and Labavitch, 1991). McCollum et al. (1989) demonstrated that proteins derived from ripe muskmelon fruit partially degraded native muskmelon hemicellulose, but the M_r changes *in vitro* were not as extensive as those observed *in situ*. M_r profiles of carnation petal hemicelluloses exposed to partially purified enzymes from senescing petal tissue were very similar to those of hemicelluloses derived from fully senescent petals (de Vetten et al., 1991).

We examined whether the changes observed in avocado hemicellulose M_r during fruit ripening, particularly the loss of large-sized polymers, were enzyme mediated. Hemicelluloses from unripe avocado fruit (RS1) were incubated with soluble protein extracts from ripe fruit (RS4). The change in M_r distribution following enzyme treatment (Figure 4-6A) involved a loss of the large-M_r polymers, an increase in polysaccharides in the range of 10.5 kDa. and also some loss of polymers in the mid-size range as compared to the control (Figure 4-6B). The enzyme-induced change in M_r of total hemicelluloses observed *in vitro* was unlike that observed during fruit ripening (Figure 4-3B, C), and could either be an indication of degradative effects that are masked by hemicellulose synthesis during ripening, or it may reflect the activity of various glycosidases and glycanases with cellular functions unrelated to hemicellulose metabolism.

The XG component of the hemicellulose samples also displayed a change in M_r distribution following incubation with the crude enzyme preparation (Figure 4-6A, B). There was a loss of large-sized polymers and the fractionated XG had an elution peak greater than 70 kDa. The size characteristics of XG after exposure to the crude enzyme preparation were similar to those found in avocado mesocarp at the soft, ripe stage (Figure 4-3C). While some of the hemicellulose components are clearly susceptible to enzyme degradation (e.g., XG), it is evident that other mechanisms, including polymer synthesis, are also involved in hemicellulose modifications during avocado ripening.

Effects of C*x*-cellulase on Xyloglucan Molecular Weight

Xyloglucan has been found to associate closely with cellulose microfibrils through hydrogen bonds (Bauer et al., 1973; Hayashi et al., 1987) while also associating with other matrix polysaccharides by covalent or non-covalent means (Bauer et al, 1973; Talbott and Ray, 1991). Several studies have linked the activity of a C*x*-cellulase-type enzyme to the hydrolysis of cell wall XG in expanding vegetative organs (Hayashi et al., 1984; Koyama et al., 1981). Hayashi et al. (1984) demonstrated that C*x*-cellulase (β-1,4-glucanase) purified from pea tissue could mediate the depolymerization of soluble or cellulose-complexed pea XG. In a study of avocado C*x*-cellulase, Hatfield and Nevins (1986) reported that the enzyme does share mechanistic similarities to the XG-hydrolyzing enzyme from pea expansion-zone tissue (Wong et al., 1977), preferring to attack β-1,4-glucosyl linkages while exhibiting no activity against β-1,3-linked glucans and only limited activity against both isolated avocado cell walls and soybean-derived XG (in terms of reducing sugar production). Hatfield and Nevins (1986) suggested that avocado C*x*-cellulase might function in the endohydrolysis of native avocado XG with a resultant decrease in XG M_r.

While the crude protein preparation from ripe avocado fruit has XGase activity (Figure 4-6) and C*x*-cellulase activity (CMC-hydrolyzing capability), only assays with purified C*x*-cellulase (Figure 4-1) and the hemicellulose substrate can test the hypothesis

that this enzyme can degrade XG directly. Hemicelluloses from RS1 avocado fruit were incubated with preparations of purified avocado C*x*-cellulase. Although the resulting profiles reveal enzyme-mediated hemicellulose changes, including a loss in mid-size polymers and an increase in the low M_r polymers (Figure 4-7A), there is no evidence of alterations in large M_r polymers, nor is XG affected compared to the control sample (Figure 4-7B). Incubation with C*x*-cellulase for periods of up to 72 h resulted in no change in XG elution behavior. The alteration in the M_r distribution of total hemicelluloses following exposure to purified C*x*-cellulase was also found with the crude protein (Figure 4-6A). A similar experiment using hemicelluloses from RS4 as substrate showed no effect on the XG profile, but did show some slight alteration in mid M_r-range polymers (Figure 4-8).

Table 4-1. Compositional analysis of iodine-precipitable XG from RS1 mesocarp and CWG from RS1 (CWG1) and RS4 (CWG4). Results are expressed as mole % and are the average of two separate derivatizations. Values in brackets indicate values as a % of the starting material.

	XG	CWG1	CWG4
Rhamnose	0.3	2.2 (0.3)	ND
Fucose	4.6	4.5 (0.6)	12.3 (1.2)
Arabinose	7.5	31.2 (3.7)	20.8 (1.8)
Xylose	23.8	28.0 (3.3)	44.6 (3.7)
Mannose	16.0	4.3 (0.6)	4.2 (0.4)
Galactose	14.3	17.4 (2.5)	5.9 (0.7)
Glucose	33.5	12.8 (1.7)	12.5 (1.4)

ND = not detected

Characterization of Xyloglucan Extract

A further experiment to clarify the reactivity of C*x*-cellulase against XG was conducted with a XG-enriched hemicellulose sample, prepared by precipitating XG as an iodine complex. In order to verify that this precipitable polymer was XG, the neutral sugar components were identified and quantified by gas chromatography. Sugars known to be involved with XG (glucose, xylose, galactose and fucose) constituted 76.5% of the sample; however, the overall neutral sugar composition (Table 4-1) did not appear to be significantly different from that of the original hemicelluloses from unripe fruit (Table 3-5, RS1), indicating that this preparation is not pure XG. Nonetheless, it does indicate that XG is the major component of 4 M alkali-extractable avocado hemicelluloses.

The M_r distribution of the precipitated XG on S-300 (Figure 4-9B) was different from that of the total hemicellulose (e.g., Figure 4-3A), eluting as a sharper peak at the exclusion limit of the column. The iodine precipitation step removed some of the polysaccharides of lower M_r and produced a more uniform XG sample. The M_r distribution of this XG-enriched isolate was unaffected by incubation with purified C*x*-cellulase (Figure 4-9A). This confirms results of earlier experiments, even though the XG used in this case contained other polymers.

The presence of other polysaccharides in the XG preparation does not necessarily indicate non-specific precipitation but may support the idea of glycosidic linkages between different hemicellulose types. There are substantial amounts of arabinose and mannose present in this XG-enriched isolate, and these, along with levels of galactose and glucose, which exceed the ratios normally found in XG, argues strongly for the presence of specific arabinogalactans and glucomannans. The alkali-soluble hemicelluloses from pea tissue partitioned into two size classes of distinctly different composition (i.e., XG and arabinogalactan; Talbott and Ray, 1992), unlike the M_r distribution of this isolate in which the component polymers co-eluted. These findings relating to avocado hemicelluloses and

XG do not sustain the contention of Talbott and Ray (1992) that inter-hemicellulose linkages via glycosidic bonds are not involved in cell wall cohesion.

Effects of C*x*-cellulase-Depleted Enzyme Extract

Although cellulase has been shown to hydrolyze soluble XG from expansion zones of pea epicotyls (Hayashi et al., 1984), the purified avocado enzyme is incapable of causing similar effects on native XG. However, XG does display a M_r downshift during avocado fruit softening and was hydrolyzed by enzyme components of a crude protein extract. Several hypotheses remain to be examined with respect to the absence of an effect of C*x*-cellulase on this polymer. The first is that C*x*-cellulase is involved in a XG-degrading complex and therefore would be ineffective in causing hydrolysis alone. This was tested by preparing a crude enzyme extract from ripe (RS4) avocado fruit from which C*x*-cellulase was removed by selective binding to acid-swollen cellulose (Figure 4-2). The cellulase-depleted enzyme preparation, when incubated with hemicelluloses from unripe fruit cell walls (RS1), caused some loss of large M_r material (Fig 4-10A) but very little alteration in the elution of polymers in the M_r range of 10.5-40 kDa. This is in contrast to that observed following hemicellulose incubation with crude or purified C*x*-cellulase (Figures 4-6 and 4-7). There was, however, a change in the elution characteristics of the XG after incubation with cellulase-depleted extracts as compared to the control (Figure 4-10B) indicating that cellulase, either alone or as a complex, cannot be involved in XG modifications.

Despite the lack of reactivity of C*x*-cellulase against XG--the hemicellulosic constituent with the most favorable structure (a β-1,4-linked glucan backbone, with a regular pattern of main-chain substitution)--there is some effect on other hemicellulose components. Evidence of this is the increase of polymers in the range of 10.5-40 kDa. in response to the presence of the purified enzyme (Figure 4-7A) and the absence of such a change with enzyme extracts not containing C*x*-cellulase (Figure 4-10A). Neutral sugar composition (Table 3-5) and linkage analysis data (Table 3-6) of hemicelluloses from

unripe (RS1) fruit indicate that glucomannan and some form of arabinogalactan could be present as well as XG. It may be that the change in molecular weight of the hemicellulose sample is due to hydrolysis of either the glycosidic linkages between these polymers and the XG, or an attack on internal linkages within the polymers themselves. In either case, it must be that the attacks are opportunistic, since similar modifications in the M_r profile were seen when the purified enzyme was incubated with RS4 hemicelluloses (Figure 4-8).

Effect of C*x*-cellulase on Cell Wall Ghosts

The second hypothesis regarding the state of reactivity of C*x*-cellulase toward XG concerns the physical condition of the XG. The activity of C*x*-cellulase has been tested against soluble substrates, whereas the polymer *in situ* is held in a fixed position via hydrogen bonds across the cellulose microfibrils. It may be that the random orientation assumed by the solvated polymer does not satisfy the catabolic requirements of the enzyme. Final experiments investigated whether the native (bound) arrangement of XG with cellulose could positively influence the recognition and binding of C*x*-cellulase. Hayashi et al. (1984) used CWG (cell walls selectively extracted to contain only XG and cellulose) to prove that pea C*x*-cellulase preferentially caused XG hydrolysis rather than attacking cellulose. The non-cellulosic neutral sugar characterization of CWG of unripe and ripe avocado fruit showed significant amounts of residual arabinose after 1 M NaOH and EDTA treatments in both ripening stages (Table 4-1). There was also a higher proportion of xylose than one would expect if this sugar were only involved with XG at both RS1 and RS4. Since the hydrogen bonds that result in microfibril cohesiveness are the same as those that result in the attachment of the glucan backbone of XG to the same microfibril, it is feasible that the trifluoroacetic acid hydrolysis of the primary XG layer could be hindered and therefore incomplete. This would result in the apparently high arabinose and xylose levels and very low glucose content of the noncellulosic portion of the CWG at both stages seen in Table 4-1.

The purpose of incubating CWG from RS1 with purified C*x*-cellulase was to investigate whether the *in situ* orientation of cellulose-complexed XG may satisfy specific conformational requirements for recognition and/or catalysis that are absent with solubilized XG, and may account for the lack of reactivity toward soluble XG. Aqueous suspensions of CWG from unripe avocado mesocarp contained higher levels of reducing sugars following a 72 h incubation with C*x*-cellulase than control samples (Table 4-2). However, total trifluoroacetic acid-hydrolyzable sugars amount to at least 12.7% of the CWG material (without accounting for the possible incomplete hydrolysis of the bound XG backbone). The action of C*x*-cellulase released approximately 0.16% (in glucose equivalents) after 72 h which, while more than the control, can be considered negligible. Total water-soluble material from a duplicate of both the treated and control samples was run through a Sephacryl S-300 gel permeation column to examine the M_r properties of any released carbohydrates. The resultant low carbohydrate levels in the M_r profiles (data not shown) confirmed that the amount of carbohydrate released by the cellulase was inconsequential and that it did not contain polymeric material.

Table 4-2. Water-soluble and 0.1 M NaOH-soluble carbohydrates produced during the incubation of CWG from RS1 with pure C*x*-cellulase. Results are expressed in $\mu g\ mg^{-1}$ CWG $\pm$ SE. Water-soluble material was assayed reductometrically (n = 3) and the alkali-soluble material was assayed using the phenol-sulfuric reagent assay (n = 4).

Incubation Treatment	Water-Soluble	0.1 M NaOH-Soluble
+ Active C*x*-cellulase	1.64 (0.23)	7.30 (1.74)
+ Denatured C*x*-cellulase	0.91 (0.18)	5.25 (0.71)

Extraction of the enzyme-treated CWG with weak alkali did not reveal any significant differences in the solubility and cohesion of polymers (Table 4-2). Therefore, the normal solubility and cohesive properties of hemicelluloses, particularly XG, were maintained even in the presence of active C*x*-cellulase. Confirming this were the iodine-binding assays which were negative for both the active treatment and denatured control samples.

Polymers soluble in 6 M NaOH were fractionated on Sephacryl S-300 and while the profiles of XG in both treatments and controls were similar (Figure 4-11A, B), the C*x*-cellulase promoted the extraction of some high M_r (non-XG) hemicelluloses from the CWG. Quantitative data were not gathered for this experiment since this would have led to compromising the amount of sample available for M_r studies. In total, it appears that even when the XG is presented in a structural form close to that found *in situ*, this polymer is not hydrolyzed by C*x*-cellulase. There is no evidence of the low M_r fragments (water-soluble) found by Hayashi et al. (1984), while dilute and concentrated alkali extracts of CWG did not show any structural modifications as a result of enzyme treatment. The increased alkali-solubility of high-M_r hemicelluloses, following C*x*-cellulase treatment of the CWG (Figure 4-11) indicates that the enzyme was able to effect a change in the intra- or inter-polymeric interaction of some hemicellulose components. At this point it is unknown whether C*x*-cellulase operates directly on some non-XG component of the hemicelluloses associated with cellulose, or acts on the microfibril--the modification causing a secondary effect on other associated polymers. As the enzyme prefers to hydrolyze β-1,4-glucosyl linkages, the second option is more likely.

Summary

The work reported here demonstrates that avocado C*x*-cellulase is unable to depolymerize solubilized XG, although the purified enzyme is capable of modifying other hemicelluloses as judged by the alteration in total hemicellulose M_r and the release of large

M_r hemicelluloses from CWG. The effects on total solubilized hemicelluloses are probably only of relevance *in vitro* since C*x*-cellulase exhibited hydrolytic activity toward similar polymers derived from ripe avocado fruit, suggesting that the polymers were persistent *in situ*. Alternatively, if the C*x*-cellulase is involved in the degradation of these polymers *in situ*, then continued synthesis may explain the apparent persistence of the affected polymers during fruit ripening and softening.

The cellulase-mediated XG depolymerization in vegetative expansion zones (Hayashi et al., 1984; Koyama et al., 1981) and the preference of avocado C*x*-cellulase for β-1,4-glucosyl linkages (Hatfield and Nevins, 1986) makes it difficult to reconcile the lack of reactivity between avocado-derived cellulase and avocado XG. The pea XG-degrading cellulase attacks XG at sites of unsubstituted glucose residues to produce nonasaccharide and heptasaccharide fragments in a fashion similar to that of fungal endoglucanases (Hayashi et al., 1984). There was no evidence for the production of oligosaccharides from avocado XG by the action of purified C*x*-cellulase.

Consideration has also been given to the possibility that C*x*-cellulase may be part of a XG-degrading complex, with only limited ability to hydrolyze XG prior to the action of other enzymes. There is XG-hydrolyzing capability within the avocado ripening-associated enzyme complement, as evidenced by the change in XG M_r following incubation with a crude enzyme preparation from ripe fruit. It is likely that the method to produce C*x*-cellulase-depleted protein extracts also removed other enzymes with the ability to bind to modified cellulose. Even so, this extract retained the ability to hydrolyze XG, producing an elution profile similar to that found in ripe fruit. Presumably, there is a specific XGase activated during avocado ripening, similar to the case of senescing carnation petals (de Vetten et al., 1992).

While the C*x*-cellulase does not have a direct effect on XG, it seems that the extractability of other polymers was affected by some action of the enzyme. It is suggested that avocado C*x*-cellulase has some degree of reactivity against cellulose, and

modifications in the microfibril structure (which may be brought about even by the simple action of binding) may cause a loss of cohesiveness among the various associated non-cellulosic polymers. While it is surprising that there may be a number of other hemicelluloses associated in some way with the cellulose, when traditionally it has been thought that only XG occupies this position, it is conceivable that disruption of the microfibrillar network could cause a change in the organization of other cell wall polymers.

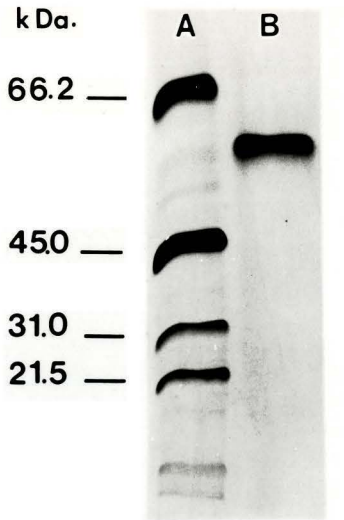

Figure 4-1. Silver-stained SDS-PAGE of purified Cx-cellulase isolated from ripe (RS4) avocado fruit. Lane A, molecular weight standards; Lane B, Cx-cellulase.

Figure 4-2. Western blot with anti-Cx-cellulase antibodies to detect the presence of Cx-cellulase. Lane A, Cx-cellulase-depleted extract (crude, soluble protein fraction unable to bind to acid-swollen cellulose); Lane B, Cx-cellulase enriched (fraction binding to acid-swollen cellulose).

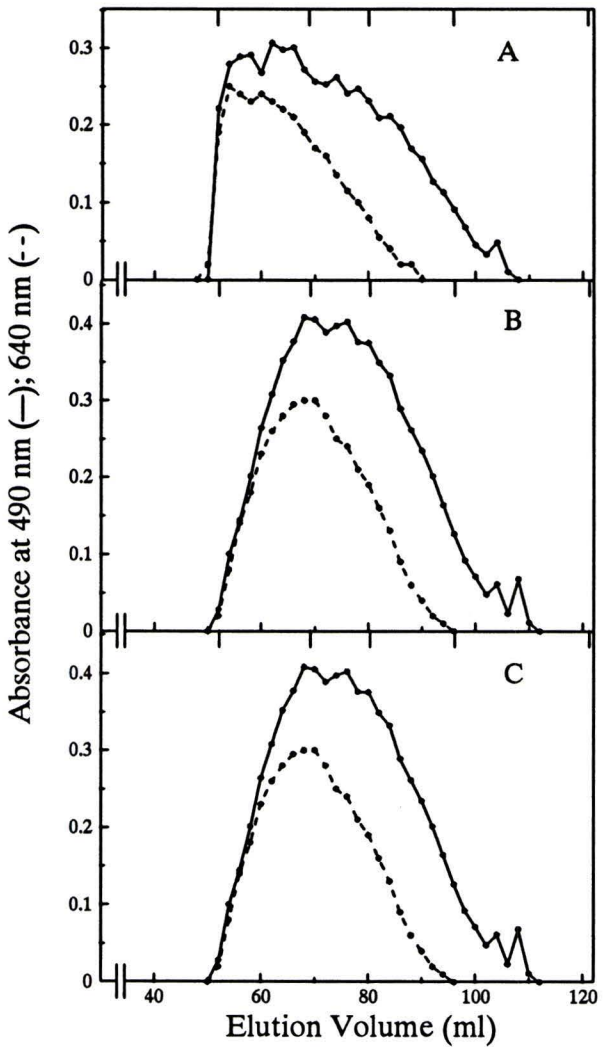

Figure 4-3. Sephacryl S-300 profiles of 4 M NaOH-soluble hemicelluloses from cell walls of RS1 (unripe, A), RS3 (climacteric peak, B) and RS4 (ripe, C) avocado fruit. Total carbohydrates abs. 490 nm (——); XG abs. 640 nm (----). Tick marks at the top of each profile indicate elution positions of standard dextrans: 5-40 x 10^3 kDa. (void volume), 70 kDa., 40 kDa., 10.5 kDa. and glucose.

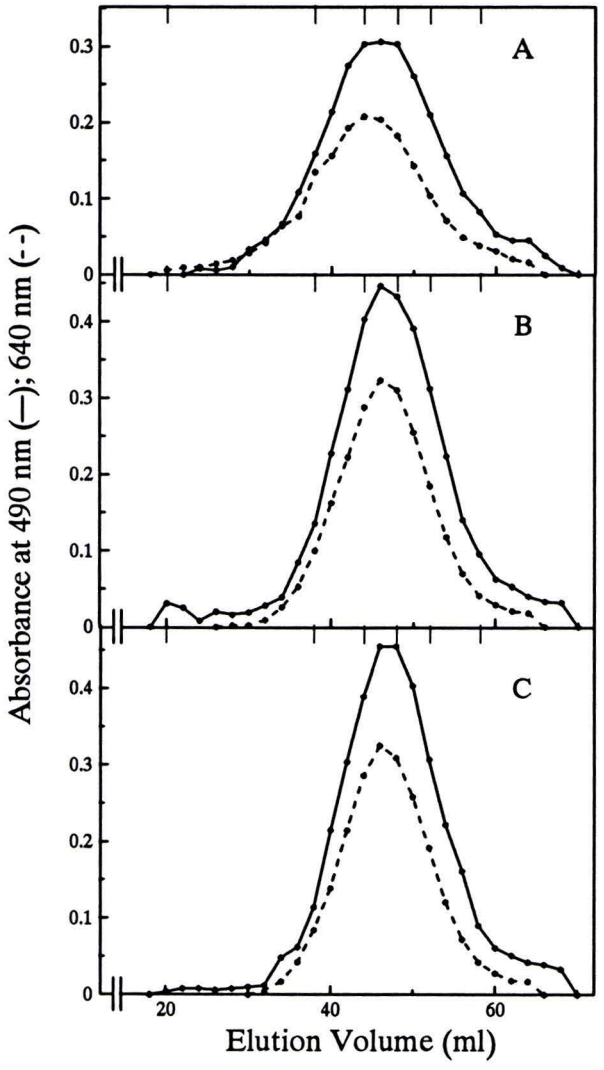

Figure 4-4. Sepharose 4B-200 profiles of 4 N NaOH-soluble hemicelluloses from RS1 (unripe, A), RS3 (climacteric peak, B) and RS4 (ripe, C) avocado fruit. Total carbohydrates abs. 490 nm (——); XG abs. 640 nm (----). Tick marks at the top of each profile indicate elution positions of standard dextrans: 5-40 x 10^3 kDa. (void volume), 500 kDa., 70 kDa., 40 kDa., 10.5 kDa. and glucose.

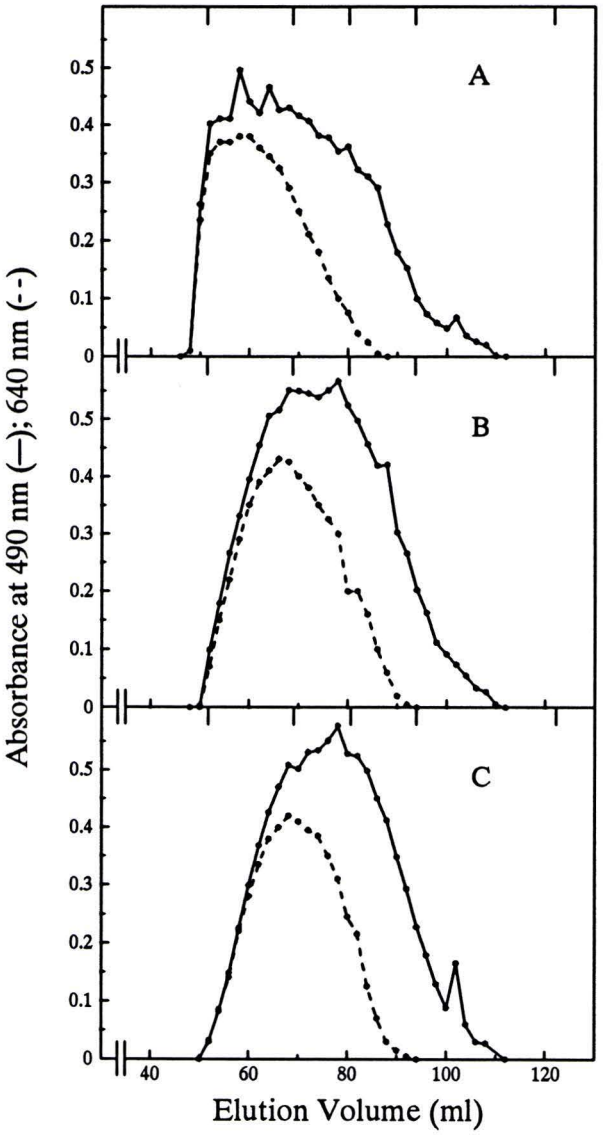

Figure 4-5. Sephacryl S-300 profiles of 4 N NaOH-soluble hemicelluloses extracted from EIS of RS1 (unripe, A), RS3 (climacteric peak, B) and RS4 (ripe, C) avocado fruit. Total carbohydrates abs. 490 nm (——); XG abs. 640 nm (----). Molecular weight markers are as for Figure 4-3.

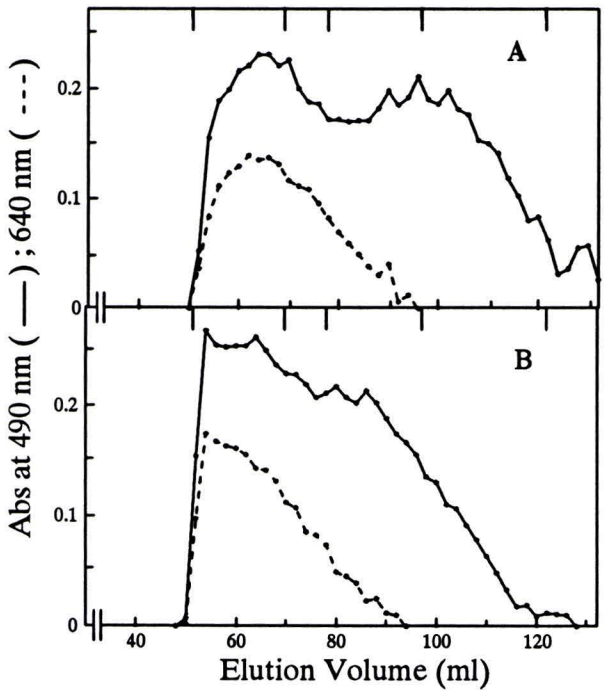

Figure 4-6. Molecular size distribution of RS1 hemicelluloses partitioned on Sephacryl S-300 following a 24-h incubation with active crude protein extract (A) or heat-denatured crude protein (B) from ripe fruit. Total carbohydrates abs. 490 nm (——); XG abs. 640 nm (----). Molecular weight markers are as for Figure 4-3.

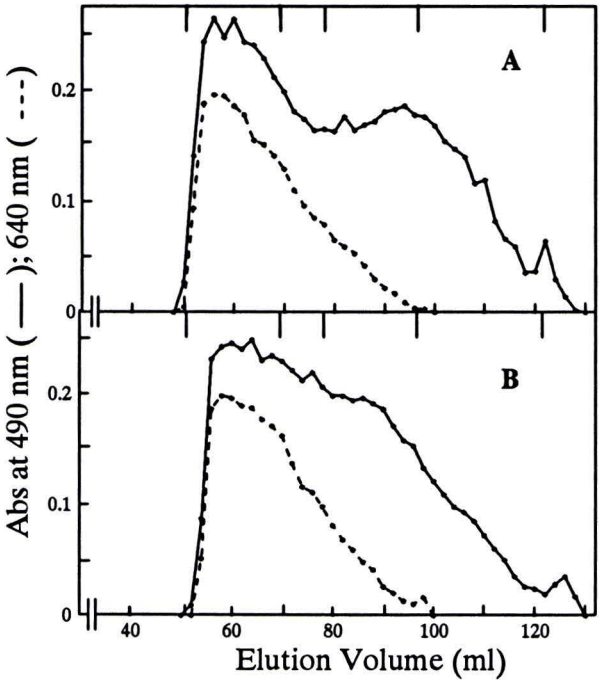

Figure 4-7. Molecular size distribution of RS1 hemicelluloses partitioned on Sephacryl S-300 following a 24-h incubation with active (A) or heat denatured (B) purified C*x*-cellulase . Total carbohydrates abs. 490 nm (——); XG abs. 640 nm (----). Molecular weight markers are as for Figure 4-3.

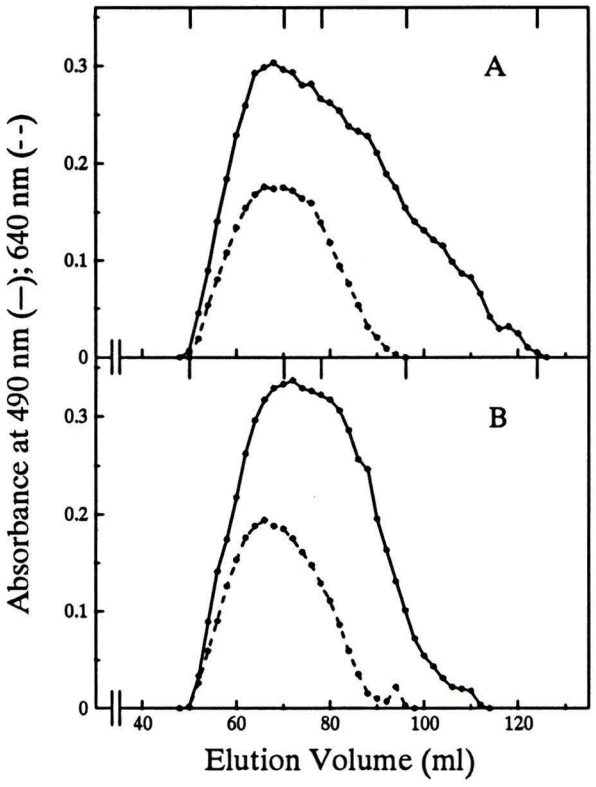

Figure 4-8. Molecular size distribution of RS4 hemicelluloses partitioned on Sephacryl S-300 following a 24-h incubation with active C*x*-cellulase (A) or heat denatured C*x*-cellulase (B). Total carbohydrates abs. 490 nm (——); XG abs. 640 nm (----). Molecular weight markers are as for Figure 4-3.

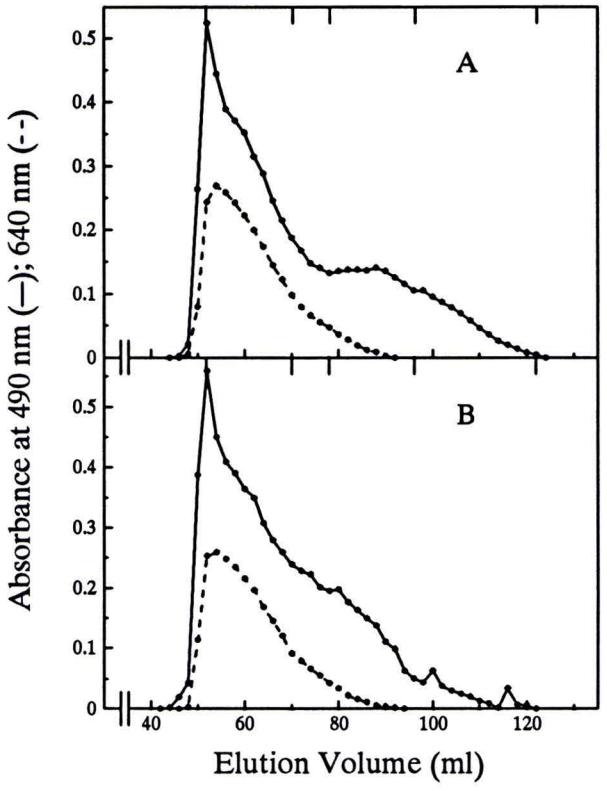

Figure 4-9. Molecular size distribution of XG-enriched hemicellulose partitioned on Sephacryl S-300 following a 24-h incubation with active C*x*-cellulase (A) or heat denatured C*x*-cellulase (B). Total carbohydrates abs. 490 nm (——); XG abs. 640 nm (----). Molecular weight markers are as for Figure 4-3.

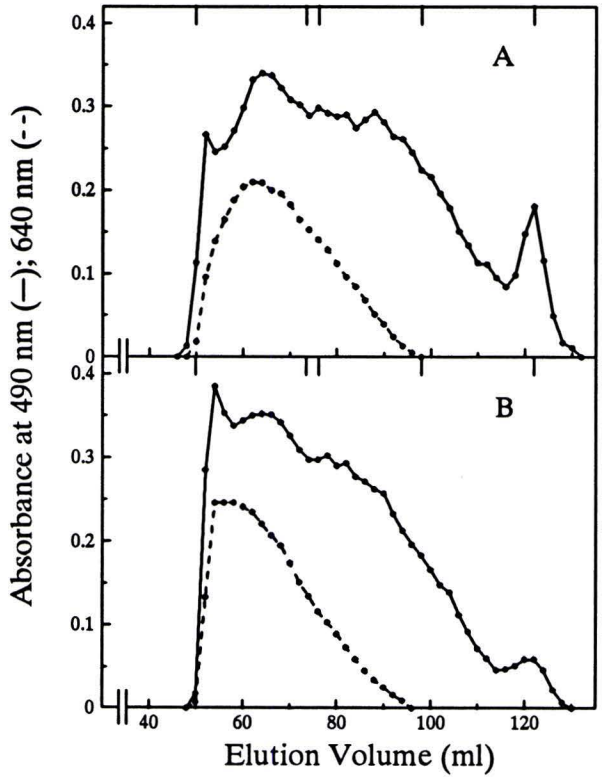

Figure 4-10. Molecular size distribution of RS1 hemicelluloses partitioned on Sephacryl S-300 following a 24-h incubation with active (A) or heat-denatured (B) cellulase-depleted enzyme extract. Total carbohydrates abs. 490 nm (——); XG abs. 640 nm (----). Molecular weight markers are as for Figure 4-3.

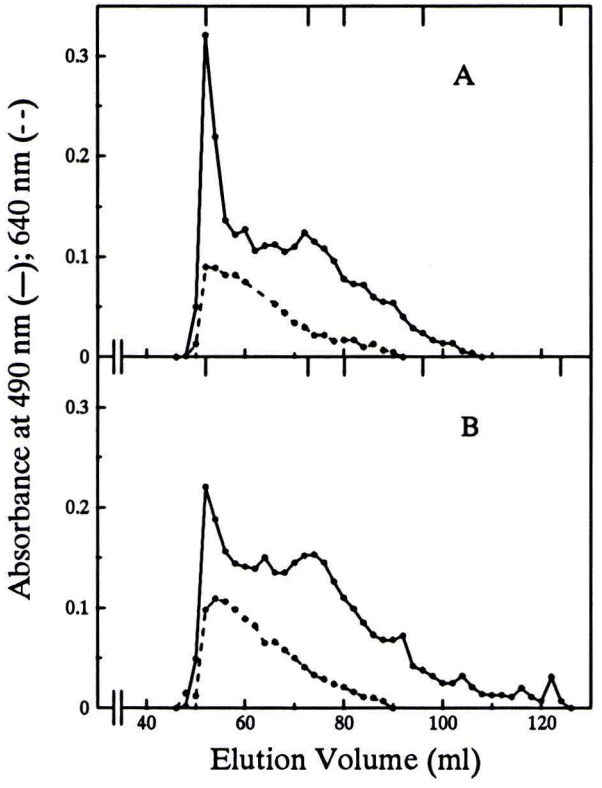

Figure 4-11. Molecular size distribution of hemicelluloses extracted from cell wall ghosts partitioned on Sephacryl S-300 following a 72 h incubation with active C*x*-cellulase (A) or heat denatured C*x*-cellulase (B). Total carbohydrates abs. 490 nm (——); XG abs. 640 nm (----). Molecular weight markers are as for Figure 4-3.

CHAPTER 5
INFLUENCE OF AVOCADO C*x*-CELLULASE ON THE STRUCTURAL FEATURES OF AVOCADO CELLULOSE

Introduction

Investigations of the effects of ripening on the fruit cell wall have focused on pectic and hemicellulosic polysaccharides and enzymatic proteins. For the most part, cellulose has been thought to be unaffected by cell wall degradative processes during fruit ripening. There are occasional reports noting a change in cellulose content during fruit ripening (Nightingale et al., 1930; Jermyn and Isherwood, 1956; Colinas-Leon and Young, 1981; Huber, 1985), but questions regarding how this may come about are usually tempered by the belief that plant systems, unlike fungi and bacteria, do not possess the enzymic capacity to achieve significant cellulose hydrolysis and that the structure of the cellulose chains renders them resistant to enzymic modification. Only the work by Huber (1985) considered that the changes in cellulose quantity in tomato gel during fruit ripening may be enzymic in nature.

Ultrastructural studies of fruit cell walls reveal a dramatic loss of middle lamella components (primarily pectins) during ripening, whereas the fibrillar cellulose appears to become swollen but the basic support structure remains intact (Pesis et al., 1978; Ben Aire et al., 1979; Platt Aloia et al., 1980). Undoubtedly, the loss of matrix material enables the changes in formerly embedded cellulose to become more visible but this does not preclude the possibility that there are alterations in the cellulose organization at the primary- or sub-microfibril level. The persisting limitation to investigations of cellulose structure has been the lack of appropriate techniques to measure such changes, given the insolubility of this

polymer in standard solvent systems and its susceptibility to solvation-related hydrolysis in harsher solvents.

The role of C*x*-cellulase in fruit ripening is an enigma, particularly in avocado fruit where the enzyme is synthesized in large quantities coincident with the onset of fruit softening. The genetic control and expression-related modification of the avocado C*x*-cellulase has been well studied (Christofferson et al., 1984; Tucker and Laties, 1984; Bennett and Christofferson, 1986), although without impact on the understanding of its physiological function in the cell wall. A genetically similar C*x*-cellulase has also been associated with abscission zones of bean tissue (Tucker and Milligan, 1991). As with fruit ripening, the enzyme in this case is believed to be involved with cell wall deterioration although, apart from immunolocalization studies, that place the enzyme in the cell wall during these critical developmental phases (Dallman et al., 1989; Sexton et al., 1981), there is no specific evidence of a particular substrate to which the enzyme may be directed.

A complication in the elucidation of the physiological role of C*x*-cellulase is that without the knowledge of the specific substrate, identification of the enzyme is reliant on assays employing synthetic substrates that likely do not reflect its function in the cell wall. C*x*-cellulase hydrolyzes β-1,4-glucans and appears to have some tolerance for substitutions on such a glucan backbone. The action of the enzyme is measured against a synthetic cellulose derivative, carboxymethylcellulose (CMC), which is a compromise at best and may lead to misinterpretation of the glycosidic functions of other intra- or extra-cellular enzymes.

Hatfield and Nevins (1986) suggested that the enzyme may hydrolyze the substituted glucan xyloglucan (XG); however, experiments described in Chapter 4 have shown that this is not the case in avocado and that the ripening-associated molecular weight (M_r) decrease of avocado XG appears to be mediated by a specific XGase. It was also shown, however, that the C*x*-cellulase could act on cell wall ghosts to increase the release of very large-sized hemicelluloses. It is unlikely that cellulase acts directly on the

linkages between hemicellulose and cellulose since these are primarily hydrogen bonds. It is possible that the enzyme could attack cellulose and cause a secondary effect of loosening the associated polymers. The aim of this work was to investigate the physical parameters of avocado cellulose such as M_r and crystallinity, with an emphasis on identifying any ripening-related changes. In addition, the physical effects of C*x*-cellulase activity on avocado cellulose were also studied in order to determine if the enzyme could modify the microfibril structure.

Materials and Methods

Plant Material

Cell wall material was prepared from avocado fruit at each ripening stage (RS) as defined in Chapter 3. Cell walls were prepared with buffered phenol (BP; Huber, 1991) to inactivate associated enzymes and were de-starched when necessary by incubation with porcine amylase for 16 h (details in Chapter 3).

Hydrated cell walls were prepared by homogenizing approximately 100 g of partially thawed avocado mesocarp from each RS in 400 ml of 40 mM N-2-hydroxyethylpiperazine-N'-2-ethane sulfonic acid (HEPES), pH 7.0 and then filtered through miracloth. The cell walls were then transferred to 200 ml of BP, stirred at room temperature for 30 min, then filtered through miracloth and washed with 2 L of cold deionized water. The sample was vigorously stirred in chloroform/methanol/water (2:1:1, v/v/v, mixed well prior to sample addition) for 30 min at room temperature. Following miracloth filtration, the sample was washed with 50% ethanol and cold deionized water. Excess water was gently squeezed out and the remaining hydrated cell walls were stored at -20°C. Prior to their use in electron microscopy, the hydrated cell walls were ground in liquid nitrogen. This allowed uniform cell wall suspensions to be mounted on the support grids.

Electron Microscopy

Fixation of avocado mesocarp for ultrastructural analysis. Mesocarp blocks approximately 1 mm^3 were cut from the mid-section (equatorial region) of avocado fruit at each of the four RS. The tissue was fixed with 4% formaldehyde and 1% glutaraldehyde in 0.1 M cacodylate buffer, pH 7.2 (Karnovskys' reagent) for 2 h, then washed with the cacodylate buffer (3 x 10 min washes). The fixed samples were dehydrated in an ethanol series (25%, 50%, 75%, 95%, each for 30 min) and then infiltrated with LR White (London Resin Co., Woking, England) at 25% and 50% resin concentrations in 95% ethanol for 2 h each, 75% resin for 16 h, and 100% resin for 2 x 4 h. The samples were embedded in 100% LR White and polymerized overnight at 60°C in 1.5 ml centrifuge tubes.

Thin sections (approximately 70 nm) of the fixed avocado mesocarp were mounted on 100-mesh, formvar-coated Ni grids and stained with uranyl acetate/lead citrate (Reynolds, 1963). Sections were viewed at 60 kV with a JEOL 100CX transmission electron microscope.

Platinum/carbon shadowing of cell wall samples. Hydrated cell wall suspensions were mounted on formvar-coated, 200-mesh Ni grids previously treated for 20 min with 0.01% poly-L-lysine to improve sample adhesion. Drops of the aqueous cell wall suspensions were rested on the grids for 30 min, then washed gently with water and air dried. Any sample manipulations, including enzyme treatments or immunolabelling (described below), were performed directly on the grids at this time. The grids were then subjected to unidirectional platinum-carbon (Pt/C) shadowing at a 15° angle in a Balzers MED 010 vacuum evaporator. Microfibrils and other cell wall materials were viewed at 60 kV with a JEOL 100CX transmission electron microscope.

Ultrastructural analyses

Cellulose localization. Cellulose microfibrils were localized in fixed mesocarp thin sections and cell wall preparations of RS1 and RS4 avocado mesocarp, following the

method of Berg et al. (1988). Briefly, the grids were blocked with 0.5% cold-water fish gelatin in incubation buffer (50 mM Na-citrate, pH 4.5 containing 1 mg ml^{-1} polyethylene glycol (PEG) and 0.02% NaN_3). The samples were exposed (20 min) to a mixture of cellulases from *Trichoderma reesei* (cellobiohydrolase I and II, and endoglucanase) conjugated to 15 nm gold. Controls were treated with the enzyme-gold conjugate diluted in incubation buffer containing 1 mg ml^{-1} CMC. At the termination of labelling, the samples were washed in blocking solution, followed by water. The mesocarp thin sections were then stained with uranyl acetate and lead citrate, while the cell wall samples were dried and shadowed as outlined above.

Immunolocalization of xyloglucan. XG was localized in cell wall samples using monoclonal antibodies (provided by Dr. M. Hahn of the Complex Carbohydrate Research Center, University of Georgia, Athens, GA) directed to the fucose moiety of the repeating heptasaccharide unit of the polymer. Grids with attached cell walls of each RS were blocked for 15 min with 1% cold-water fish gelatin in high-salt Tween buffer (HST; 20 mM Tris-HCl, pH 7.2, containing 500 mM NaCl and 0.01% Tween). The XG antibodies or standard mouse ascites fluid (Sigma Chemical Co., St Louis, MO) were diluted 1 in 100 with the gelatin/HST buffer and were used to label the grids for 1 h at room temperature. The grids were washed with HST and phosphate-buffered saline solution (PBS; 10 mM Na-phosphate pH 7.4, containing 150 mM NaCl) and then treated with goat anti-mouse gold conjugate diluted in PBS for 1 h at room temperature. After washes in PBS and water, the grids were air-dried and then shadowed with Pt/C.

Preparation of avocado C*x*-cellulase-gold complex. C*x*-cellulase (280 µg) was precipitated in acetone for 1 h at -80°C, redissolved in 100 µl of 4 mM NaOAc, pH 5.0 and then added quickly and with stirring to 5 ml of a 15 nm gold sol (prepared by a citrate reduction of AuCl and provided by Ms. D. Akin, J. Hillis Miller Health Center, University of Florida, Gainesville, FL). Bovine serum albumin (BSA) and PEG (5 mg each) were also added and the protein-gold complex was centrifuged at 25 400 x *g* for 1 h. The

protein-gold conjugate pellet was suspended in 50 mM NaOAc, pH 5.0 containing 1 mg ml^{-1} each of PEG and BSA and its stability was confirmed after overnight storage at 4°C. Aliquots of the complex were stored at -80°C.

Labelling of cell walls and Avicel with avocado C*x*-cellulase-gold complex. The binding location of the C*x*-cellulase-gold was examined using substrates of Avicel (wood cellulose) and hydrated cell wall preparations of RS1 and RS4 (shadowed) and thin sections of Avicel embedded in Spurrs resin (provided by Dr. G.W. Erdos, Electron Microscopy Core Laboratory, University of Florida, Gainesville, FL) for conventional transmission electron microscopy. Samples mounted on Ni grids were blocked with 5% cold-water fish gelatin in the gold suspension buffer. The labelling protocol followed that described above for cellulose labelling.

Procedures for immunolocalization of C*x*-cellulase using polyclonal antibodies

Polyclonal antibodies against C*x*-cellulase were obtained according to the procedure outlined in the Appendix. Several methods were examined in an effort to optimize specific conditions for localization of C*x*-cellulase. Cell wall samples mounted on Ni grids were blocked with 1% gelatin or BSA diluted in PBS or HST for 15 min. The grids were exposed to antibodies or preimmune serum (for controls) diluted in PBS buffer or 1% gelatin in HST for 1 h at room temperature or overnight at 4°C. After washing with PBS (3 x 10 min) the samples were incubated with either Protein A-gold or goat anti-rabbit-gold diluted with 1% gelatin in PBS or HST, or PBS alone for 1 h at room temperature. The grids were washed with PBS and water, then air-dried prior to shadowing with Pt/C. A number of samples including cell walls of each RS, and cell walls pretreated with C*x*-cellulase were used for immunolocalization purposes.

Ultrastructural analysis of avocado cell walls and Avicel treated with C*x*-cellulase

Hydrated cell walls from RS1 and RS4 avocado fruit (approximately 1 mg dry weight each), suspended in 600 µl of 40 mM NaOAc, pH 5.0, containing 0.02% NaN_3, were incubated with 40 µg of C*x*-cellulase for 12 h at 34°C and then stored at -30°C while

still in the hydrated state. Controls contained buffer in place of the active enzyme. Avicel (1 mg) was treated similarly. The cellulase-treated samples were mounted onto Ni grids in the usual way and shadowed.

In order to examine the effect of C*x*-cellulase on the cell wall organization of fresh avocado tissue, mesocarp tissue blocks (approximately 1 mm^3) were removed from the mid-section (equatorial region) of unripe fruit and were incubated at 34°C for 30 min with semipurified C*x*-cellulase. This enzyme was partially purified from a crude enzyme extract of RS4 mesocarp using CM-Sephadex ion exchange chromatography (Chapter 4). This procedure retained the C*x*-cellulase enzyme but resulted in much reduced polygalacturonase activity. The unripe avocado tissue blocks were treated with 10 000 viscosity units of C*x*-cellulase activity in 50 mM NaOAc, pH 5.0 (4 ml total volume). At the termination of incubation the tissue was fixed, embedded in LR White and thin sections prepared for transmission electron microscopy.

Molecular Weight Determination of Avocado Cell Walls and Avicel

The objectives of this experiment were to ascertain the M_r distribution of cellulose in the cell walls of ripening avocado mesocarp and to investigate the effects of C*x*-cellulase on the M_r of cellulose. The solvent most effective in cellulose solubilization (LiCl in dimethylacetamide [DMAC]; McCormick et al., 1985) is not specific for cellulose and is also able to solubilize all cell wall polysaccharides. Special care was taken during the solubilization and chromatography procedures to eliminate moisture in all reagents and equipment.

Preparation of cell walls and Avicel for solubilization. For M_r analysis of cell wall polysaccharides, destarched cell walls from each RS were ground to 40 mesh in a Wiley mill prior to solubilization. Cellulose from each RS was prepared by extracting pectin and hemicellulose from destarched cell walls using 6 M NaOH with 26 mM $NaBH_4$ (3 x 2 h). The samples were washed with water until the pH of the filtrate was neutral and then partially dehydrated by washing in 80% ethanol followed by 100% acetone. After air-

drying, the cellulose was ground to 40 mesh in a Wiley mill. The non-cellulosic neutral sugar composition of these samples was analyzed by alditol acetate derivatization and gas chromatography using the method described in Chapter 3.

Treatment of cell walls and Avicel with Cx-cellulase. To assess the effects of enzyme activity on the M_r distribution of cell wall polymers, samples (60 mg) of destarched cell walls from RS1 or Avicel were incubated with 200 µg of purified Cx-cellulase or 2.6 mg of crude enzyme protein extracted from ripe avocado mesocarp according to the protocol described in Chapter 4. The incubation buffer was 40 mM NaOAc, pH 5.0, 0.02% NaN_3 and the reaction volume in all cases was 11 ml. The incubation was for 24 h at 34°C, with occasional stirring. Controls contained heat-denatured crude enzyme. The suspensions were filtered through Whatman 934-AH filters and the filtrates tested for total sugars (Dubois et al., 1956). The residual material (cell walls or Avicel) was washed thoroughly with water followed by 80% ethanol and 100% acetone (30 ml in each case). All samples were then air dried, ground to 40 mesh using a Wiley mill and stored with desiccant.

General protocol for solubilization and molecular weight determination of cell walls. Approximately 45 mg samples of avocado cell walls, Avicel or Cx-cellulase-treated material were solubilized in DMAC containing 0.5% LiCl according to the procedure of Timpa (1991). Briefly, all dried, powdered samples were activated in DMAC at 150°C with stirring for 2 h, then cooled to 100°C prior to the addition of dry LiCl. The suspensions were stirred at 100°C for 2 h, then equilibrated at 50°C overnight followed by alternate heating at 100°C and shaking at room temperature. Total volume for each sample was 50 ml.

Approximately 3 ml of each solution containing cell walls or Avicel dissolved in 0.5% LiCl/DMAC were filtered through a 0.5 µm Teflon filter directly into Waters WISP autosampler vials using a vacuum-driven extraction apparatus. The HPLC system used for sample fractionation was equipped with four Ultrastyragel gel permeation columns

(10^3, 10^4, 10^5, and 10^6, Waters/Millipore, Milford, MS) connected in series and run in DMAC with 0.5% LiCl at a flow rate of 1 ml min^{-1}. The columns and solvent system were operated at 80°C. A dual viscometric- and refractive index-detection system with Unical software (Viscotek Corp., Porter, TX) enabled the calculation of viscosity and concentration at each retention volume leading to the production of M_r profiles for each sample. The gel permeation system was calibrated using universal calibration with polystyrene standards of 2890, 1260, 710, 355, 190, 102, 43.9, 19.6, 10.3 and 6.2 kDa. (Toyo Soda, Tokyo, Japan).

X-ray Diffraction Analysis

The crystallinity of cellulose in samples of avocado cell walls at each RS, microcrystalline Avicel and cell walls from unripe avocado fruit treated with C*x*-cellulase, was calculated from x-ray diffraction signals. Cell wall matrix polysaccharides do not possess crystalline characteristics, but contaminating starch was removed from the samples as a precautionary measure.

Preparation of cell walls and Avicel for x-ray diffraction. Destarched cell walls from each RS were ground to 40 mesh in a Wiley mill prior to solubilization. To assess the effects of enzyme activity, destarched RS1 cell walls or Avicel were incubated with 400 µg of purified C*x*-cellulase in 40 mM NaOAc, pH 5.0 with 0.02% NaN_3. Buffer replaced the enzyme in controls. The total reaction volume was 20 ml, with incubation for 24 h at room temperature. Following incubation, the samples were filtered on GF/C paper (Whatman) and washed with 10 ml of water. This filtrate was retained and tested for the presence of carbohydrate (Dubois et al, 1956). The remaining material was washed with 80% ethanol and 100% acetone (400 ml of each solvent), air dried, and milled to 40 mesh.

In another experiment, cell walls from unripe fruit (120 mg) were incubated with approximately 1 mg of either crude, cellulase-depleted, or cellulose-binding enzyme preparations isolated from ripe avocado mesocarp. These enzyme extracts were prepared as detailed in Chapter 4. Cellulose-binding enzymes are classified as buffer-soluble

proteins from ripe fruit that bind to acid-swollen cellulose and are released by 100 mM Tris buffer, pH 8.0. Active enzyme was replaced with heat-denatured crude enzyme extract in control samples. All other experimental conditions were as described for incubation with the pure enzyme.

X-ray diffraction. All powdered samples were formed into discs approximately 13 mm in diameter and 1 mm thick using a sample press set to 7000 psi . Diffraction signals were collected at 3^{o} min^{-1} between the angles of 5^{o} and 45^{o} in a Phillips APD 3720 diffractometer equipped with a Cu x-ray source with emission at 0.154 nm. Crystallinity indices were calculated by calculating the difference in the heights of the crystalline and amorphous peaks (in mm) and expressing it as a percentage of the crystalline peak height (Segal et al., 1959). Signal peak height, width at half height, and area were also recorded from diffractograms. Values were averaged from the analysis of two separate samples.

Results and Discussion

Ultrastructural Analysis of Avocado Mesocarp

Effects of ripening on cell wall and microfibril organization

Ultrastructural analysis of thin sections from RS1 and RS4 mesocarp (Figure 5-1) reveal a loss of middle lamella material from the cell wall during avocado fruit ripening. Similar changes in avocado fruit have been noted by Pesis et al. (1978) and Platt Aloia et al. (1980) and the loss of density in the middle lamella correlates well with the demonstrated decrease in fruit firmness and the increasing solubility of cell wall pectins during avocado ripening (Chapter 3). Cellulose has traditionally been associated with the primary cell wall, yet cellulase-gold conjugates localized this polymer throughout the cell wall and in wall junction areas of unripe avocado fruit (Figure 5-2A). Controls (not shown) contained minimal label. The middle lamella was originally thought to be composed solely of pectic material but Moore and Staehelin (1988) also localized XG in this region.

During avocado ripening, there is a reduction in cellulose labelling in the middle lamella although there is still strong labelling in the primary wall regions (Figure 5-2B). The overall decrease in cellulose labelling appears to be much more marked than the 19% decrease between RS1 and RS4 based on quantitative assessment of cellulose content (Chapter 3). It is possible that with the ripening-induced solubility changes of middle lamella pectins, the microfibrils are no longer anchored and are either washed away during sample preparation or redistributed to the outer edges of the primary cell wall. Also possible is that the loss of binding density reflects a disruption in the microfibrils themselves. While there is no precedence for this in the literature, the change in hemicellulose solubility from cell wall ghosts following the action of C*x*-cellulase (Chapter 4) supports the idea.

Platinum/carbon shadowing of isolated cell walls reveals details not observed with thin sections and is particularly effective in resolving cellulose microfibrils (Figure 5-3). The avocado cell wall matrix material usually appeared as large clumps, similar to those observed in onion cell walls (McCann et al., 1990). The cell walls used in this study were prepared under aqueous conditions to prevent excessive polymer aggregation before mounting on the grids. In Pt/C shadowed cell walls of unripe, preclimacteric fruit, the dominant feature is conglomerated matrix material (Figure 5-3A and B). At RS3, and more so at RS4 (Figure 5-3C and D), the microfibrils are found free of extraneous cell wall material and also show signs of being untwisted from a more secondary organization. Localization with fungal cellulase-linked gold revealed that the matrix material of RS1 contained embedded cellulose, and that any free microfibrils were rather short and thick (Figure 5-4A and B). In ripe avocado fruit (RS4, Figure 5-4C and D), the microfibrils were found to be long and filamentous, with only occasional associations with massed cell wall matrix. The controls treated with the enzyme-gold pre-adsorbed with CMC (Figure 5-4B, D) showed considerable background distortion after shadowing. This is thought to be due to CMC adhering to the formvar coating on the grids and may explain why, in

some cases, there was background gold labelling, particularly where gold particles have clumped together (Figure 5-4D).

Xyloglucan has been demonstrated to be linked to cellulose microfibrils via hydrogen bonds (Bauer et al., 1973; Hayashi and Maclachlan, 1984; Hayashi et al., 1987). In tomato fruit there is degradation of the XG as evidenced by a broadening M_r distribution and a reduction in the average M_r (Huber and Lee, 1986). In avocado fruit there is a more moderate ripening-associated change in XG polymer length that is apparent in fruit at the climacteric peak (RS3, Chapter 4). It was of interest to investigate whether this enzyme-induced hydrolysis reduced the binding of XG to cellulose microfibrils, since the XG is believed to prevent the fasciation of cellulose and to allow the microfibrils to slide past one another during expansion growth (Hayashi et al., 1987; Hayashi, 1989). The XG was labelled using monoclonal antibodies directed to the fucose moiety on the side branches of the glucan backbone. Figure 5-5 shows that XG is found in and around cell wall matrix material in unripe fruit and continues to be associated with microfibrils even in fruit at the soft, ripe stage. There was no labelling in the controls (not shown). The pattern of XG localization closely followed that of cellulose, particularly at RS3 and RS4.

Immunolocalization of C*x*-cellulase in isolated avocado cell walls

Dallman et al. (1989) immunolocalized C*x*-cellulase in thin sections of avocado mesocarp tissue and detected it throughout the cell wall in ripe fruit. Similarly, Cu precipitation demonstrated that cellulase of tobacco flower abscission zones was associated with fibrillar components of the middle lamella (Lieberman et al., 1982). While XG binding to cellulose is persistent throughout ripening (Figure 5-5), the C*x*-cellulase of avocado fruit does not attack this polymer (Chapter 4), nor does it cause hydrolysis of middle lamella pectins (data not shown). There is a strong possibility that the C*x*-cellulase is binding to cellulose since the cellulose is fibrillar in nature and is also found throughout the cell wall of ripening avocado fruit.

To investigate whether C*x*-cellulase does bind to cellulose microfibrils, immunocytochemical localization was attempted on whole cell walls of ripening fruit using purified polyclonal antibodies directed to the protein portion of the enzyme, followed by Pt/C shadowing. Unfortunately, immunolocalization of the enzyme was not successful, despite varying the assay conditions including buffers, gold label and blocking proteins. While there was often good gold labelling in the samples treated with antibodies, in some cases around cellulose microfibrils, there was always non-structural binding and high background labelling with the control samples of preimmune serum. A number of factors could have contributed to this, including enzyme denaturation, removal of enzyme during sample preparation, and non-specific gold labelling. The cell walls used for microscopy were hydrated but treated with BP, which inactivates cell wall enzymes (Huber, 1991). There are no complete details on the nature of this deactivation although it is likely to involve denaturation--with consequences on the structure and orientation of the enzyme. Both factors are an integral part of the recognition between antibody and antigen, and distortions at this level may account for the lack of antibody binding; however, aqueous cell wall preparations and whole tissue homogenates (not treated with BP) did not show significant labelling over the controls. Therefore, phenol-induced denaturation may not explain the lack success in the localization studies.

The binding constant of C*x*-cellulase to specific cell wall polysaccharides is unknown. The enzyme can be extracted from avocado tissue using NaCl concentrations in the range of 0.4 M (Awad and Lewis, 1980) although most extractions are typically performed with higher salt concentrations. The initial blocking treatments of sections prior to immunolocalization utilize buffers such as PBS and HST, both with reasonably high NaCl concentrations (150 mM and 500 mM, respectively). It is possible that the enzyme is tenuously bound to the cell wall and the buffer-salt concentrations were sufficient to cause enzyme release and subsequent removal during grid washing.

Non-specific gold labelling was also a problem due to the electrostatic attraction of the gold to the grid material and to the formvar coating. Such problems are not usually encountered with normal immunolocalization on thin sections since the gold is not attracted to resin to the extent that it is on exposed formvar. Gold conjugated to goat anti-rabbit IgG gave a reduced background compared to Protein A-gold. The problem was also slightly alleviated by blocking non-protein sites on the grids with 5% protein rather than the standard 1%. Cold water-fish gelatin acted as a better block than BSA. The most effective step to circumvent the non-specific binding was pre-adsorbing the protein-gold conjugate in 1% gelatin in the dilution buffer. Presumably the gelatin is better able to disperse and neutralize the charge effects of the gold in suspension than when it is present as a protective layer on a coated grid.

The preimmune controls also seemed to be prone to strong background labelling, even though there was no such effects in the ELISA assays (Appendix) or Western blots (Chapter 4). This problem persisted even after the preimmune serum was pre-adsorbed with protein from unripe avocado fruit (similar to the affinity purification technique used for the antibodies). There was often more label on control samples than on antibody-treated cell walls.

The lack of strong C*x*-cellulase-antibody binding was also apparent in assays where the antibody was used in attempts to inhibit the viscometric activity of the enzyme. These experiments were carried out under normal viscometric assay conditions (Chapter 4) and the enzyme was normally pre-adsorbed with the antibody overnight at 1°C. No antibody-induced inhibitory effects were seen on the viscometric activity of the enzyme and similar results were found if activity was assayed using reductometric methods to detect the production of reducing sugars. In both experiments, the enzyme and antibody concentrations were varied to check for prosome effects. Inhibition of activity is not necessarily an indicator of an enzyme-antibody interaction, since the antibodies may be directed to areas on the enzyme other than the active site. Nonetheless, one could expect

there to be some reduction in the rate of enzyme activity as a consequence of a large protein such as IgG (approximately 150 kDa.) attaching anywhere on a smaller protein. Many enzymes have carbohydrate chains associated with some part of the active or binding site and C*x*-cellulase has been shown to possess carbohydrate chains rich in mannose and glucose (Bennett and Christofferson, 1986) although it has not been demonstrated where these are located in relation to the active site. A significant number of antibodies in the C*x*-cellulase polyclonal preparation were found to be directed to the carbohydrate of this and other cell wall enzymes (see Appendix) and were removed to enhance the antiserum specificity. It was thought that if there was some involvement of the carbohydrate at the active site of Cx-cellulase the inclusion of carbohydrate-directed antibodies would cause enzyme inactivation. This did not prove to be the case. In all experiments, the preimmune serum did not show affinity for the enzyme, nor produce any anti-viscometric effects in C*x*-cellulase/CMC assays.

While there were problems with the antibody binding in direct enzyme assays and in immunolocalization experiments, there was always high reactivity of the antibody towards the protein immobilized on nitrocellulose paper in dot blots with non-denatured protein or in Western blots. The procedure for immunolocalization was also successful for identifying XG. It is believed that the polyclonal antibodies used here for C*x*-cellulase were low-affinity antibodies, and that binding effects could have been improved by repeated injections of the antigen over a number of weeks during antibody production in the rabbit. Alternatively, monoclonal antibodies can be selected for certain properties such as active site interference. Either of these techniques may have enhanced the immunocytochemical localization of C*x*-cellulase. While the inability to localize C*x*-cellulase in the cell walls of ripening avocado fruit using whole cell walls and shadowing could indicate that the enzyme does not remain wall bound, it appears more likely that limiting factors are inherent to the antibody preparation.

Labelling of cell walls with avocado C*x*-cellulase-gold conjugates

As an alternative to localizing C*x*-cellulase in cell walls of ripening avocado fruit (discussed above), the purified enzyme was directly conjugated to 15 nm gold particles and incubated on grids containing hydrated cell walls of RS1 and RS4 or Avicel. This approach attempted to identify the site of enzyme binding, while circumventing the use of low affinity antibody probes. The direct labelling technique, however, was ineffective in identifying the site of C*x*-cellulase binding, possibly due to insufficient gold associated with the C*x*-cellulase during the conjugate preparation. It has also been noted that some enzyme-gold conjugates are more effective if the enzyme is heat-denatured prior to conjugation (Vian et al., 1991). The linkage of protein to gold does not necessarily inhibit enzyme activity and the substrate and label may wash away.

Treatment of cell walls with C*x*-cellulase

To investigate whether the C*x*-cellulase could cause a structural change in the microfibrils evident by Pt/C shadowing, cell walls of RS1 and RS4 avocado fruit were incubated with purified C*x*-cellulase or buffer for 12 h. Similar experiments were performed with Avicel. The samples were mounted onto grids and shadowed as usual. Microfibrils were not distinct in RS1 control samples and the few free microfibrils were short and thick (Figure 5-6B). In contrast, microfibrils in walls treated with cellulase appeared to be unravelled and frayed (Figure 5-6A), similar to microfibrils seen at RS3 (Figure 5-3C). In RS4 cell walls and Avicel, treatment with C*x*-cellulase caused a further unravelling of already-free cellulose microfibrils (Figure 5-7; Figure 5-8). Disintegration was not evident but the microfibrils seem to be extremely striated in a manner suggesting a reduction to a sub-formation of the micro fibril. This effect has not been reported for C*x*-cellulases of plant origin, but does seem to be consistent with the general action of C*x*-cellulases in fungal cellulase complexes. Sprey and Bochem (1991) found that purified endoglucanase from *Trichoderma reesei* could cause untwisting of microfibrils of *Sinapis alba* seed-slime cellulose. The endoglucanase of *Cellulomonas fimi* has binding and catalytic domains

that seem able to cause two distinct effects, the overall activity being to burrow into the microfibril and disrupt the tightly organized structure with some capability to hydrolyze ('polish') the frayed edges caused by the penetration (Din et al., 1991). The endoglucanases from *T. reesei*, *C. fimi* and avocado belong to different subclasses based on hydrophobic cluster analysis of the catalytic domain (Beguin, 1991). Despite this difference in grouping, they all appear to possess the capability to modify the cellulose microfibril. Obviously the fungal glucanases have enhanced activity when joined by the other members of the cellulase complex, whereas in avocado only one enzyme is involved. This may explain why the fruit synthesize such high levels of the C*x*-cellulase.

A close analysis of the organization of the cell wall of mesocarp from unripe avocado following incubation of mesocarp blocks with a semipure C*x*-cellulase (polygalacturonase-free) preparation revealed a change in density across the cell wall in comparison to buffer controls (Figure 5-9) which, in light of the effects on microfibrils seen in Figure 5-6, could be due to a loss of cohesion in the cell wall caused by disruption of the cellulose framework. Incubation of thin sections of fixed unripe mesocarp with purified C*x*-cellulase also indicate that some portions of the cell wall are affected by the enzyme (not shown), leaving the regular, consistent density of the control unripe cell wall quite variable in some areas.

Molecular Weight Analysis

Solubilization of cellulose

The investigation of molecular weight of avocado cellulose was carried out in the USDA laboratory of Dr. J.D. Timpa, in New Orleans, LA. While it has been shown in Chapter 3 and 4 that pectins and hemicelluloses undergo changes in M_r to varying extents, a similar approach to studying of cellulose is complicated by difficulties in extracting this polymer and identifying an appropriate solvent and separation system to measure the M_r accurately.

The stability of cellulose is due in large part to the cooperative reinforcement of hydrogen bonding along the length of the polymer. While this is advantageous in a structural sense, solubilization of cellulose for analytical studies is more difficult than for other cell wall polymers. Various procedures have been attempted using various solvents, including cadoxen (a mixture of cadmium acetate and ethylenediamine; Brett, 1981) and dimethylsulphoxide with paraformaldehyde (Johnson et al, 1976). Derivatization methods such as nitration increase the solubility of the cellulose and have also been utilized (Blaschek et al., 1982). There are serious limitations with these techniques, however. Solvents that are effective in dispersing and solubilizing cellulose often cause inadvertent hydrolysis, resulting in questionable absolute M_r data. Derivatization/precipitation is reliant on the efficiency of the substitution reactions, although the technique is usually very specific and the cellulose remains undegraded. The method used here for cellulose solubilization and gel permeation chromatography employs a solvent of LiCl in DMAC (McCormick et al., 1985) in which the Li^+ is believed to complex with the DMAC and the Cl^- associates with the cellulose through a hydrogen bond (Dawsey and McCormick, 1990). This interaction has been shown to effectively solubilize cellulose from a variety of sources without solvent-induced hydrolysis.(McCormick et al., 1985; Timpa, 1991).

Both the residual cellulose remaining after pectin and hemicellulose removal and whole cell walls were used in the analysis of cellulose M_r during avocado fruit ripening. While removing the pectin and hemicellulose from the cell walls results in a sample highly enriched in cellulose, the strong alkali used in the procedure is likely to alter the structure of the remaining cellulose. Treating cotton with strong alkali (mercerization) modifies the crystallinity properties and changes the cellulose chain orientation from parallel to antiparallel (Warwicker et al., 1966; French, 1985). While the cellulose is not dissolved by this process, some polymer cleavage likely occurs. To circumvent this problem, total cell walls as well as enriched cellulose samples were tested at each RS.

Molecular weight distribution of avocado cell wall polysaccharides

Figure 5-10 shows the M_r characteristics of total cell wall polysaccharides during ripening. The M_r distribution represents the population distribution of the proportion of species present at each M_r, with the same concentration of cell wall applied to the HPLC column each time. The LiCl/DMAC solvent can solubilize all cell wall components, therefore each profile presumably contains pectins, hemicelluloses and cellulose. In all cases, there are two distinct peaks which tend to become sharper and narrower as ripening progresses. The first peak (low M_r polymers) exhibits a M_r downshift during ripening. RS1 and 2 are similar, while at RS3 the peak height is reduced as well as the average M_r. At RS4, while the average M_r of the first peak has not changed, the shape has sharpened. On the basis of the elution profiles in Chapters 3 and 4, this low M_r peak probably contains hemicelluloses and pectins.

The second peak, of much higher average M_r, probably contains pectin and cellulose. The shape and position of this second peak is similar for RS1 to RS3, but there is a proportional loss of material at the leading edge and an increase in average M_r at RS4. Cell wall components of very high M_r appear unaffected during avocado fruit ripening, while there is increasing solubility of some polymers (pectins) and reduction in M_r of both pectin and hemicelluloses (Chapters 3 and 4).

Characterization of cellulose isolated from avocado cell walls

Compositional analysis of the cellulose-enriched samples (Table 5-1) revealed that there were considerable amounts of non-cellulosic sugars present despite the extensive alkali extraction procedure employed to remove pectins and hemicellulose. The procedures used to produce the cellulose sample were similar to those suggested by Edelmann and Fry (1992) for full xyloglucan removal. The neutral-sugar data illustrate that other polymers remain tenaciously associated with the cellulose. The total percentage of cellulose in the cellulose-enriched samples ranged from 78.6% at RS1 to 85.4% at RS4 (w/w). Arabinose, glucose and galactose were the main non-cellulosic sugars present at

RS1 and while glucose levels increased slightly, galactose declined sharply during avocado fruit ripening. Arabinose increased at RS2 and RS3 but decreased at RS4. It is possible the arabinose and galactose participate in an arabinogalactan that is strongly associated with cellulose by interactions other than hydrogen bonds (which would be disrupted by strong alkali). Trifluoroacetic acid hydrolyzes non-crystalline polymers, but it is possible the glucose in the neutral sugar fractionation (Table 5-1) could be derived from amorphous regions of the cellulose if the acid penetrated this less tightly bound layer on the microfibril periphery.

Table 5-1. Non-cellulosic neutral sugars of cellulose-enriched cell wall samples from each RS. Results are expressed as mole %. Values in brackets indicate values as a % of the starting material.

	RS1	RS2	RS3	RS4
Rhamnose	7.2 (2.4)	8.1 (2.0)	5.9 (1.9)	0.6 (0.1)
Fucose	ND	ND	ND	ND
Arabinose	38.0 (11.0)	40.1(9.4)	43.3 (12.2)	29.7 (3.9)
Xylose	7.0 (4.1)	4.8 (1.1)	9.3 (2.7)	11.1 (1.5)
Mannose	0.4 (0.1)	0.1 (0.1)	3.2 (1.2)	0.8 (0.2)
Galactose	26.1 (8.7)	23.8 (6.5)	10.8 (3.7)	1.7 (0.3)
Glucose	21.4 (7.1)	23.2 (6.5)	27.6 (9.2)	26.2 (8.8)

ND = not detected

Molecular weight distribution of cellulose-enriched cell wall polymers

The M_r distribution of cellulose-enriched samples from each RS is illustrated in Figure 5-11. A notable feature of these profiles is that the average M_r in all cases is lower than at each corresponding stage for the total cell wall samples (Figure 5-10). This is likely due to disruptive effects of the 6 N NaOH used to remove hemicelluloses and

pectins. While the interpretation of absolute M_r may be compromised, the comparison of M_r distribution among the various ripening stages is still valid. Between RS1 and RS2, there is a loss of medium-sized polymers, while at RS3 a reduction in lower M_r polymers is obvious along with a slight upshift in the average M_r. Despite these differences, the profiles of RS1 to RS3 are of broad distribution and appear skewed toward smaller M_r polysaccharides. Unlike the profiles of total cell wall polymers, the average M_r of cellulose-enriched polymers from ripe fruit (RS4) does not appear to be significantly different from the other stages; however, the M_r profile is symmetrical and displays a much narrower distribution, quite similar to that of whole RS4 cell walls. While absolute M_r comparisons are hampered by the effect of the alkali treatment employed in preparing the cellulose enriched polymers, similar trends in M_r distribution are apparent in the cellulose-enriched samples and the large-M_r component of whole cell walls during avocado fruit ripening.

Effects of C*x*-cellulase on the molecular weight distribution of Avicel

When Avicel was incubated with C*x*-cellulase or a crude enzyme extract from ripe avocado fruit, there was a loss of lower M_r material such that the sample contained a proportionally greater amount of higher M_r cellulose polymers (Figure 5-12). It was thought that since avocado cellulase is apparently not associated with an enzyme complex similar to those found in bacterial and fungal systems, it would be unable to effect any change in cellulose. This idea was based on the lack of reducing sugars produced following incubation of avocado cellulase with cell walls (Hatfield and Nevins, 1986, and also found here). Solubility changes, however, are not necessarily an appropriate indicator of enzyme action, whereas examination of the M_r of the products is often more revealing. The change in M_r profile of cellulose following incubation with either purified C*x*-cellulase or a crude enzyme extract is open to two interpretations. First, under the influence of avocado C*x*-cellulase, lower M_r cellulose may have become associated into higher M_r chains. There is speculation that low levels of C*x*-cellulase may act on tomato XG in an

endotransgylcosylase fashion (Dr. G. Maclachlan, McGill University, Montreal, Quebec, Canada; personal communication). If avocado C*x*-cellulase acts similarly towards cellulose, one might expect polymers of much higher M_r to be evident also; however, since even low levels of avocado C*x*-cellulase can hydrolyze CMC, condensation does not appear to be a satisfactory explanation of events occurring with cellulose in response to C*x*-cellulase activity. Second, it is possible that C*x*-cellulase preferentially hydrolyzed the lower M_r cellulose chains, resulting in a sample containing a greater proportion of large-M_r chains. Since C*x*-cellulase clearly exhibits endo-glucanase activity, this is a more acceptable explanation for its effects on Avicel. Presumably the cellulase present in the crude enzyme extract is operating in the same manner. The question remains, however, as to the fate of the hydrolyzed cellulose. Levels of glucose equivalents in the post-incubation filtrate, solubilized from Avicel by C*x*-cellulase or crude enzyme extract were 6 $\mu g\ mg^{-1}$ and 5 $\mu g\ mg^{-1}$, respectively, indicating that minimal solubilization occurred during enzyme incubation. The insoluble fragments produced by the action of the cellulase would be easily solubilized by LiCl/DMAC but may be of too low M_r to fractionate on the HPLC column system. Glucose itself elutes beyond the solvent peak (Dr. J. Timpa, Southern Regional Research Center, USDA-ARS, New Orleans, LA, personal communication). The very low M_r chains of the cellulose controls are fractionated, therefore it is difficult to accept that smaller, yet still buffer-insoluble cellulose fragments cannot be similarly visualized. It is possible that the resolution of the gel permeation column series is questionable at these low M_r. Nevertheless, the evidence clearly shows that avocado C*x*-cellulase can influence the M_r of cellulose.

Effects of C*x*-cellulase activity on the molecular weight distribution of cell walls

When either the purified C*x*-cellulase or crude enzyme extract from ripe avocado fruit were incubated with total cell walls from unripe fruit, there was a clear reduction, both in amount and M_r, of the second, high M_r peak (Figure 5-13). Preliminary assays of C*x*-cellulase using partially de-esterified pectin confirmed that the purified enzyme does

not alter the M_r of pectin and, on the premise that this peak does not contain hemicellulose, it is suggested that C*x*-cellulase has reduced the M_r of cellulose in the cell walls of avocado fruit. A similar experiment with the cellulose-enriched samples from RS1 incubated with C*x*-cellulase was not performed. As this cellulose was exposed to strong alkali during preparation and, consequently, its crystallinity properties altered, any M_r modification in this case would have little relevance to the situation *in situ*.

While there is a definite loss of the high-M_r peak (interpreted as a loss of cellulose) in cell walls from unripe avocado fruit under the influence of added C*x*-cellulase, this type of M_r distribution change is not evident during normal ripening. This discrepancy may be due to the changing elution characteristics of other polymers in the cell walls during ripening. The decrease in M_r of large polysaccharides in cell walls following C*x*-cellulase treatment could be due to an attack on the amorphous component of the microfibrils. The extent of hydrolysis of cellulose appears to be moderated to some extent, however, since soluble fragments were not produced. The action of the enzyme on Avicel may be occurring in the same manner by attacking the more weakly associated, amorphous portions of the microfibrils.

Analysis of Cell Wall Crystallinity by X-Ray Diffraction

General features

Investigations into the crystallinity properties of avocado cellulose were prompted by reports of specific cellulases, so-called 'low value' cellulases, which exhibit a preference for amorphous cellulose (Klyosov, 1990). Several lines of evidence have also pointed to the role of endoglucanase in 'high value' cellulase systems to be that of attacking the amorphous regions of the microfibrils. Wood and McCrae (1979) suggested this from the preference of endoglucanase for modified cellulose substrates such as CMC and acid-swollen cellulose rather than crystalline Avicel or cotton. Monoclonal antibodies for the endoglucanase of *Trichoderma reesei* have been employed to localize this enzyme on amorphous domains of aspen cellulose (Nieves et al., 1991). Sprey and Bochem

(1991) and Din et al. (1991) noted structural effects on cellulose following incubation with purified endoglucanase from *Cellulomonas fimi*, suggesting that while the enzyme may not be able to cause complete polymer solubilization, it may provide access to the inner crystalline regions of the microfibril. Din et al. (1991) showed that particular enzymic domains could also provide different functionalities for the enzyme. While the C*x*-cellulase from avocado fruit is not be within the same structural classification as many of the more thoroughly characterized endoglucanases of fungal and bacterial origin (Beguin, 1990), it does have in common with these enzymes the ability to hydrolyze CMC and the inability to hydrolyze crystalline cellulose. Crystallinity assessments add insight into the changes that may occur if the avocado Cx-cellulase attacks the amorphous regions of cellulose microfibrils, since if these areas are reduced the cellulose becomes proportionally enriched in the residual crystalline component.

Crystallinity index considerations

The interplay between the matrix and crystalline content of the cell wall becomes important in the calculation of crystallinity index values using the method of Segal et al., (1959). This calculation was formulated for experiments dealing with relatively pure forms of cellulose (e.g., cotton, Avicel) where the only amorphous material is derived from the cellulose itself. Investigations into the crystalline content of cell walls containing a variety of complex polysaccharides introduces a complication in the interpretation of powder diffraction signals. It has not been demonstrated how the matrix material of the cell wall, itself of amorphous nature, contributes to x-ray diffraction signals. An additional complicating factor in the interpretation of the diffraction signals is that the composition of the cell walls changes during ripening. Indeed, the relative amount of cellulose increased from 31% in cell walls of unripe fruit to 54 % in cell wall samples from ripe fruit. Mixtures of Avicel and citrus pectin were examined to determine if non-cellulosic wall components (pectin being the most predominant) could potentially confound assessments of cellulose crystallinity in cell walls. Diffractograms recording the x-ray diffraction

signals for all cell wall samples containing cellulose consist of a sharp peak pertaining to the crystalline fraction of the cellulose (usually in the diffraction angle range of 20° - 22°), and a smaller, broader peak related to the amorphous content of the cellulose (measured at 18°). Results of these test runs as well as those for the ripening series appear in Table 5-2.

Table 5-2. Crystalline peak height, width (at half height), area and crystallinity index calculated from x-ray diffraction data of Avicel:pectin test samples and cell walls of ripening avocado mesocarp. Units of signal measurement are mm.

	Height	Width	Area	Crystallinity Index (%)
Avicel	254	10.5	2667	81.1
Avicel:Pectin (2:1)	122	11	1342	75.8
Avicel:Pectin (1:2)	52	12.5	650	51.9
Pectin	8		-	-
Cell Walls: RS1	44	18.3	805	41.3
RS2	40	18	720	44.6
RS3	42	18	738	44.8
RS4	74	17.3	1280	49.8

Decreasing Avicel content (increasing pectin content) of the standards led to a decrease in the height and area of the crystalline cellulose peak. The crystallinity index decreased with decreasing cellulose content despite there being no actual change in the crystallinity of the Avicel in the standards. The quantity-dependent nature of this parameter indicates that it may not be a reliable measure of crystallinity for cell wall samples of varying cellulose concentrations. There was also an increase in peak width (measured at half the peak height) as the Avicel content of the standard samples decreased

This indicates that the particle size of the crystalline material has decreased and that the crystalline material is increasingly dispersed. Increasing the pectin content of the Avicel standards did not increase the size of the amorphous cellulose peak (data not shown) and did not appear to influence the signal pattern. In the sample containing 100% pectin, there were no apparent diffraction peaks, and only a low background signal. No crystallinity index could be calculated for this.

Crystallinity of avocado cell walls during fruit ripening

While the cellulose content of the avocado cell walls increased from 31% to 54% with ripening (within the cellulose content range of the two standard Avicel:pectin mixtures) the crystalline signals were lower and broader than the standards and the peak height, area and crystallinity index did not increase at the same rate as the standards. These data indicate that the crystallinity of the cellulose in avocado cell walls is much lower than that of Avicel. Clearly, the crystallinity of the cellulose from these two sources is different, since in this case the matrix material has no quantitative influence on the diffraction signals. The increase in peak area reflects the increasing amount of cellulose present in each cell wall sample, and these values are in line with the increases observed in the Avicel:pectin samples. As ripening proceeds, there is also a decrease in the peak width, indicating that the crystalline particles are becoming less dispersed, and possibly increasing in size. This may be interpreted as a complete disruption of the amorphous cellulose chains, with the remaining cellulose having a higher crystalline content. In the only other studies of cellulose crystallinity in cell walls during development there was no significant relationship between crystallinity and growth of developing asparagus spears (Sterling, 1957) and a change in the crystallinity index from only 50% to 51% in ripening peach fruit (Sterling, 1961). These data were not discussed in relation to the cellulose content.

Effects of C*x*-cellulase activity on unripe avocado cell wall crystallinity

When total cell walls of unripe avocado fruit were treated with purified C*x*-cellulase the magnitude of the crystalline signal from the x-ray diffraction data increased as did the crystallinity index (Table 5-3). The peak width decreased and the area remained constant. While the area of the crystalline cellulose peak is dependent on the total amount of cellulose present (crystalline and amorphous), the action of C*x*-cellulase would not have led to a proportional increase in the amount of cellulose since it is unable to attack pectins or XG, and did not produce significant levels of soluble sugars during incubation. Therefore, the peak area is constant. The alteration in the dimensions of the diffraction signal must be due to a change in the crystallinity of the cellulose itself, probably due to the action of the enzyme on the amorphous regions of the microfibrils. That the peak width narrows somewhat after enzyme action also indicates that there is a modification in cellulose crystalline particle size.

In cell walls treated with various enzyme preparations from ripe avocado mesocarp, the effects on crystallinity were not clear (Table 5-3). In the crude extract (protein extracted in high-salt buffer and soluble in 20% ammonium sulfate), there is the full complement of cell wall hydrolases, including C*x*-cellulase and polygalacturonase. The action of this extract should result in a loss of matrix polysaccharides and a proportional enrichment of the cell wall with cellulose, similar to that occurring during fruit ripening. In actuality, the crystallinity index did increase but the other signal dimensions were not altered to the same extent as found in cell walls during avocado ripening. The cellulase-depleted enzyme extract did not contain C*x*-cellulase (Chapter 4) but would have contained most of the other cell wall hydrolases. There was a noticeable decline in the size, width and area of the crystalline signal following treatment of the cell walls with this enzyme preparation, although the crystallinity index was increased above that of the control. This would indicate that the signal related to the amorphous cellulose was comparatively low. The sum of the results from the cell walls treated with cellulase-

depleted enzyme extract indicate that there may be glycosidases present that can reduce the amount of amorphous cellulose. The cellulase-enriched enzyme extract acted on the cell walls in a manner that increased the peak height and area, but left the peak width (an indicator of crystalline particle size and dispersal) unchanged. The crystallinity index was increased over that of the control, but did not differ markedly from that caused by the cellulase-depleted enzyme extract. This result is in contrast to the effects of crude extracts or purified C*x*-cellulase; however, the effects of mixtures of enzymes obscure the issue of crystallinity by changing the composition of the cell walls (particularly matrix polysaccharides). For this reason the experiments to examine enzyme effects using purified C*x*-cellulase are more indicative of the true activity of this enzyme although its activity *in situ* is in association with the whole complement of cell wall hydrolases.

Effect of C*x*-cellulase activity on crystallinity of Avicel

When the microcrystalline cellulose Avicel was incubated with pure C*x*-cellulase, the interpretation of the x-ray diffraction signal pattern was simplified due to the one polymer-one enzyme situation where the crystallinity index could be applied without confoundment from the presence of other polysaccharides. In these experiments, the crystallinity was not altered by the enzyme, although the peak area increased above that of the control through contributions by both the height and width of the signal (Table 5-3). This would imply that there is more cellulose present, but the same amounts of material were used for incubation in each case and there were no differences in the soluble sugars produced in the reaction (data not shown). The magnitude of the crystalline signal for Avicel is over seven times that of the cell walls of avocado fruit. It is possible that at these high levels the sensitivity of the detector declines and the peak heights are not as reliable. The initial crystallinity value of Avicel is high and the levels of amorphous cellulose would be correspondingly low. In this light, the lack of a change in the crystallinity of Avicel treated with C*x*-cellulase is consistent with the proposed activity of Cx-cellulase on only amorphous cellulose.

Table 5-3. Crystalline peak height, width (at half height), area and crystallinity index calculated from x-ray diffraction data following incubation of RS1 cell walls with purified C*x*-cellulase or crude enzyme preparations and controls. Units of peak measurement are mm.

Treatment	Height	Width	Area	Crystallinity Index (%)
RS1 Cell Walls:				
+ C*x*-cellulase	45	16.8	756	46.0
+ Buffer Control	41	18.3	750	42.7
RS1 Cell Walls:				
+ Crude Extract	44	17.8	783	45.2
+ Cellulase-Depleted	39	16.5	644	44.8
+ Cellulase-Enriched	49	17.8	872	44.8
+ Heat-Denatured Crude	46	17.8	819	42.7
Avicel:				
+ C*x*-cellulase	376	12	4512	83.4
+ Buffer	345	10.5	3623	83.9

Summary

During avocado fruit ripening there is a loss of cellulose and a major increase in the production and activity of the enzyme C*x*-cellulase. The experiments described here were designed to investigate whether C*x*-cellulase has effects on cellulose that are not apparent with conventional methods of analysis. Because of difficulties associated with solubilizing cellulose, changes in M_r effected by C*x*-cellulase have previously gone undetected. Since the cellulose network acts as a type of extra-cellular skeleton, any change in the M_r could have a marked influence on the strength of the cell wall.

Disruption of the cellulose network, even without the hydrolysis of glycosidic bonds, may serve to change the cohesive properties of the cell wall, and may even facilitate the passage of cell wall hydrolases through the wall.

Ultrastructural studies reported here and elsewhere (Pesis et al., 1978; Platt Aloia et al., 1980) have noted the loss of middle lamella material in the cell walls of ripening avocado fruit. Cytochemical localization shows that cellulose is found throughout the cell wall but is also reduced in the middle lamella during ripening. It is clear from Pt/C shadowing that the microfibrils become less associated with matrix material as ripening progresses and that they become untwisted and unravelled during this time. Even so, there is still strong binding of XG to the microfibrils which supports the findings of Chapter 4 that XG undergoes only moderate hydrolysis during ripening, and that this is not mediated by C*x*-cellulase. Presumably, if the enzyme could solubilize the XG bound to cellulose there would be a marked reduction of this polymer along the fibril. However, this was not seen and it is apparent that M_r modification does not alter the binding properties of XG to cellulose.

The effects of C*x*-cellulase on cellulose microfibrils observed ultrastructurally point to a change in the nature of fibril organization rather than a complete breakdown of the cellulose network. In cell walls of unripe fruit the enzyme appears to cause untwisting of the microfibrils whereas in cell walls from ripe fruit, which have already been exposed to C*x*-cellulase, the effect of added enzyme is to cause further striations and reveal elementary fibril substructure. A similar effect was seen following the action of cellulase on Avicel. None of these enzyme-substrate incubates showed significant release of soluble products, but analysis of the M_r distributions showed two distinct effects. The Avicel, which possesses a high degree of crystallinity, displayed an increase in average M_r due to a loss of lower M_r components. The cell wall sample from unripe fruit exhibited an erosion of the polymers of highest M_r. While these two effects may seem opposed, the physical results of such activity seen ultrastructurally are very similar in that cellulose

organization is disrupted. It is proposed that C*x*-cellulase attacks the cellulose microfibril at its most accessible sites, the integral and peripheral amorphous areas. There is no evidence at this point regarding the extent of coverage of XG on the outer surface of the cellulose, but since the XG chains have a much lower M_r than the cellulose of the cell wall, and the quantity of XG is comparatively low in comparison to other polysaccharides in the avocado cell wall, it is anticipated that the coverage is not complete and the frequency of gaps may be high. If this is the case, C*x*-cellulase would have some means of access to the microfibril and may cause some cleavage of the relatively loosely held amorphous cellulose chains. Din et al. (1991) proposed that the binding domain of *Cellulomonas fimi* endoglucanase could burrow into the microfibril, exfoliating the structure and releasing ends of elementary fibrils. Parallels between the mode of action of bacterial and fungal endoglucanases and the avocado C*x*-cellulase should be drawn cautiously due to the lack of information regarding the binding/catalysis kinetics of C*x*-cellulase (stemming from a previous lack of knowledge regarding the enzyme substrate). Nevertheless, the evidence from both the M_r distribution and microfibril ultrastructure following incubation with avocado C*x*-cellulase tends to indicate that this enzyme binds and disrupts the amorphous regions of the cellulose microfibril.

The x-ray diffraction data supports the view that C*x*-cellulase targets the amorphous areas of the microfibril. Following exposure to C*x*-cellulase there was an increase in the crystallinity index of cell walls from unripe fruit. Since the cellulose content did not alter significantly during this incubation (the crystallinity peak areas are similar) and the added enzyme was pure, the crystallinity index in this case is a reliable indicator of the changes associated with the action of the enzyme. In addition, the crystalline peak shape sharpened following C*x*-cellulase activity which is an additional sign of increasing crystalline nature of the cellulose. These results reflect the enzyme-related disruption of the integral or peripheral amorphous areas of the microfibril, which reduces

the quantity of amorphous cellulose associated with the fibrils and proportionately increases the amount of crystalline material.

It is difficult to demonstrate that alterations in the cellulose organization occur during normal avocado fruit ripening since changes in cell wall matrix polymers also occur during this time. The methods used to assess cell wall crystallinity and M_r were sensitive to the presence of matrix polysaccharides, but ultrastructural observations indicated that during avocado fruit ripening, cellulose microfibrils unravelled to reveal the elementary fibril substructure.

The consequences of the action of C*x*-cellulase on the cellulose component of ripening avocado fruit would be to cause initial softening, prior to middle lamella dissolution by other cell wall hydrolases such as polygalacturonase. Softening of the mesocarp tissue occurs prior to the climacteric and is well associated with the onset of cellulase production. Considerable cellulose is lost from the middle lamella region during ripening. Dallman et al. (1989) immunolocalized C*x*-cellulase throughout the cell wall and speculated that the enzyme could be delivered to the center of the cell wall via the endoplasmic reticulum-derived plasmodesmata. This mechanism was proposed due to the low frequency of both Golgi-mediated vesicular fusion and cellulase deposition at the cell wall edges. From this viewpoint the reduction of cellulose in the middle lamella during ripening is reasonable due to the access of cellulase to this region of the cell wall. Activity of C*x*-cellulase in the middle lamella (a region regarded as having a cementing function in the cell wall) would provide a loss of cellular cohesion, contributing to the initial softening of the avocado mesocarp.

Figure 5-1. Transmission electron micrographs of the cell walls of (A) unripe and (B) ripe avocado mesocarp. Tissue was embedded in LR White, and sections were stained with uranyl acetate and lead citrate.

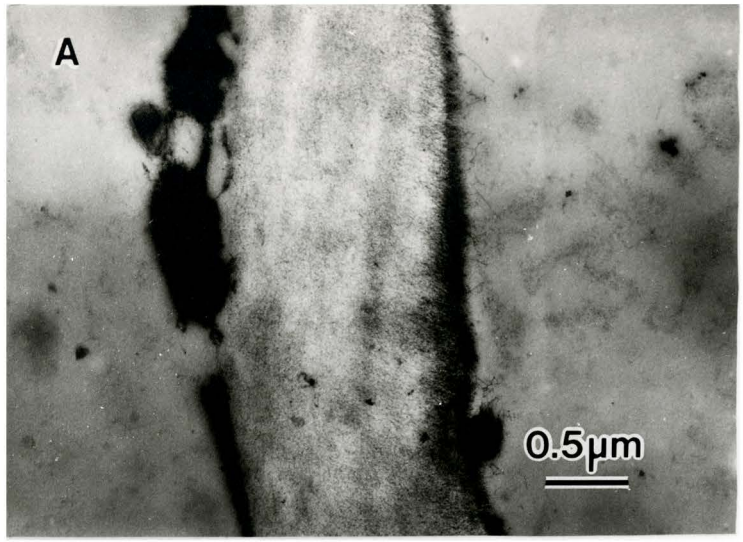
A
0.5μm

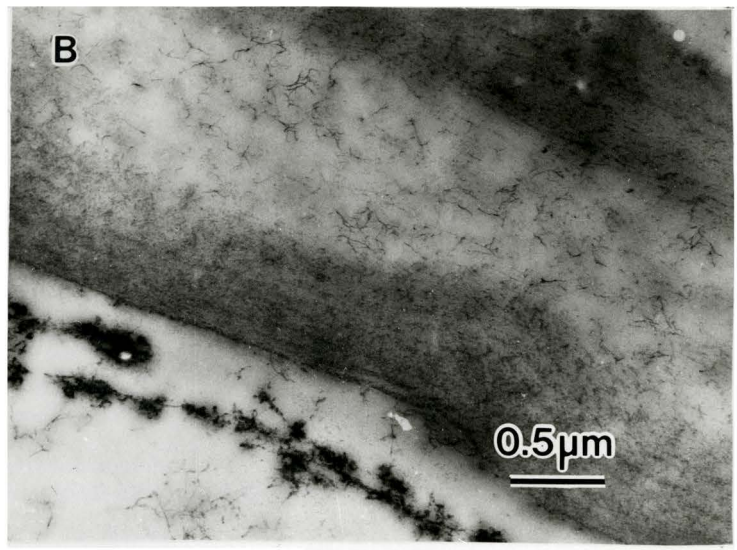
B
0.5μm

Figure 5-2. Enzyme-gold localization of cellulose in cell walls of avocado mesocarp. Sections of LR White-embedded tissue from (A) unripe and (B) ripe avocado fruit were treated with a fungal cellulase-gold conjugate and then stained with uranyl acetate and lead citrate.

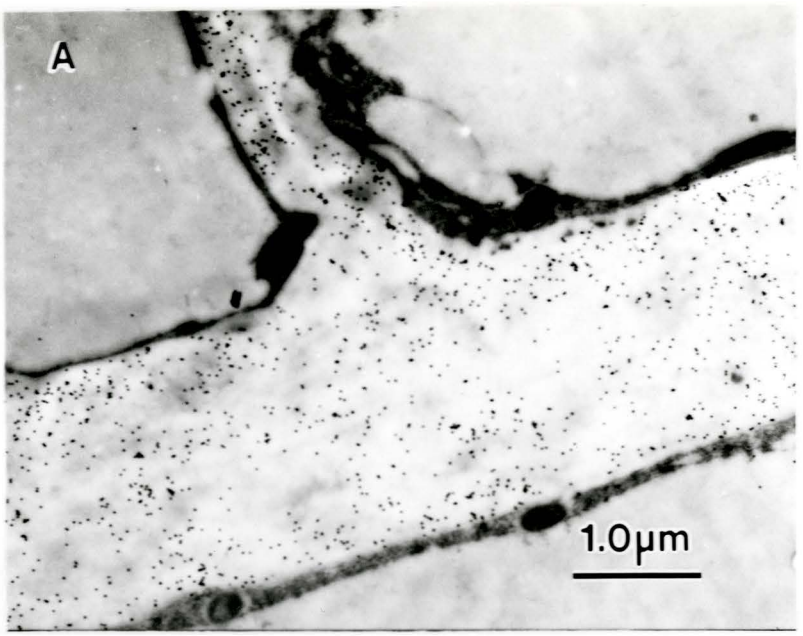
A
1.0μm

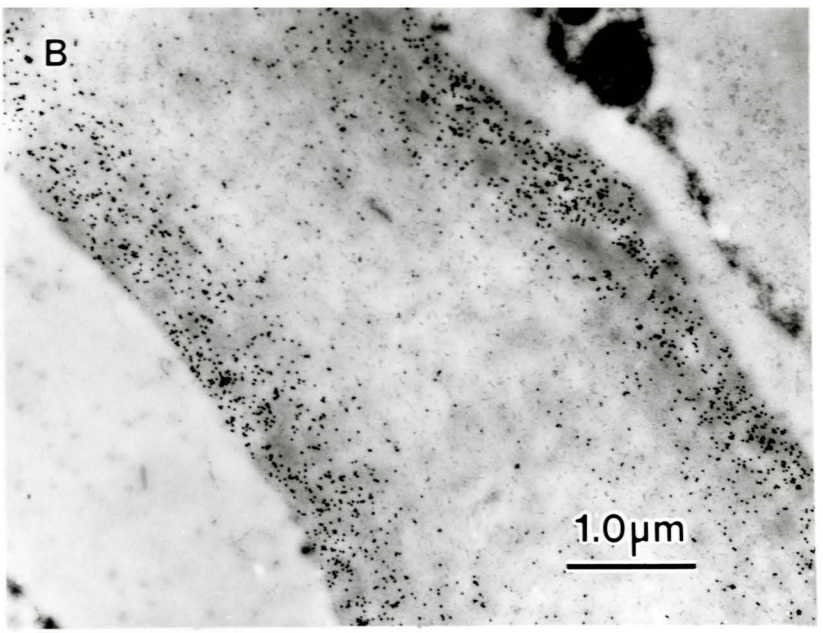
B
1.0μm

Figure 5-3. Electron micrographs of platinum/carbon-shadowed cell walls isolated from avocado mesocarp at each ripening stage. Walls at RS1 (A) and RS2 (B) are predominantly composed of clumps of matrix material. At RS3 (C) and RS4 (D) microfibrils are found free of matrix material and show signs of unravelling.

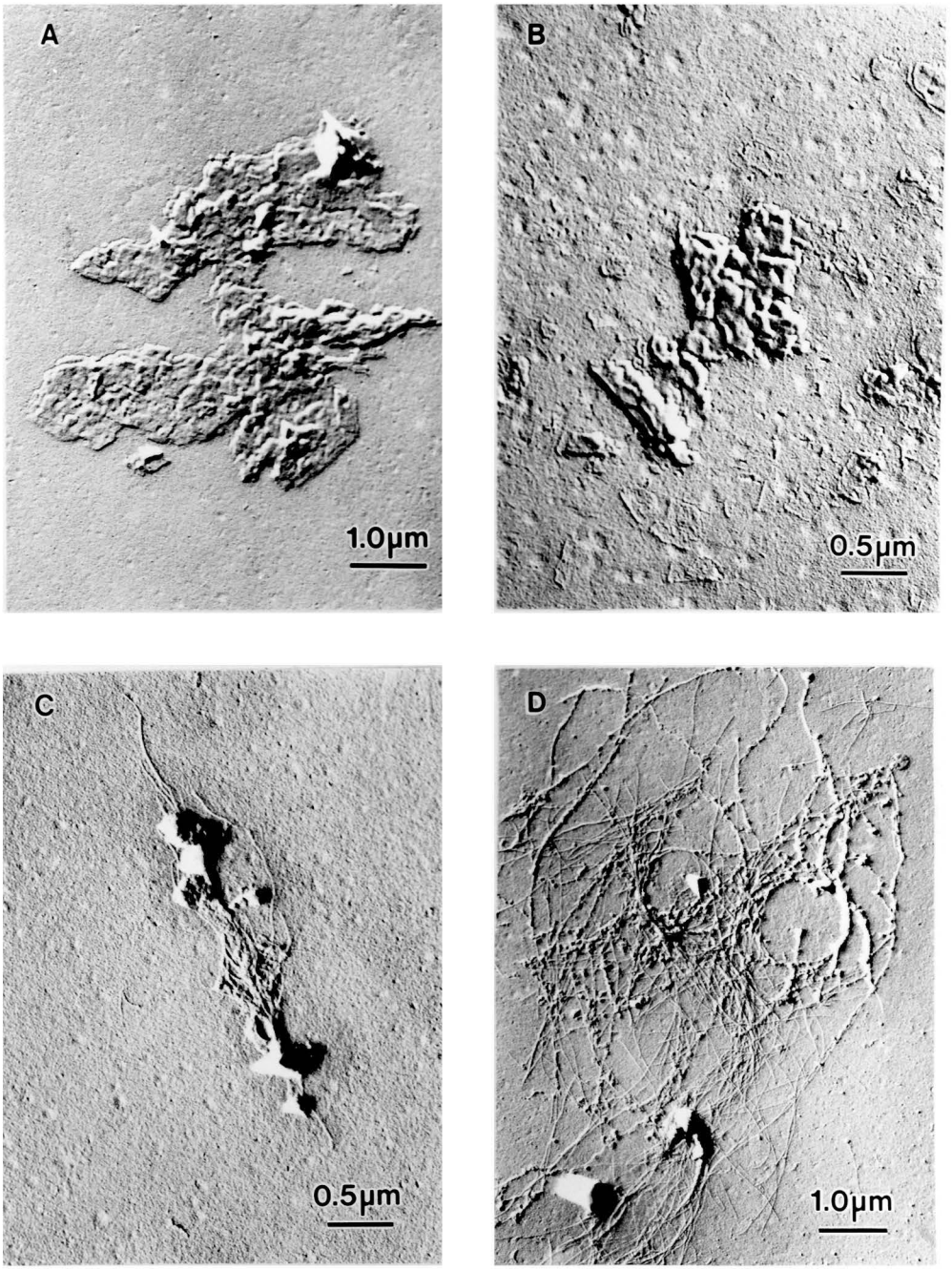
A
1.0μm
B
0.5μm
C
0.5μm
D
1.0μm

Figure 5-4. Enzyme-gold localization of cellulose in platinum/carbon-shadowed cell walls isolated from unripe and ripe avocado fruit. The fungal cellulase-gold probe localized cellulose associated with clumps of matrix material in cell walls of unripe avocado mesocarp (A), while in ripe fruit (C), cellulose microfibrils were found free. Localization controls were cell walls of unripe (B) and ripe (D) mesocarp, treated with enzyme-gold preabsorbed to carboxymethylcellulose.


0.5µm
A

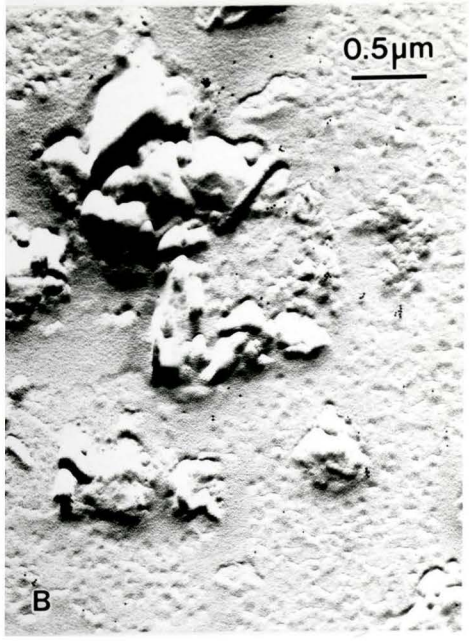
0.5µm
B


0.5µm
C


0.5µm
D

Figure 5-5. Immunolocalization of xyloglucan in platinum/carbon-shadowed cell walls isolated from RS1 (A), RS2 (B), RS3 (C) and RS4 (D) avocado fruit. Cell walls were labelled with murine monoclonal antibodies directed to the fucose residue of xyloglucan, followed by a goat-anti-mouse IgG-gold conjugate. Xyloglucan is closely associated with clumps of matrix polysaccharides at RS1 and RS2, and is found on the surface of cellulose microfibrils at RS3 and RS4.

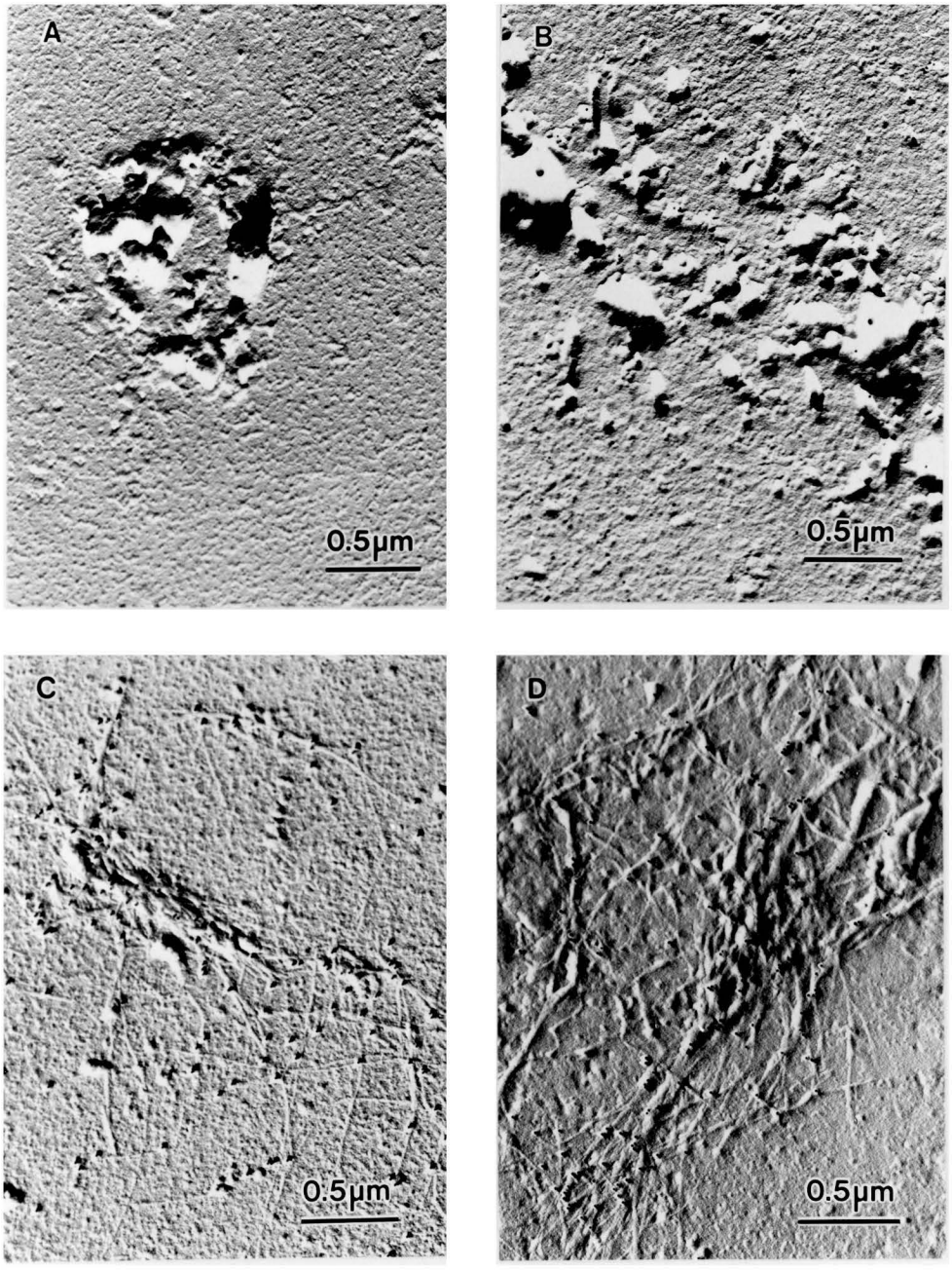
A
0.5μm
B
0.5μm
C
0.5μm
D
0.5μm

Figure 5-6. Platinum/carbon-shadowed cell walls from unripe avocado fruit after 12 h incubation with pure C*x*-cellulase (A) or buffer (B). Microfibril organization is disrupted, and substructure is readily evident in cell walls treated with C*x*-cellulase.

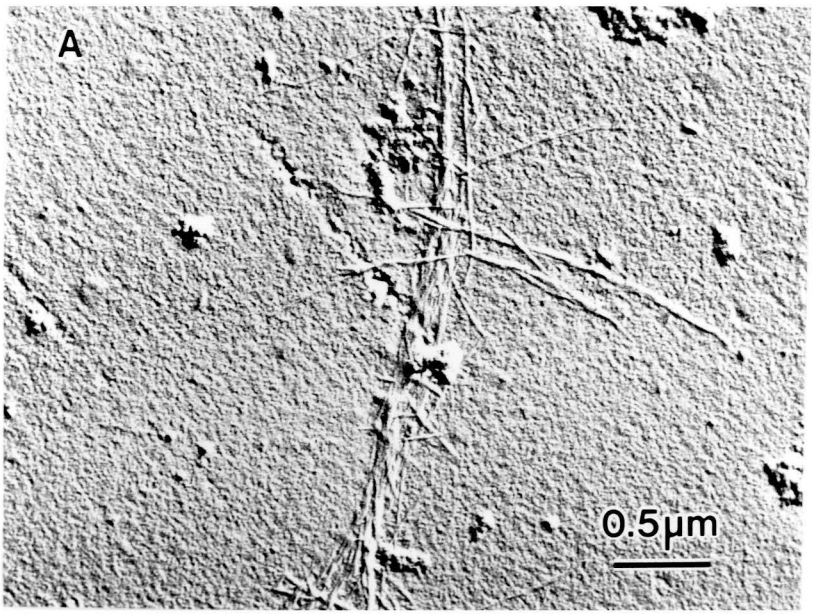
A
0.5μm

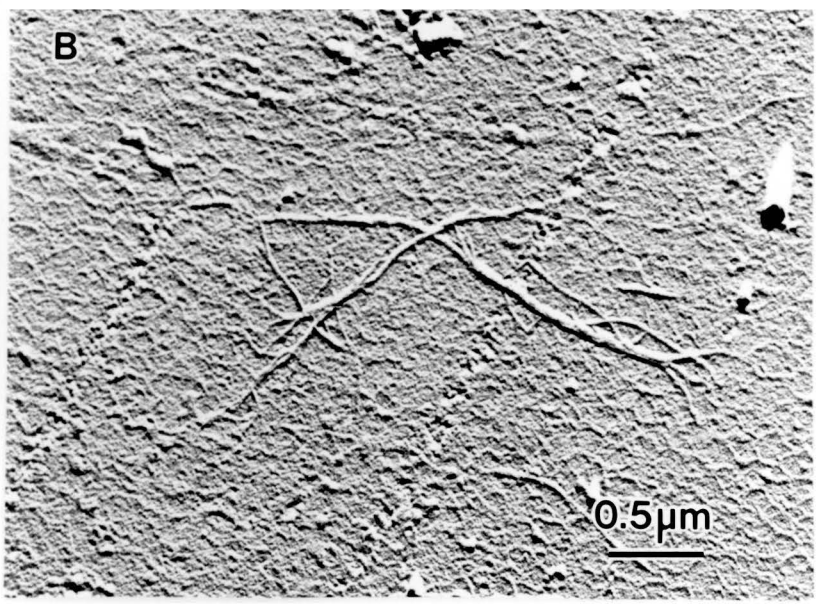
B
0.5μm

Figure 5-7. Platinum/carbon-shadowed cell walls from ripe avocado fruit after 12 h incubation with pure C*x*-cellulase (A) or buffer (B).

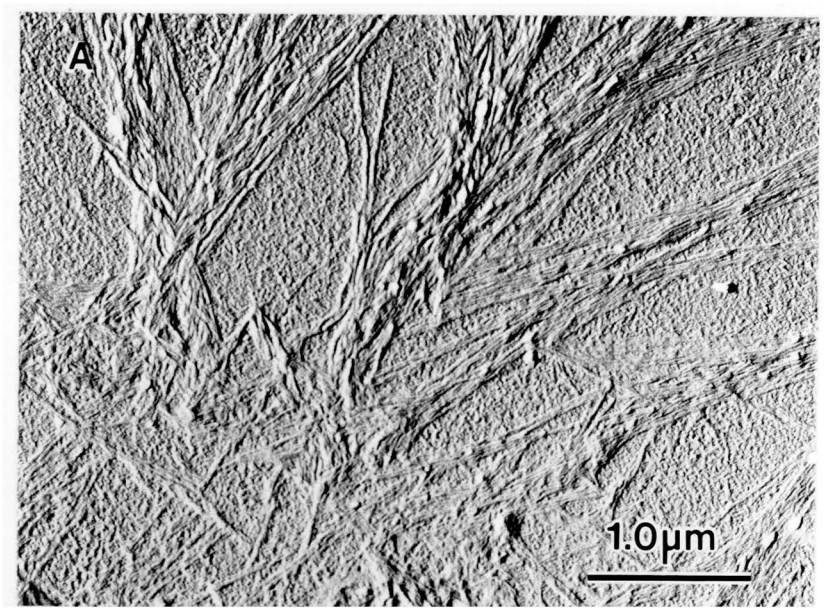
A
1.0μm

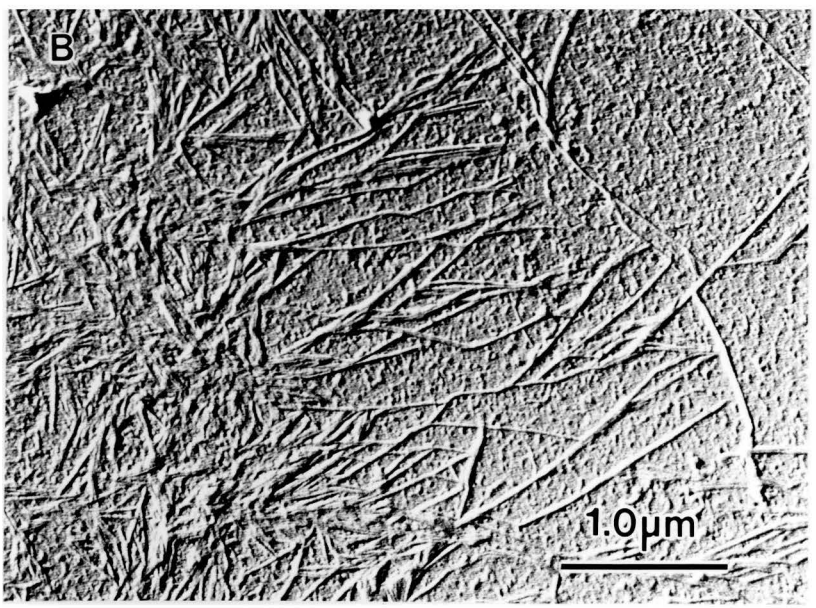
B
1.0μm

Figure 5-8. Platinum/carbon-shadowed cellulose microfibrils of Avicel following a 12 h incubation with pure C*x*-cellulase (A) or buffer (B).

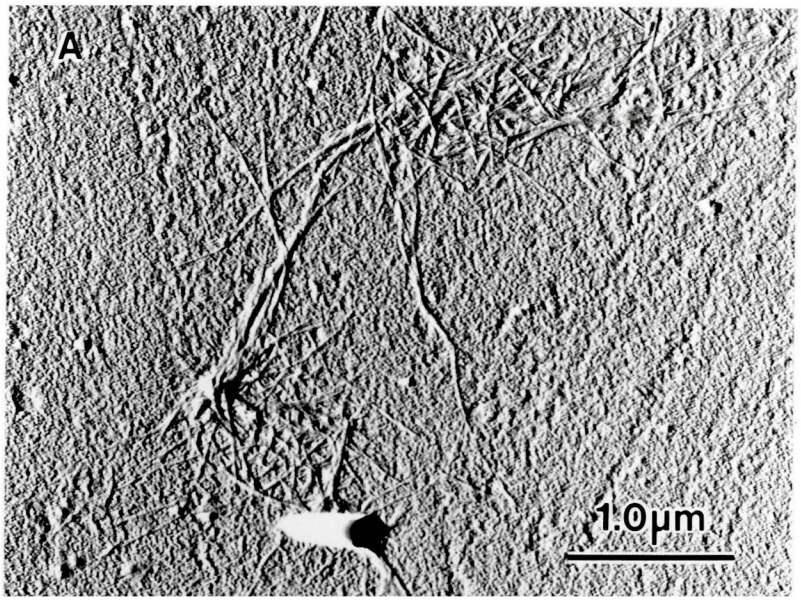
A
1.0μm

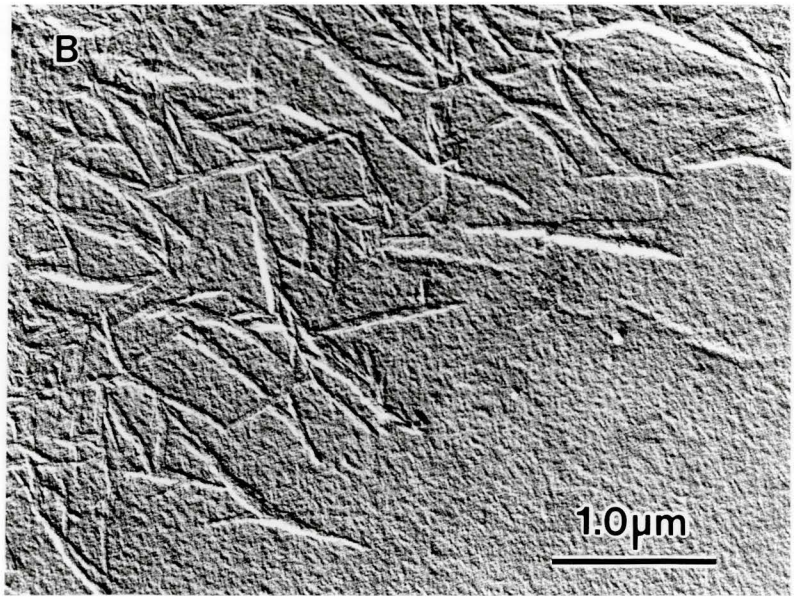
B
1.0μm

Figure 5-9. Electron micrographs of cell walls from C*x*-cellulase treated avocado mesocarp. Fresh, unripe avocado tissue was incubated for 30 min in partially-purified C*x*-cellulase (A) or buffer (B), then fixed and infiltrated with LR White. Sections were stained with uranyl acetate and lead citrate.

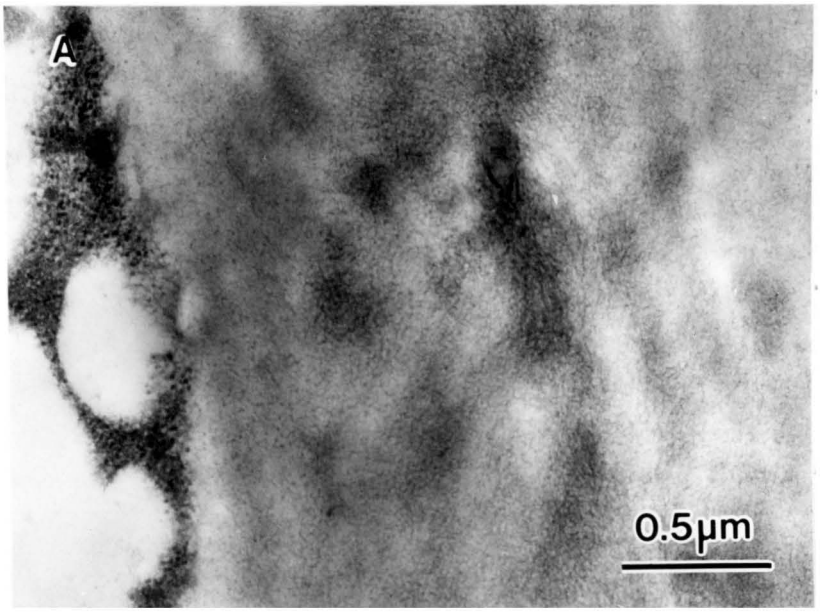
A
0.5μm

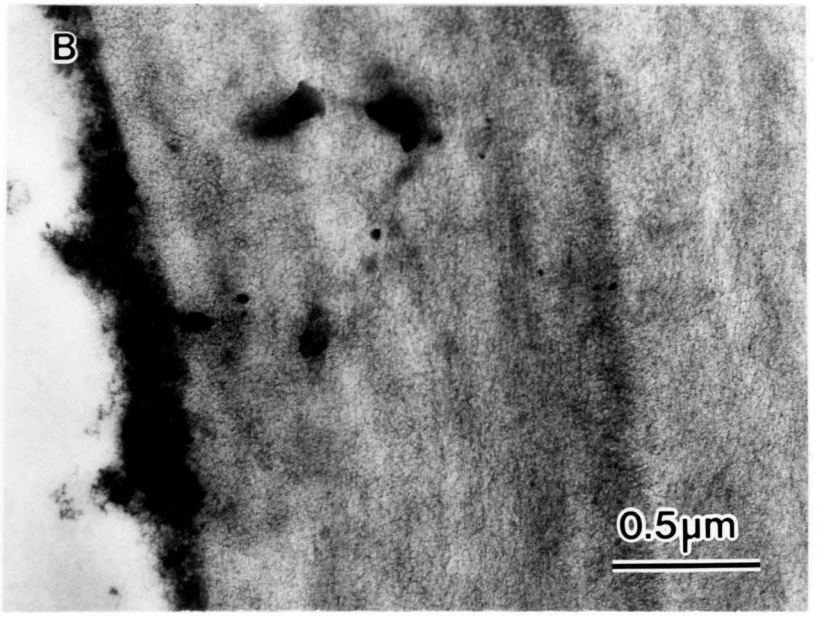
B
0.5μm

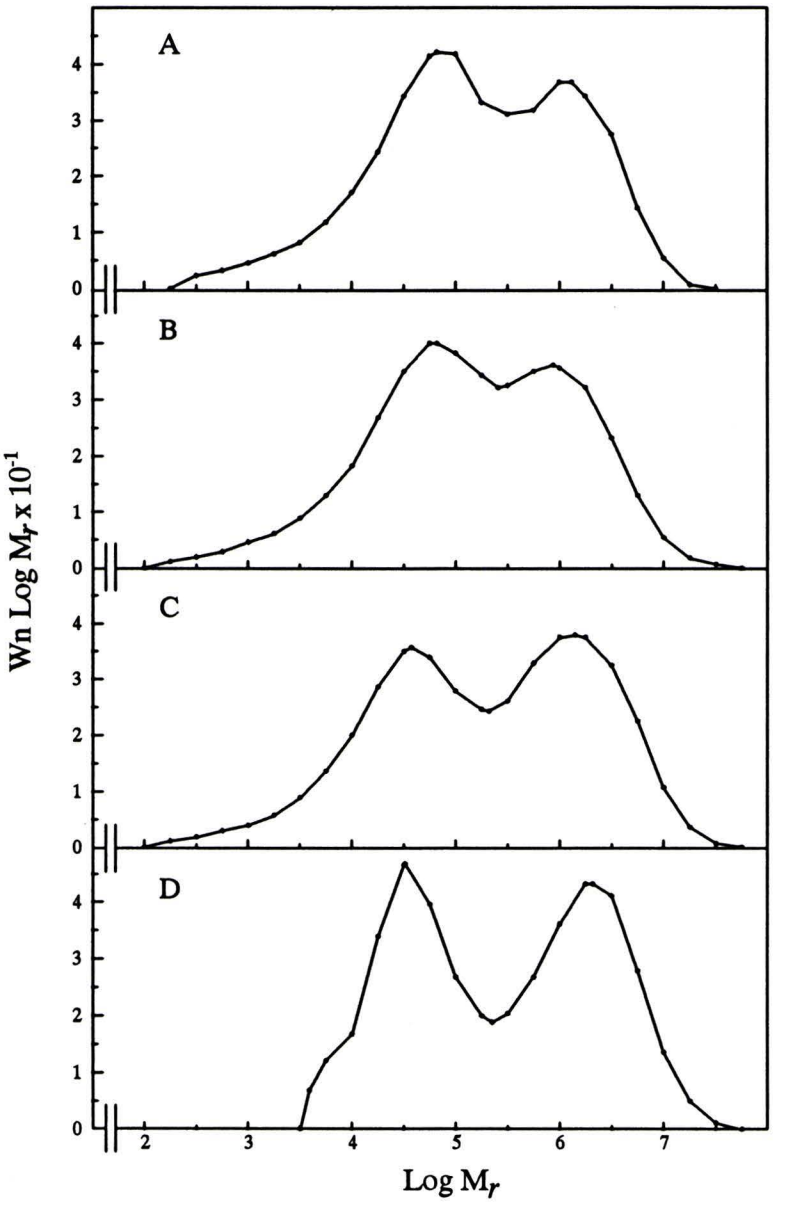

Figure 5-10. Molecular weight distribution of cell walls of (A) RS1, (B) RS2, (C) RS3 and (D) RS4 solubilized in dimethylacetamide with 0.5% LiCl and fractionated by HPLC.

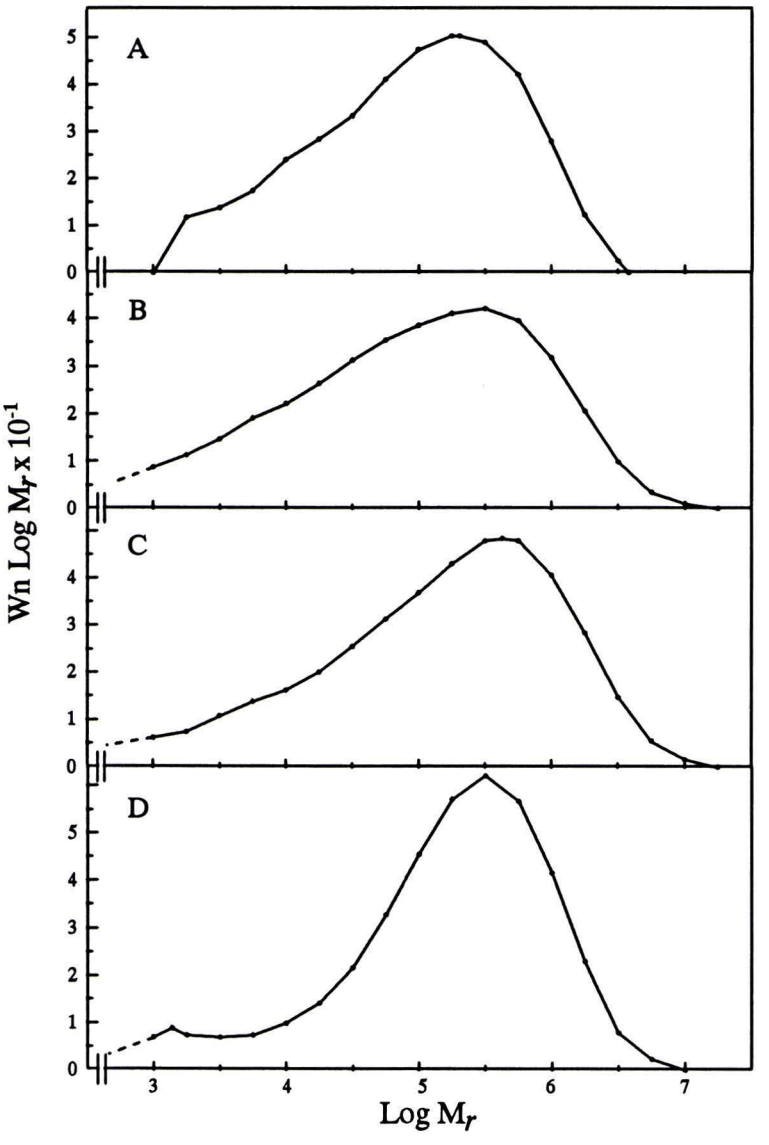

Figure 5-11. Molecular weight distribution of isolated cellulose from (A) RS1, (B) RS2, (C) RS3 and (D) RS4 cell wall material. Samples were solubilized in dimethylacetamide containing 0.5% LiCl and were fractionated by HPLC.

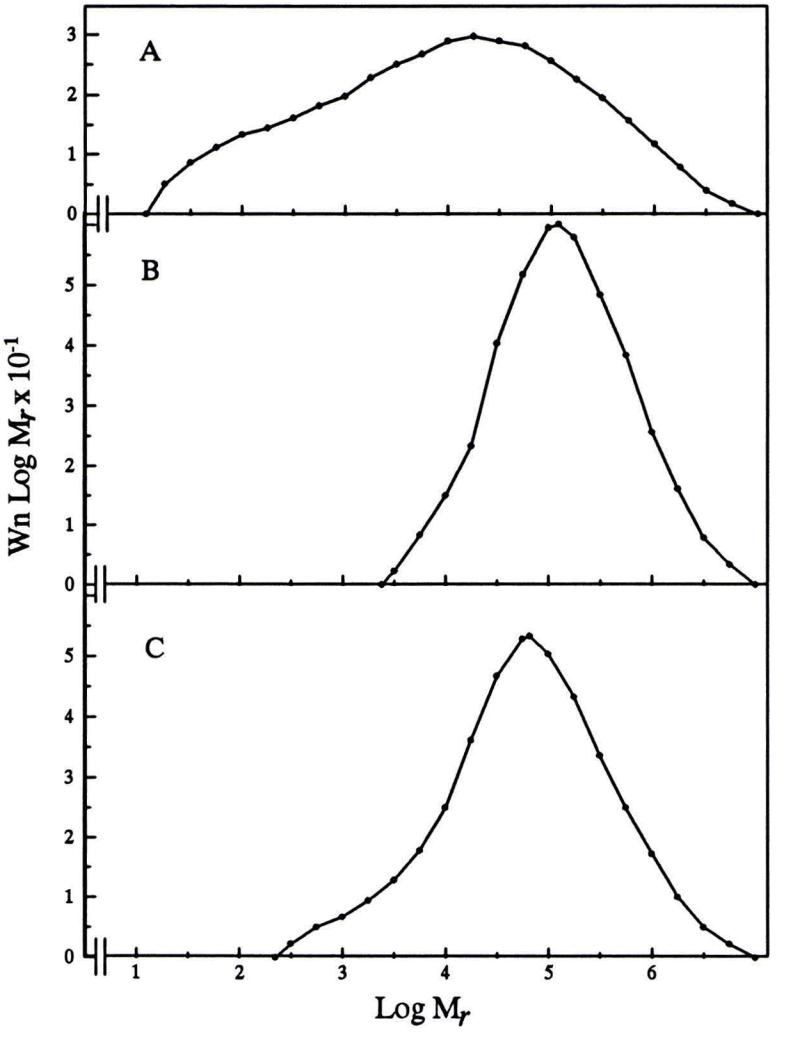

Figure 5-12. Molecular weight distribution of Avicel following incubation with (A) denatured crude enzyme, (B) active crude enzyme or (C) purified C*x*-cellulase extracted from ripe avocado mesocarp. Samples were solubilized in dimethylacetamide containing 0.5% LiCl and were fractionated by HPLC.

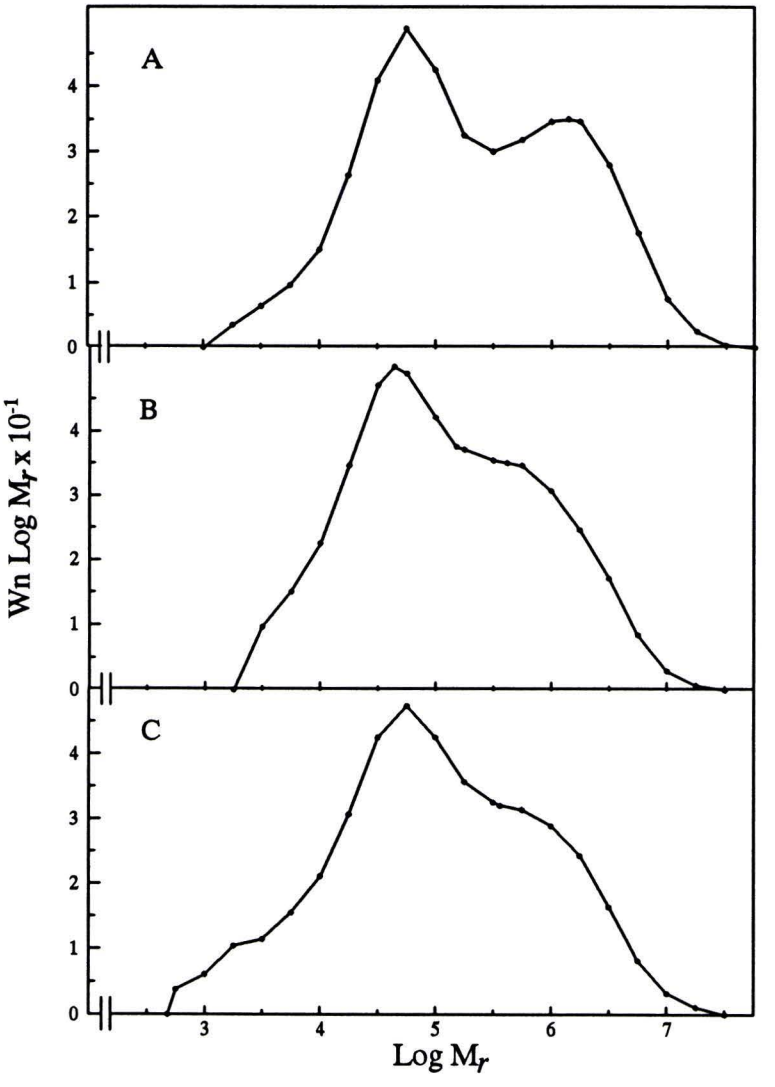

Figure 5-13. Molecular weight distribution of RS1 cell wall material following incubation with (A) denatured crude enzyme, (B) active crude enzyme or (C) pure C*x*-cellulase extracted from ripe avocado mesocarp. Samples were solubilized in dimethylacetamide containing 0.5% LiCl and were fractionated by HPLC.

CHAPTER 6
SUMMARY AND CONCLUSIONS

The primary objectives of this work were to identify the physiological changes in the cell wall during avocado mesocarp softening and to examine the function of C*x*-cellulase in the loss of cell wall integrity occurring during ripening. There is a dramatic loss of mesocarp firmness during avocado ripening, beginning prior to the ethylene/respiration climacteric and closely allied with the onset of C*x*-cellulase accumulation (identified by carboxymethylcellulose [CMC] hydrolysis). Polygalacturonase, one of the other principal cell wall hydrolases, does not appear until after the climacteric and after softening has been initiated.

The Role of Pectin Degradation During Softening

As the avocado mesocarp softens there is an increase in total pectin content, with an increasing percentage of this becoming ionic in nature and able to be solubilized by buffers containing chelators. This increase in chelator-soluble pectin indicates an increase in the interaction of pectin with calcium ions in the cell wall by two possible mechanisms: synthesis of qualitatively new pectin during ripening, or a proportional decrease in the degree of pectin esterification (probably due to pectinmethylesterase activity). Coincident with this quantitative change is a decrease in the molecular weight (M_r) of the chelator-soluble pectin, with the production of soluble pectic oligomers. The production of pectic oligomers occurs after the climacteric and is temporally associated with the increase in polygalacturonase activity.

While the incubation of chelator-soluble pectin from unripe avocado fruit with soluble enzyme extracts from ripe mesocarp decreased the amount of high-M_r pectin, the

alteration in M_r distribution was not as extensive as that seen during ripening. It is tempting to conclude from this that the alterations in soluble pectic polymers are mediated only by extensive enzyme action over a prolonged period of time. However, there are also indications that the pH optima for avocado polygalacturonase may be higher and of a narrower range than the equivalent enzyme in tomato fruit (Dr. D.J. Huber, University of Florida, Gainesville, FL; personal communication) and consequently the results of this experiment may not be a true indication of the mode of pectin degradation *in situ*. The production of pectic oligomers in avocado may be influenced by the high metabolic rate persisting in the fruit even after the climacteric surge of ethylene production has passed. It should be remembered that avocados only become palatable to the consumer (and therefore defined as 'ripe') when the fruit has softened beyond the textural preference for other ripened fruit, such as peaches and tomatoes.

While the importance of polygalacturonase activity to the loss of fruit firmness has been undermined by experiments involving antisense technology (Sheehy et al., 1988; Smith et al., 1988; Giovannoni et al., 1989), a recent report has provided support for the long-held belief that polygalacturonase activity does influence tomato fruit firmness (Kramer et al., 1992). In the case of avocado fruit, there is already a 52% decrease in mesocarp firmness before polygalacturonase becomes noticeably active, indicating that the initial loss of cell wall integrity occurs independent of this enzyme. The onset of softening also occurs without a change in the solubility or M_r characteristics of pectin. This finding does not eliminate a role for polygalacturonase in mesocarp softening since the enzyme is extremely active in the latter phases of ripening (where it may be involved in pectic oligomer production), but it does emphasize the possible involvement of other cell wall-loosening processes, particularly C*x*-cellulase activity, as being involved in the initial stages of mesocarp softening.

Xyloglucan Susceptibility to C*x*-cellulase Activity

In the development of models for the interaction of polymers in the plant cell wall, the role of xyloglucan (i.e., to hydrogen-bond to the periphery of cellulose microfibrils)is perhaps the least controversial. Xyloglucan (XG) appears to be the major hemicellulosic component of avocado fruit, and while it undergoes little quantitative change during ripening, there is a moderate decrease in the average M_r of this polymer. C*x*-cellulase is not involved in enzyme-mediated alteration of XG M_r in avocado fruit. This finding is in contrast to the situation described by Hayashi et al. (1984) and Hayashi (1989) for XG depolymerization during expansion growth in vegetative tissues and also suggested by Hatfield and Nevins (1986) for avocado cell walls. However, not only has it been demonstrated here that avocado C*x*-cellulase does not attack XG, but that enzyme extracts from ripe avocado fruit, with the C*x*-cellulase removed by affinity chromatography, decrease the average M_r of XG from unripe fruit cell walls to an extent similar to that seen in ripe fruit. It seems likely that a specific XGase is responsible for XG hydrolysis in avocado fruit, as is the situation in senescing carnation petals (de Vetten et al., 1991).

An explanation for the lack of reactivity of avocado C*x*-cellulase toward XG lies in the approximately twofold increase in release of soluble sugars from CMC 4M as compared to CMC 7M following incubation with avocado C*x*-cellulase (Hatfield and Nevins, 1986). CMC 4M has an average of 4 carboxymethyl substitutions per 10 glucose residues as compared to 7 of every 10 for the CMC 7M (Hatfield and Nevins, 1986). The reactivity differences were interpreted as being due to an enzymic preference for longer areas of unsubstituted glucan or at least less regular substitutions found in the CMC 4M. The maximum length of a XG sidechain is 3 glycosyl residues--considerably longer than the carboxymethyl sidegroup of the CMC glucan. The extent and frequency of substitution in XG varies among plant sources (Hayashi and Delmer, 1988; Hayashi, 1989), and has not been determined for the avocado polymer. Fucose is a constituent of

avocado XG and it is commonly thought that this residue occupies a terminal position on XG side-chains, being linked to the glucan chain via xylose and galactose (Hayashi, 1989). Compositional analysis of an avocado XG identified the four component sugars (glucose, xylose, galactose and fucose) in a ratio 7:5:3:1 (Chapter 4). It is possible that the iodine precipitation method was not exclusive for XG, therefore glucose, xylose and galactose may be involved in other polymers in this extract. However, the extent of contamination is thought to be low, given the congruence of the M_r distributions of total sugars and XG of the solubilized precipitate (Chapter 4). The frequency of substitution of the avocado XG, while slightly less than the classical ratio of 4:3:1:1 (Hayashi, 1989) is similar to that of derivatized groups in CMC 7M. In the orientation imposed *in situ* (hydrogen binding to the cellulose microfibril), the position of these side-chains could face outward in such a way as to restrict enzyme access to the unsubstituted glucose units. It is possible that the frequency and orientation of side-groups in XG hinders the access of C*x*-cellulase to potential hydrolysis sites through steric effects. It also appears that the enzyme retains this inability to attack the unsubstituted glucose units when the XG is solubilized, indicating that the avocado cellulase probably has very low tolerance for side-group interference.

In their work identifying C*x*-cellulase as the enzyme responsible for XG breakdown in pea epicotyl expansion zones, Hayashi et al. (1984) found that the unsubstituted glucose residue lying between the repeating branched subunits was susceptible to hydrolysis, and that cleavage at this point was responsible for the almost exclusive production of nonasaccharide fragments. Therefore it appeared that while this expansion-zone cellulase could tolerate the presence of substitutions, the enzyme did not attack between substituted glucose residues. There is no record of studies comparing the structural and/or sequence parallels of the avocado and expansion-zone cellulases. The only demonstrable similarities occur in the action against CMC, the absence of affinity for crystalline cellulose, and the preference for β-1,4-glucosyl linkages. Therefore, in the absence of data indicating conserved sequences and tertiary structure, the ability of pea

epicotyl cellulase to hydrolyze XG should not be interpreted as characteristic of fruit-derived cellulases but merely an indication that C*x*-cellulase is capable of degrading β-1,4-glucans. It is likely that avocado C*x*-cellulase is more sensitive to steric hindrances such as the position of side-chains than its expansion-zone counterpart and this would explain its lack of reactivity against native XG.

Additional evidence that the lack of XGase-like activity of C*x*-cellulase is based on structural preferences comes from the work of Hatfield and Nevins (1986) who compared the M_r of CMC 7M and *Avena* mixed-linkage glucans following incubation with avocado C*x*-cellulase and found that the *Avena* glucans (no branches) were fragmented to an extent that they eluted at the total volume of a Bio-Gel A1.5 gel permeation column. In contrast, C*x*-cellulase did not produce any fragments of this size from CMC. These results support the hypothesis that C*x*-cellulase from avocado fruit is sensitive to substitution and derivatization of the glucan backbone. While the enzyme is known as a 'CMCase', this activity appears only to indicate its ability to hydrolyze β-1,4-linkages. Consequently, the lack of C*x*-cellulase-mediated hydrolytic activity toward avocado XG can be at least partially explained by the inability of the enzyme to gain access to free, unsubstituted regions of the β-1,4-glucan polymer.

Influence of Ripening on Cell Wall Architecture

Localization of cellulose in thin sections of avocado mesocarp showed that this polymer extends throughout the avocado cell wall. Vian et al. (1992) found a similar distribution in the elongating region of mung bean hypocotyls. During ripening there is a reduction in the cellulose located in the middle lamella and also a loss of density in this region corresponding to the extensive solubilization of pectin. Such structural changes have also been recognized by Pesis et al. (1978) and Platt Aloia et al. (1980). C*x*-cellulase has been localized throughout the avocado cell wall, with release to the middle lamella regions suggested to be via the plasmadesmata (Dallman et al., 1989). In combination,

these findings suggest a spatial relationship between C*x*-cellulase and cellulose in avocado fruit.

McCann et al. (1990) studied the cell walls of onion tissue using deep-etching and rotary shadowing of homogenized, rapid-frozen cell wall material. This technique revealed cellulose microfibrils in a lattice arrangement which expanded with the chemical removal of pectins, collapsed following treatment with 1 M KOH, and swelled after a subsequent 4 M KOH treatment (removing associated hemicelluloses) had swollen the remaining cellulose microfibrils. These workers stressed the dual role of matrix polysaccharides to not only prevent the cellulose from fasciation but to anchor the microfibrils in fixed positions for structural integrity. It has been shown here that while avocado XG experiences a slight reduction in average M_r, including the loss of the longest polymers, it still remains bound to cellulose microfibrils throughout ripening. Immunolocalization of XG using fucose-specific monoclonal antibodies revealed a pattern of binding that strongly resembles that for the localization of cellulose in platinum/carbon shadowed samples. In unripe avocado fruit cell walls the microfibrils appear to be embedded in matrix material. The quantitative loss of pectin during ripening improves the visibility of microfibrils but there is no evidence of a cellulose network similar to that remaining in onion tissue after the chemical removal of pectins (McCann et al., 1990). Even allowing for the differences in preservation techniques (rapid freezing and etching as opposed to direct adherence to formvar-coated grids) the cellulose of the avocado mesocarp is tangled, and shows signs of untwisting even prior to the attainment of edible ripeness.

Effect of Ripening on Physical Parameters of Cellulose

Most studies of cellulose structure have utilized relatively pure celluloses derived from cotton and ramie, therefore the influence of matrix polysaccharides has not been considered. Although matrix polysaccharides do not directly alter the physical properties of cellulose (e.g., crystallinity, M_r), they profoundly influence the measurement of such

parameters, and this must be taken into account in interpreting data . In the case of avocado cell walls, ripening-associated proportional changes in the quantities of matrix polysaccharides and cellulose complicate the issue and prevent any definitive assessment of the changing crystallinity pattern of cellulose. Although there is an increase in the crystallinity index and an increase in crystalline particle size, neither of these measurements appears to be entirely independent of cellulose concentration. From M_r distributions of LiCl/dimethylacetamide (DMAC)-solubilized cell walls, it is clear that polymers with an average M_r between 10^5 and 10^6 Da. are lost during ripening and that there is a proportional enrichment in larger polysaccharides. It is difficult to attribute the M_r changes to any particular cell wall component (e.g., cellulose) since LiCl/DMAC solubilizes all cell wall polysaccharides.

Influence of Avocado C*x*-cellulase Activity on Cellulose

When cell walls from unripe avocado fruit were incubated with purified C*x*-cellulase, there was negligible production of reducing sugars but there was a distinct effect on cellulose structure in terms of M_r, crystallinity and microfibril organization. The current view of cellulose organization is that individual microfibrils are composed of small, elementary fibrils (Blackwell, 1982) although this was disputed as a misinterpretation of early electron micrographs by Preston (1974).

Ultrastructural analysis of cell walls from unripe fruit showed that C*x*-cellulase caused microfibril disruption, exposing the elementary fibril substructure in contrast to the short, thick microfibrils characteristic of cell walls from unripe fruit. Cellulose microfibrils from ripe avocado fruit and from Avicel were similarly affected by cellulase activity, even though the microfibrils in each instance were already dispersed. Sprey and Bochem (1991) noted that the action of an endoglucanase from *Trichoderma reesei* caused fraying of primary fibrils, seen at various positions along the length of seed slime cellulose microfibrils . The overall organization of the individual fibers was not completely

disrupted. Clearly, the nature of the substrate (and possibly the absence of associated polysaccharides) has some bearing on the efficacy of enzyme action.

C*x*-cellulase causes a reduction in average M_r of large polysaccharides from cell walls of unripe fruit. Since LiCl/DMAC appears to be a universal solvent, there is no way of conclusively identifying the target polymer from M_r distribution data. However, cellulose and pectins are the only cell wall polymers in the particular size range affected, and since the enzyme does not attack pectins, the substrate is believed to be cellulose. This conclusion appears valid in light of the other experimental results detailing the effects of C*x*-cellulase on the cell wall.

The endo-hydrolysis of the cellulose is relatively mild in comparison to that experienced by pectin during ripening, and does not result in solubilization. This suggests that C*x*-cellulase does not have multiple hydrolytic opportunities and may diffuse away after catalytic action on cellulose. It is thought that fruit cellulases do not possess separate binding and catalytic sites (Dr. A.B. Bennett, University of California, Davis, CA; personal communication) although this has not been experimentally verified. If this is the case for avocado C*x*-cellulase, there is some justification for the weak substrate binding. Additional support for this comes from the failure of C*x*-cellulase localization experiments, even in samples where it was added directly to grid-mounted cell wall samples. It is likely that the enzyme binding constant is low. The availability of amorphous cellulose binding surfaces (free of XG) could also be limiting.

C*x*-cellulase treatment of cell walls from unripe fruit led to an increase in the crystallinity index and an increase in the crystalline particle size without an alteration in the cell wall composition. It appears that the action of C*x*-cellulase has disrupted the amorphous material associated with the inner crystalline part of the microfibril, leaving the cellulose proportionately enriched in crystalline material. It has been shown that fungal endoglucanases preferentially bind to amorphous regions of the microfibril and their ability to bind and hydrolyze is reduced as the number of amorphous sites decreases (Ooshima et

al., 1983, Walker and Wilson, 1991) and the proportion of crystalline material (and hence the crystallinity index) increases (Bertran and Dale; 1985, Sinitsyn et al., 1991). It is proposed that the avocado C*x*-cellulase binds to the amorphous sites of the microfibril in areas of reduced XG association in a similar manner. The increase in avocado cellulose crystallinity and evidence of M_r reduction in response to C*x*-cellulase activity authenticate this proposed enzyme function.

Implications of C*x*-cellulase Activity in Mesocarp Softening

Both cellulose and C*x*-cellulase have been localized throughout the cell wall of ripening avocado fruit The selective, moderated disruption of this extensive cellulose network during the early phases of ripening would result in a reduction in the cohesive properties of the cell wall--not only by affecting the support structure of the wall but by altering its interactions with the cell wall matrix polysaccharides. Treatment of cell wall ghosts with C*x*-cellulase caused a loosening of the interactions of remaining matrix polysaccharides without affecting the M_r of these polymers, providing evidence that a change in the organization of the microfibril can physically disrupt an interpolymeric complex even though the matrix polymers affected are not hydrolyzed by the enzyme.

APPENDIX
POLYCLONAL ANTIBODIES AGAINST C*x*-CELLULASE

Antibody production

Polyclonal antibodies to C*x*-cellulase were raised in a female New Zealand White rabbit at the facilities of Dr. K. Kelly, Alachua, FL. Pure C*x*-cellulase was separated from a partially purified enzyme extract of ripe avocado fruit by passage through a preparative (1.5 mm diameter) 10% polyacrylamide gel using denaturing conditions (1.6% SDS). The position of the band corresponding to C*x*-cellulase was identified using a temporary stain of 0.25 mM KCl with 1 mM dithiothreitol and then removed from the gel. This sample was thoroughly homogenized with elution buffer (50 mM NaOAc, pH 5.0, containing 1 mM dithiothreitol and 150 mM NaCl) by forcing both gel strip and buffer through a syringe several times. Injections were made at several lower body sites in the rabbit, using Freunds Complete adjuvant. Boosts of the antigen in Freunds Incomplete adjuvant were made at 44 and 58 days post-injection and the rabbit was bled terminally at 90 days post injection. A sample of blood drawn from the rabbit prior to the injection of antigen served as the preimmune control.

Antibody testing procedure

The level of affinity of antibody for antigen was tested periodically using the ELISA technique. Initially the tests were run using the antiserum and pre-immune serum against semi-pure C*x*-cellulase and polygalacturonase from avocado fruit. Flat-bottomed 96 well ELISA plates were coated with antigen (100 µl at 4 µg ml^{-1}) overnight at 4°C, then blocked for 1 h at room temperature with 1% bovine serum albumin in PBS (300 µl

well^{-1}). The primary antibody was applied (100 µl well^{-1}) for 1 h at room temperature followed by the secondary antibody (goat anti-rabbit whole molecule alkaline phosphatase conjugate (Sigma Chemical Co., St Louis, MO) under similar conditions. The plate was washed four times with phosphate-buffered saline (PBS) containing 0.02% NaN_3 and 0.5% Tween between each step. The reaction in each well was developed with the application of 1 mg ml^{-1} para-nitrophenyl phosphate (Sigma) in carbonate buffer, pH 9.6. The intensity of the yellow color reaction was quantified by absorbance values at 405 nm, usually after 30 min incubation in the substrate.

The titer of the antibody/antigen reaction is the dilution of antibody used at the mid-point of the linear slope in an ELISA where the concentration of antibody is varied with constant antigen. It is therefore a measure of the affinity of the antibody. The titer of the whole antiserum was extremely high (approximately 6400) for both semi-purified C*x*-cellulase and polygalacturonase in the initial assays; the assays for preimmune recognition was negative. Lauriere et al. (1989) found that the carbohydrate portions of the glycosylated enzyme β-fructosidase from carrot cell walls were highly antigenic. To identify if the cross-reactivity of the antiserum was due to a recognition of carbohydrate chains on the enzymes, an ELISA was performed with pretreatment of the semi-pure C*x*-cellulase and polygalacturonase substrates with sodium periodate. The periodate cleaves glycosyl residues between C-2 and C-3, thereby destroying structural recognition of carbohydrate chains on each protein by the antiserum (Woodward et al., 1985). The colorimetric assay for antigen/antibody reaction in the ELISA tests was negative for polygalacturonase and reduced the titer for the recognition of the C*x*-cellulase sample to 3200, demonstrating that a number of the antibodies were directed to carbohydrate sidechains.

In order to remove the carbohydrate-directed antibodies, the antiserum was passed through a column (1 cm wide, 3 cm high) of either Sepharose CL 4B (Sigma) or Affi-Gel (Bio-Rad, Richmond, CA) which had been conjugated to soluble protein from unripe

(RS1) avocado fruit (Bennett and Christofferson, 1984). Each column (1.5 cm wide, 3 cm high) was operated in 10 mM Tris, pH 8.0. The non-binding portion of the serum was found to have no recognition for polygalacturonase in ELISA assays but retained its affinity for C*x*-cellulase extracts. Further purification and concentration of the polyclonal antibodies was attained by affinity chromatography using a Protein A-Sepharose (Sigma) column (1.5 cm wide, 3 cm high). The IgG components of the serum bound to this column when circulated in phosphate-buffered saline (PBS), and were released with 100 mM glycine/HCl buffer at pH 3.0. Column fractions (1 ml) were immediately neutralized in 75 µl of 1 M Tris, pH 8.0. The eluted fractions were pooled and dialyzed against PBS (4 x 1 L, 22 h total). This antibody sample was used for Western blotting and ultrastructural immunolocalization purposes.

REFERENCES

Abeles, F.B. & Biles, C.L. 1991. Cellulase activity in developing apple fruits. Sci. Hort. 47: 77-87.

Abeles, F.B. & Takeda, F. 1989. Increased cellulase activity during blackberry fruit ripening. HortScience 24: 851.

Abeles, F.B. & Takeda, F. 1990. Cellulase activity and ethylene in ripening strawberry and apple fruits. Sci. Hort. 42: 269-275.

Addicott, F.T. & Wiatr, S.M. 1977. Hormonal controls of abscission: biochemical and ultrastructural aspects. In: Plant Growth Regulators. Springer-Verlag, Berlin. Ed. P.E. Pilet. pp. 249-258.

Ahmed, A.E. & Labavitch, J.M. 1977. A simplified method for accurate determination of cell wall uronide content. J. Food Biochem. 1: 361-365.

Ahmed, A.E. & Labavitch, J.M. 1980. Cell wall metabolism in ripening fruit I: cell wall changes in ripening 'Bartlett' pears. Plant Physiol. 65: 1009-1013.

Albersheim, P., Nevins, D.J., English, P.D. & Karr, A. 1967. A method for the analysis of sugars in plant cell wall polysaccharides by gas-liquid chromatography. Carbohydr. Res. 5: 430-345.

Awad, M. 1977. Variation in cellulase content of Fuerte avocado fruit after harvest. HortScience 12: 406.

Awad, M. & Lewis, L.N. 1980. Avocado cellulase: extraction and purification. J. Food Sci. 45: 1625-1628.

Awad, M. & Young, R.E. 1979. Post harvest variation in cellulase, polygalacturonase and pectinmethylesterase in avocado fruits in relation to respiration and ethylene production. Plant Physiol. 64: 306-308.

Bacic, A., Churms, S.C., Stephen, A.M., Cohen, P.B. & Fincher, G.B. 1987. Fine structure of the arabinogalactan-protein from *Lolium multiflorum*. Carbohydr. Res. 162: 85-93.

Bal, A.K., Verma, D.P.S., Byrne, H. & Maclachlan, G.A. 1980. Subcellular localization of cellulases in auxin treated pea. J. Cell Biol. 69: 97-105.

Barnes, M.F. & Patchett, B.J. 1976. Cell wall degrading enzymes and the softening of senescent strawberry fruit. J. Food Sci. 41: 1392-1395.

Bartley, I.M. 1978. Exo-polygalacturonase of apple. Phytochemistry 17: 213-216.

Bartley, I.M., Knee, M. & Casimir, M.A. 1982. Fruit softening I: changes in cell wall composition and endo-polygalacturonase in ripening pears. J. Exp. Bot. 33: 1248-1255.

Bauer, W.H., Talmadge, K.W., Keegstra, K. & Albersheim, P. 1973. The structure of plant cell walls II: the hemicellulose of the walls of suspension-cultured sycamore cells. Plant Physiol. 51: 174-187.

Beguin, P. 1990. Molecular biology of cellulose degradation. Annu. Rev. Microbiol. 44: 219-248.

BeMiller, J.N. 1986. An introduction to pectins: structure and properties. In: Chemistry and Function of Pectins. American Chemical Society, Washington, DC. Ed. M.L. Fishman & J.J. Jen. pp 2-12.

Ben Aire, R., Sonego, L. & Frenkel, C. 1979. Changes in the pectic substance of ripening pears. J. Amer. Soc. Hort. Sci. 104: 500-505.

Bennett, A. B. & Christofferson, R.E. 1986. Synthesis and processing of cellulase from ripening avocado fruit. Plant Physiol. 81: 830-835.

Berg, R.H., Erdos, G.W., Gritzali, M. & Brown, R.D. 1988. Enzyme-gold affinity labelling of cellulose. J. Electron Microsc. Tech. 8. 371-379.

Bertran, M. S. & Dale, B.E. 1985. Enzymatic hydrolysis and recrystallization behavior of initially amorphous cellulose. Biotechnol. Bioeng. 27: 177-181.

Biale, J.B. 1941. Climacteric rise in respiration rate of the 'Fuerte' avocado fruit. Proc. Amer. Soc. Hort. Sci. 39: 137-142.

Biale, J.B. 1960. The postharvest biochemistry of tropical and sub-tropical fruits. Adv. Food Res. 10: 293-354.

Biale, J.B. & Young, R.E. 1971. The avocado pear. In: The Biochemistry of Fruits and their Products. Academic Press Inc., New York. Ed. A.C. Hulme. pp. 11-63.

Biale, J.B., Young, R.E. & Olmstead, A.J. 1954. Fruit respiration and ethylene production. Plant Physiol. 29: 168-174.

Biggs, M.S. & Handa, A.K. 1988. Temporal regulation of polygalacturonase gene expression in fruits of normal, mutant and heterozygous tomato genotypes. Plant Physiol. 89: 117-125.

Blackwell, J. 1982. The macromolecular organization of cellulose and chitin. In: Cellulose and Other Natural Polymers Systems. Biogenesis, Structure and Degradation. Plenum Press, New York. Ed. R.M. Brown Jr. pp. 403-428.

Blaschek, W., Koehler, H., Semler, U. & Franz, G. 1982. Molecular weight distribution of cellulose in primary cell walls. Planta 154: 550-555.

Blumenkrantz, N. & Asboe-Hansen, G. 1973. New method of quantitative determination of uronic acids. Anal. Biochem. 54: 484-489.

Bower, J.P. & Cutting, J.G. 1988. Avocado fruit development and ripening physiology. Hort. Rev. 10: 229-271.

Brady, C.J., MacAlpine, G., McGlasson, W.B. & Ueda, Y. 1982. Polygalacturonase in tomato fruits and the induction of ripening. Aust. J. Plant Physiol. 9: 171-178.

Brett, C.T. 1981. Polysaccharide synthesis from GDP-glucose in pea epicotyl slices. J. Exp. Bot. 32:1067-1077.

Buescher, R.W. & Tigchelaar, E.C. 1975. Pectinesterase, polygalacturonase and C*x*-cellulase activities and softening. HortScience 10: 624-625.

Burg, S.P. & Burg, E.A. 1964. Evidence of a naturally occurring inhibitor of ripening. Plant Physiol. 39: (suppl.) x.

Byrne, H., Christou, N.V., Verma, D.P.S. & Maclachlan, G.A. 1975. Purification and characterization of two cellulases from auxin treated pea epicotyls. J. Biol. Chem. 250: 1012-1018.

Cass, L.G., Kirven, K.A. & Christofferson, R.E. 1990. Isolation and characterization of a cellulase gene family member expressed during avocado fruit ripening. Mol. Gen. Genet. 223: 76-86.

Cassab, G.I. & Varner, J.E. 1988. Cell wall proteins. Annu. Rev. Plant Physiol. Plant Mol. Biol. 39: 321-353.

Christofferson, R.E., Tucker, M.L. & Laties, G.G. 1984. Cellulase gene expression in ripening avocado fruit: the accumulation of cellulase mRNA and protein as demonstrated by cDNA hybridization and immunodetection. Plant Mol. Biol. 3: 385-391.

Christofferson, R.E., Warm, E. & Laties, G.G. 1982. Gene expression during fruit ripening in avocado. Planta 155: 52-57.

Colinas-Leon, M.T. & Young, R.E. 1981. The cell wall in ripening avocados. Calif. Av. Soc. Ybk. 1981: 113-117.

Cummings, K. & Schroeder, C.A. 1942. Anatomy of the avocado fruit. Calif. Av. Soc. Ybk. 1942: 56-64.

Dallman, T.F., Thomson, W.W., Eaks, I.L. & Nothnagel, E.A. 1989. Expression and transport of cellulase in avocado mesocarp during ripening. Protoplasma 151: 33-46.

Darvill, A.G., NcNeil, M. & Albersheim,.P. 1978. Structure of plant cell walls VIII: a new pectic polysaccharide. Plant Physiol. 62: 418-422.

Dawsey, T.R. & McCormick, C.L. 1990. The lithium chloride/dimethylacetamide solvent for cellulose: a literature review. J. Mat. Sci.-Rev. Macromol. Chem. Phys. 30: 405-440.

de Vetten, N.C. & Huber, D.J. 1990. Cell wall changes during the expansion and senescence of carnation (*Dianthus caryophyllus*) petals. Physiol. Plant. 78: 447-454.

de Vetten, N.C., Huber, D.J. & Gross, K.C. 1991. Endoglycanase-catalyzed degradation of hemicelluloses during development of carnation (*Dianthus caryophyllus*) petals. Plant Physiol. 95: 853-860.

de Vries, J.A., Voragen, A.G.J., Rombouts, F.M. & Pilnik, W. 1986. Structural studies of apple pectins with pectolytic enzymes. In: Chemistry and Function of Pectins. American Chemical Society, Washington, DC. Ed. M.L. Fishman & J.J. Jen. pp. 2-12.

del Campillo, E., Durbin, M. & Lewis, L.N. 1988. Changes in two forms of membrane-associated cellulase during ethylene-induced abscission. Plant Physiol. 88: 904-909.

del Campillo, E., Reid, P.D., Sexton, R. & Lewis, L.N. 1990. Occurrence and localization of 9.5 cellulase in abscising and nonabscising tissues. Plant Cell 2: 245-254.

DellaPenna, D., Alexander, D.C. & Bennett, A.B. 1986. Molecular cloning of tomato fruit polygalacturonase: analysis of polygalacturonase mRNA levels during ripening. Proc. Natl. Acad. Sci. USA 83: 6420-6424.

Din, N., Gilkes, N.R., Tekant, B., Miller, R.C., Warren A.J. & Kilburn, D.G. 1991. Non-hydrolytic disruption of cellulose fibres by the binding domain of a bacterial cellulase. Bio/Technol. 9: 1096-1099.

Dische, Z. 1953. Qualitative and quantitative colorimetric determination of heptoses. J. Biol. Chem. 204: 983-997.

Dolendo, A.L., Luh, B.S. & Pratt, H.K. 1966. Relation of pectic and fatty acid changes to respiration rate during ripening of avocado fruits. J. Food Sci. 31: 332-336.

Dubois, M.K.A., Hamilton, J.K., Rebers, P.A. & Smith, F. 1956. Colorimetric method for determination of sugars and related substances. Anal. Chem. 28: 350-356.

Durbin, M.L. & Lewis, L.N. 1988. Cellulases in *Phaseolus vulgaris*. In: Methods in Enzymology, Vol. 162, Part A. Academic Press Inc., New York. Ed. W.A. Wood & S.T. Kellog. pp. 342-351.

Durbin, M.L., Sexton, R. & Lewis, L.N. 1981. The use of immunological methods to study the activity of cellulase isozymes (β-1,4-glucan-4-glucanohydrolase) in bean leaf abscission. Plant Cell Env. 4: 67-73.

Eaks, I.L. 1980. Respiratory rate, ethylene production and ripening response of avocado fruit to ethylene and propylene following harvest at different maturities. J. Am. Soc. Hort. Sci. 105: 744-747.

Edelmann, H.G. & Fry, S.C. 1992. Factors that affect the extraction of xyloglucan from the primary cell walls of suspension-cultured rose cells. Carbohydr. Res. 228: 423-431.

Fan, D.F. & Maclachlan, G. 1966. Control of cellulase activity by indole acetic acid. Can. J. Bot. 44: 1035-1034.

Farkas, V. & Maclachlan, G. 1988. Stimulation of pea β-1,4-glucanase activity by oligosaccharides derived from xyloglucan. Carbohydr. Res. 184: 213-219.

Fincher, G.B., Stone, B.A. & Clarke, A.E. 1983. Arabinogalactan-proteins: structure, biosynthesis and function. Annu. Rev. Plant Physiol. 34: 47-70.

Food and Agricultural Organization. 1991. Annual Yearbook: Production. Vol. 44. Statistics Divison, Economic and Social Policy Department, FAO, Rome.

French, A.D. 1985. Physical and theoretical methods of determining the supramolecular structure of cellulose. In: Cellulose Chemistry and its Applications. Ellis Horwood Ltd. New York. Ed. T.P. Nevell & S. H. Zeronian. pp. 84-111.

Fry, S.C. 1986. *In vivo* formation of xyloglucan nonasaccharide: a possible biologically active fragment. Planta 169: 443-453.

Fry, S.C. 1988. The Growing Plant Cell Wall: Chemical and Metabolic Analysis. John Wiley & Sons Inc., New York.

Fry, S.C. 1989. The structure and functions of xyloglucan. J. Exp. Bot. 40: 1-11.

Giovannoni, J.J., DellaPenna, D., Bennett, A.B. & Fischer, R.L. 1989. Expression of a chimeric polygalacturonase gene in transgenic *rin* (Ripening Inhibitor) tomato fruit results in polyuronide degradation but not fruit softening. Plant Cell 1: 53-63.

Gonzalez, A.R. & Brecht, P.E. 1978. Firmness of harvested *rin* and normal tomatoes as affected by ethylene. HortScience 13: 42-43.

Grant, C.T., Morris, E.R., Rees, D.A., Smith, P.J.C. & Thom, D. 1973. Biological interactions between polysaccharides and divalent cations: the egg-box model. FEBS Lett. 32: 195-198.

Greve, L.C. & Labavitch, J.M. 1991. Cell wall metabolism in ripening fruit V: analysis of cell wall synthesis in ripening tomato pericarp tissue using a D-[U-^{13}C]glucose tracer and gas chromatography-mass spectrometry. Plant Physiol. 97: 1456-1461.

Gross, K.C. 1986. Composition of ethanol-insoluble polysaccharides in water extracts of ripening tomatoes. Phytochemistry 25: 373-376.

Gross, K.C. & Sams, C.E. 1984. Changes in cell wall neutral sugar composition during fruit ripening: a species survey. Phytochemistry 23: 2457-2461.

Gross, K.C. & Wallner, S.J. 1979. Degradation of cell wall polysaccharides during tomato fruit ripening. Plant Physiol. 63: 117-120.

Hall, C.B. 1963. Cellulase in tomato fruits. Nature 200: 1010-1011.

Harriman, R.W., Tieman, D.M. & Handa, A.K. 1991. Molecular cloning of tomato pectin-methylesterase gene and its expression in Rutgers, Ripening Inhibitor, Nonripening, and Never Ripe tomato fruits. Plant Physiol. 97: 80-87.

Hasegawa, S. & Smolensky, D.C. 1971. Cellulase in dates and its role in fruit softening. J. Food Sci. 36: 966-967.

Hatfield, R. & Nevins, D.J. 1986. Characterization of the hydrolytic activity of avocado cellulase. Plant Cell Physiol. 27: 541-552.

Hayashi, T. 1989. Xyloglucans in the primary cell wall. Annu. Rev. Plant Physiol. Plant Mol. Biol. 40: 139-168.

Hayashi, T. & Delmer, D.P. 1988. Xyloglucan in the cell walls of cotton fiber. Carbohydr. Res. 181: 273-277.

Hayashi, T. & Maclachlan, G.A. 1984. Pea xyloglucan and cellulose I: macromolecular organization. Plant Physiol. 75: 596-604.

Hayashi, T., Wong, Y.S. & Maclachlan, G.A. 1984. Pea xyloglucan and cellulose II: hydrolysis by pea endo-1,4-β-glucanases. Plant Physiol. 75: 605-610.

Hayashi, T., Marsden, M.P.F. & Delmer, D.P. 1987. Pea xyloglucan and cellulose V: xyloglucan-cellulose interactions *in vitro* and *in vivo*. Plant Physiol. 83: 384-389.

Hinton, D.M. & Pressey, R. 1974. Cellulase activity in peaches during ripening. J. Food Sci. 39: 783-785.

Hobson, G.E. 1963. Pectinesterase in normal and abnormal tomato fruit. Biochem. J. 86: 358-365.

Hobson, G.E. 1964. Polygalacturonase in normal and abnormal tomato fruit. Biochem. J. 92: 324-332.

Hobson, G.E. 1968. Cellulase activity during the maturation and ripening of tomato fruit. J. Food Sci. 33: 588-592.

Horton, R.F. & Osborne, D.J. 1967. Senescence, abscission and cellulase activity in *Phaseolus vulgaris*. Nature 214: 1086-1088.

Hoson, T., Masuda, Y., Sone, Y. & Misaki, I. 1991. Xyloglucan antibodies inhibit auxin-induced elongation and cell wall loosening of azuki bean epicotyls but not of oat coleoptiles. Plant Physiol. 96: 551-557.

Huber, D.J. 1983a. Polyuronide degradation and hemicellulose modifications in ripening tomato fruit. J. Amer. Soc. Hort. Sci. 108: 405-409.

Huber, D.J. 1983b. The role of cell wall hydrolases in fruit softening. Hort. Rev. 5: 169-219.

Huber, D.J. 1984. Strawberry fruit softening: the potential roles of polyuronides and hemicelluloses. J. Food Sci. 49: 1310-1315.

Huber, D.J. 1985. A possible role for cellulose and Cx-cellulase activity in locular gel formation in tomato fruit. HortScience 20: 442-443.

Huber, D.J. 1987. Postharvest senescence: an introduction to the symposium. HortScience 22: 853-854.

Huber, D.J. 1991. Acidified phenol alters tomato cell wall pectin solubility and calcium content. Phytochemistry 30: 2523-2527.

Huber, D.J. & Lee, J.H. 1986. Comparative analysis of pectins from pericarp and locular gel in developing tomato fruit. In: Chemistry and Function of Pectins, ACS Symposium Series 310. American Chemical Society, Washington, DC. Eds. M.L. Fishman, J.J. Jen. pp. 141-156.

Huber, D.J. & Lee, J.H. 1988. Uronic acid products release from enzymically active cell wall from tomato fruit and its dependencey on enzyme quantity and distribution. Plant Physiol. 87: 592-597.

Huber, D.J. & Nevins, D.J. 1981. Partial purification of endo- and exo-β-D glucanase enzyme from *Zea mays* L. seedlings and their involvement in cell wall autohydrolysis. Planta 151: 206-214.

Jarvis, M.C. 1984. Structure and properties of pectin gels in plant cell walls. Plant Cell Env. 7: 153-164.

Jarvis, M.C., Hall, M.A., Threfall, D.R. & Friend, J. 1981. The polysaccharide structure of potato cell walls: chemical fractionation. Planta 152: 93-100.

Jermyn, M.A. & Isherwood, F.A. 1956. Changes in the cell wall of the pear during ripening. Biochem. J. 63: 123-130.

Johnson, D.C., Nicholson, M.D. & Haigh, F.C. 1976. Dimethylsulfoxide/ paraformaldehyde: a non-degrading solvent for cellulose. Appl. Polym. Symp. 28: 931-943.

Keegstra, K., Talmadge, K.W., Bauer, W.D. & Albersheim, P. 1973. The structure of plant cell walls III: a model of the walls of suspension-cultured sycamore cells based on the interconnections of the macromolecular components. Plant Physiol. 51: 188-196.

Keller, B., Sauer, N. & Lamb, C.J. 1988. Glycine-rich cell wall proteins in bean; gene structure and association of the protein with the vascular system. EMBO J. 7: 3625-3633.

Klyosov, A.A. 1990. Trends in biochemistry and enzymology of cellulose degradation. Biochemistry 29: 10577-10585.

Knee, I.M. 1973. Polysaccharide changes in cell walls of ripening apples. Phytochemistry 12: 1543-1549.

Knee, I.M. 1978. Metabolism of polymethylgalacturonate in apple fruit cortical tissue during ripening. Phytochemistry 17: 1261-1264.

Knee, I.M., Sargent, J.A. & Osborne, D.J. 1977. Cell wall metabolism in developing strawberry fruits. J. Exp. Bot. 28: 377-396.

Koch, J.L. & Nevins, D.J. 1989. Tomato fruit cell wall I: use of purified tomato polygalacturonase and pectinmethylesterase to identify developmental changes in pectins. Plant Physiol. 91: 816-822.

Koehler, E.D., Lewis, L.N., Shannon, L.M. & Durbin, M.L. 1981. Purification of a cellulase from kidney bean abscission zones. Phytochemistry 20: 409-412.

Kooiman, P. 1960. A method for the determination of amyloid in plant seeds. Recl. Trav. Chim. Pays-Bas. 79: 675-678.

Koyama, T., Hayashi, T., Kato, Y. & Matsuda, K. 1981. Degradation of xyloglucan by wall-bound enzymes from soybean tissue I: occurrence of xyloglucan-degrading enzymes in soybean cell wall. Plant Cell Physiol. 22: 1191-1198.

Koyama, T., Hayashi, T., Kato, Y. & Matsuda, L. 1983. Degradation of xyloglucan by wall-bound enzymes from soybean tissue II: degradation of the fragment heptasaccharide from xyloglucan and the characteristic action pattern of the α-D-xylosidase in the enzyme system. Plant Cell Physiol. 24: 155-162.

Kramer, M., Sanders, R., Bolkan, H., Waters, C., Sheehy, R.E. & Hiatt, W.R. 1992. Postharvest evaluation of transgenic tomatos with reduced levels of polygalacturonase: processing, firmness and disease resistance. Postharvest Biol. Technol. 1: 241-255.

Labavitch, J.M. 1981. Cell wall turnover in plant development. Annu. Rev. Plant Physiol. 32: 385-406.

Labavitch, J.M. & Ray, P.M. 1974. Relationship between promotion of xyloglucan metabolism and induction of elongation by indole acetic acid. Plant Physiol. 54: 499-502.

Ladisch, M.R., Lin, K.W., Voloch, M. & Tsao, G.T. 1983. Process considerations in the enzymatic hydrolysis of biomass. Enzyme Microb. Technol. 5: 38-102.

Lashbrook, C.C., Giovannoni, J.J., Stott, J., Fischer, R.L. & Bennett, A.B. 1991. Functional analysis of cellulase (endo-β-1,4-glucanase) gene expression in transgenic tomato fruit. Plant Physiol 96: 6.

Lauriere, M., Lauriere, C., Chrispeels, M.J., Johnson, K.D. & Sturm, A. 1989. Characterization of a xylose-specific antiserum that reacts with the complex asparagine-linked glycans of extracellular and vacuolar glycoproteins. Plant Physiol. 90: 1182-1188.

Lee, Y.H. & Fan, L.T. 1982. Kinetic studies of enzymatic hydrolysis of insoluble cellulose: analysis of the initial rates. Biotechnol. Bioeng. 24: 2383-2406.

Lester, G.E. & Dunlap, J.R. 1985. Physiological changes during development and ripening of 'Perlita' muskmelon fruits. Sci. Hort. 26: 323-331.

Lewis, C.E. 1978. The maturity of avocados--a general review. J. Sci. Food Agric. 29: 857-866.

Lewis, L.N. & Varner, J.E. 1970. Synthesis of cellulase during abscission of *Phaseolus vulgaris* leaf explants. Plant Physiol. 46: 194-199.

Lewis, L.N., Lew, F., Reid, P.D. & Barnes, J.E. 1970. Isozymes of cellulase in the abscission zone of *Phaseolus vulgaris*. In: Plant Growth Substances. Springer-Verlag, Berlin. Ed. D.J. Carr. pp. 233-239.

Lewis, L.N., Linkins, A.E., O'Sullivan, S. & Reid, P.D. 1974. Two forms of cellulase in bean plants. In: Proceedings of the 8th International Conference on Plant Growth Substances. Hirokawa Publishing Co. Inc., Tokyo. pp. 701-718.

Lieberman, L.J., Valdovinos, J.G. & Jensen, T.E. 1982. Ultrastructural localization of cellulase in abscission cells of tobacco flower pedicels. Bot. Gaz. 143: 32-40.

Maclachlan, G. & Brady, C. 1992. Multiple forms of 1,4-β-glucanase in ripening tomato fruits include a xyloglucanase activatable by xyloglucan oligosaccarides. Aust. J. Plant Physiol. 19: 137-146.

Maclachlan, G. & Perrault, J. 1964. Cellulase from pea epicotyls. Nature 204: 81-82.

McCann, M.C., Wells, B. & Roberts, K. 1990. Direct visualization of cross-links in the primary plant cell wall. J. Cell Sci. 96: 323-334.

McCollum, T.G., Huber, D.J. & Cantliffe, D.J. 1989. Modification of polyuronides and hemicelluloses during muskmelon fruit softening. Physiol. Plant. 76: 303-308.

McCormick, C.L., Callais, P.A. & Hutchinson, B.H. 1985. Solution studies of cellulose in lithium chloride and N,N-dimethylacetamide. Macromolecules 18: 2394-2401.

McDougall, G.J. & Fry, S.C. 1988. Inhibition of auxin stimulated growth of pea stem segments by a specific nonasaccaride of xyloglucan. Planta 175: 412-416.

McDougall, G.J. & Fry, S.C. 1990. Xyloglucan oligosaccharides promote growth and activate cellulase: evidence for a role of cellulase in cell expansion. Plant Physiol. 93: 1042-1048.

McNeil, M., Darvill, A.G. & Albersheim, P. 1980. The structure of plant cell walls X: rhamnogalacturonan I, a structurally complex pectic polysaccharide in the walls of suspension-cultured sycamore cells. Plant Physiol. 66: 1128-1134.

McNeil, M., Darvill, A., Albersheim, P. & Fry, S. 1984. Structure and function of the primary cell walls of plants. Annu. Rev. Biochem. 53: 625-663.

Merril, C.R. 1990. Gel staining techniques. In: Methods in Enzymology, Vol. 182. Academic Press Inc., San Diego, CA. Ed. M.P. Deutscher. pp. 477-488.

Milner, Y. & Avigad, G. 1967. A copper reagent for the determination of hexuronic acids and certain ketohexoses. Carbohydr. Res. 4: 359- 361.

Mitcham, E.J. & McDonald, R.E. 1992. Cell wall modification during ripening of 'Keitt' and 'Tommy Atkins' mango fruit. J. Amer. Soc. Hort. Sci. In press.

Mitcham, E.J., Gross, K.C. & Ng, T.J. 1989. Tomato fruit cell wall synthesis during development and senescence. Plant Physiol. 89: 477-481.

Mitcham, E.J., Gross, K.C. & Ng, T.J. 1991. Ripening and cell wall synthesis in normal and mutant tomato fruit. Phytochemistry 30: 1777-1780.

Moore, P.J. & Staehelin, L.A. 1988. Immunogold localization of the cell wall matrix polysaccharides rhamnogalacturonan I and xyloglucan during cell expansion and cytokinesis in *Trifolium pratense* L.: implication of secretory pathways. Planta 176: 433-445.

Moore, P.J., Darvill, A., Albersheim, P & Staehelin, L.A. 1986. Immunogold localization of xyloglucan and rhamnogalacturonan I in the cell walls of suspension-cultured sycamore cells. Plant Physiol. 82: 787-794.

Nelson, N. 1944. A photometric adaptation of the Somogyi method for the determination of glucose. J. Biol. Chem. 153: 375-380.

Nevell, T. P. & Zeronian, S.H. 1985. Cellulose chemistry fundamentals. In: Cellulose Chemistry and its Applications. John Wiley & Sons, New York. Ed. T.P. Nevell & S.H. Zeronian. pp. 15-29.

Nieves, R.A., Ellis, R.P., Todd, R.J., Johnson, T.J.A., Grohmann, K. & Himmel, M.E. 1991. Visualization of *Trichoderma reesei* cellobiohydrolase I and endoglucanase I on aspen cellulose by using monoclonal antibody-colloidal gold conjugates. Appl. Environ. Microbiol. 57: 3163-3170.

Nightingale, G.T., Addoms, R.M. & Blake, M.A. 1930. Development and ripening of peaches as correlated with physical characteristics, chemical composititon and histological structure of the fruit flesh: III. New Jersey Agr. Expt. Sta. Bull. 2-16.

Nirody, B.S. 1922. Investigations in avocado breeding. Calif. Av. Soc. Ybk. 1921-1922: 65-78.

Nishitani, K. & Masuda, Y. 1983. Auxin-induced changes in the cell wall xyloglucans: effects of auxin on the two different subfractions of xyloglucans in the epicotyl cell wall of *Vigna angularis*. Plant Cell Physiol. 24: 345-355.

Ogawa, K., Hayashi, T. & Okamura, K. 1990. Conformational analysis of xyloglucans. Int. J. Biol. Macromol. 12: 218-222.

O'Neill, M.A. & Selvendran, R.R. 1983. Isolation and partial characterization of a xyloglucan from the cell walls of *Phaseolus coccineus*. Carbohydr. Res. 111: 239-255.

Ong, E., Greenwood, J.M., Gilkes, N.R., Kilburn, D.G., Miller, R.C. & Warren, R.A.J. 1989. The cellulose-binding domains of cellulases: tools for biotechnology. Trends Biotechnol. 7: 239-243.

Ooshima, H., Sakata, M. & Harano, Y. 1983. Adsorption of cellulase from *Trichoderma viride* on cellulose. Biotechnol. Bioeng. 25: 3103-3114.

Osborne, D.J. 1989. Abscission. CRC Crit. Rev. Plant Sci. 8: 103-130.

Pesis, E., Fuchs, Y. & Zauberman, G. 1978. Cellulase activity and fruit softening in avocado. Plant Physiol. 61: 416-419.

Pharr, D.M. & Dickinson, D.B. 1973. Partial characterization of C*x*-cellulase and cellobiase from ripening tomato fruits. Plant Physiol. 52: 577-583.

Platt Aloia, K.A. & Thomson, W.W. 1981. Ultrastructure of the mesocarp of mature avocado fruit and changes associated with ripening. Ann. Bot. 48: 451-465.

Platt Aloia, K.A., Thomson, W.W. & Young, R.E. 1980. Ultrastructural changes in the walls of ripening avocados: transmission, scanning and freeze fracture microscopy. Bot. Gaz. 141: 366-373.

Pressey, R. & Avants, J.K. 1982. Solubilization of cell walls by tomato polygalacturonases: effects of pectinesterases. J. Food Biochem. 6: 57-74.

Preston, R.D. 1974. The Physical Biology of Plant Cell Walls. Chapman & Hall, London.

Ray, J., Knapp, J.E., Grierson, D., Bird, C. & Schuch, W. 1988. Identification and sequence determination of a cDNA clone for tomato pectinesterase. Eur. J. Biochem. 174: 119-124.

Redgwell, R.J., Melton, L.D. & Brasch, D.J. 1990. Cell wall changes in kiwifruit following post harvest ethylene treatment. Phytochemistry 29: 399-407.

Redgwell, R.J., Melton, L.D. & Brasch, D.J. 1991. Cell-wall polysaccharides of kiwifruit (*Actinidia deliciosa*): effect of ripening on the structural features of cell-wall materials. Carbohydr. Res. 209: 191-202.

Redgwell, R.J., Melton, L.D. & Brasch, D.J. 1992. Cell wall dissolution in ripening kiwifruit (*Actinidia deliciosa*): solubilization of the pectic polymers. Plant Physiol. 98: 71-81.

Reid, P.D., Strong, H.G., Lew, F. & Lewis, L.N. 1974. Cellulase and abscission in the red kidney bean. Plant Physiol. 53: 732-737.

Reynolds, E.S. 1963. The use of lead citrate at high pH as an electron opaque stain in electron microscopy. J. Cell Biol. 17: 208-212.

Roe, B. & Bruemmer, J.H. 1981. Changes in pectic substance and enzymes during ripening and storage of 'Keitt' mangos. J. Food Sci. 46: 186-189.

Ryall, A.L. & Pentzer, W.T. 1982. Handling, Transportation and Storage of Fruits and Vegetables. Vol. 2. AVI Publishing Co. Inc., Westport, Connecticut.

Schroeder, C.A. 1953. Growth and development of the 'Fuerte' avocado fruit. Proc. Am. Soc. Hort Sci. 61: 103-109.

Segal, L., Creely, J.J., Martin, A.E. & Conrad, C.M. 1959. An empirical method for estimating the degree of crystallinity of native cellulose using the x-ray diffractometer. Textile Res. J. 19: 786-794.

Selvendran, R.R. 1975. Analysis of cell wall material from plant tissues: extraction and purification. Phytochemistry 14: 1011-1017.

Sexton, R., Durbin, M.L., Lewis, L.N. & Thomson, W.W. 1980. Use of cellulase antibodies to study leaf abscission. Nature 283: 873-874.

Sexton, R., Durbin, M.L., Lewis, L.N. & Thomson, W.W. 1981. The immunocytochemical localization of 9.5 cellulase in abscission zones of bean (*Phaseolus vulgaris* cv. Red Kidney). Protoplasma 109: 335-347.

Seymour, G.B., Harding, S.E., Taylor, A.J., Hobson, G.E. & Tucker, G.A. 1987. Polyuronide solubilization during ripening of normal and mutant tomato fruit. Phytochemistry 26: 1871-1875.

Sheehy, R.E., Kramer, M.K. & Hiatt, W.R. 1988. Reduction of polygalacturonase activity in tomato fruit by antisense RNA. Proc. Natl. Acad. Sci. USA 85: 8805-8809.

Sitrit, Y., Riov, J. & Blumenfeld, A. 1986. Regulation of ethylene biosynthesis in avocado fruit during ripening. Plant Physiol. 81: 130-135.

Sinitsyn, A.P., Gusakov, A.V. & Vlasenko, E.Y. 1991. Effect of structural and physico-chemical features of cellulosic substrates on the efficiency of enzymatic hydrolysis. Appl. Biochem. Biotechnol. 30: 43-59.

Smith, P.K., Krohn, R.I., Hermanson, G.T., Mallia, A.K., Gartner, F.H., Provenzano, M.D., Fugimoto, E.K., Goeke, N.M., Olson, B.J. & Klenk, D.C. 1985. Measurement of protein using bicinchoninic acid. Anal. Biochem. 150: 76-85.

Smith, C.J.S., Watson, C.F., Ray, J., Bird, C.R., Morris, P.C., Schuch, W. & Grierson, D. 1988. Antisense RNA inhibition of polygalacturonase gene expression in transgenic tomatoes. Nature 334: 724-726.

Sobotka, F.E. & Stelzig, D.A. 1974. An apparent cellulase complex in tomato (*Lycoperscion esculentum*) fruit. Plant Physiol. 53: 759-763.

Sprey, B. & Bochem, H.P. 1991. Electron microscopic observations of cellulose microfibril degradation by endocellulase from *Trichoderma reesei*. FEMS Microbiol. Letts. 78: 183-188.

Starrett, D.A. & Laties, G.G. 1991. The effect of ethylene and propylene pulses on respiration, ripening advancement, ethylene-forming enzyme, and 1-aminocyclopropane-1-carboxylic acid synthase activity in avocado fruit. Plant Physiol. 95: 921-927.

Sterling, C. 1957. Cellulose micelles in developing fibers of asparagus. Acta Botanica Neer. 6: 458-471.

Sterling, C. 1961. Physical state of cellulose during ripening of peach. J. Food Sci. 26: 95-98.

Stevenson, T.T., Darvill, A.G. & Albersheim, P. 1988. Structural features of the plant cell-wall polysaccharide rhamnogalacturonan II. Carbohydr. Res. 182: 207-220.

Stout, A.B. 1923. A study in cross-pollination of avocados in Southern California. Calif. Av. Soc. Ybk. 1922-1923: 29-45.

Strahm, A., Amado, R. & Neukom, H. 1981. Hydroxyproline-galactoside as a protein polysaccharide linkage in a water-soluble arabinogalactan-protein from wheat endosperm. Phytochemistry 20: 1061-1063.

Talbott, L.D. & Ray, P.M. 1992. Molecular size and separability features of pea cell wall polysaccharides: implications for models of primary wall structure. Plant Physiol. 98: 357-368.

Talmadge, K.W., Keegstra, K., Bauer, W.D. & Albersheim, P. 1973. The structure of plant cell walls I: the macromolecular components of the walls of suspension-cultured sycamore cells with a detailed analysis of pectic polysaccharides. Plant Physiol. 51: 158-173.

Theologis, A. & Laties, G.G. 1978. Respiratory contribution of the alternate path during various stages of ripening in avocado and banana fruits. Plant Physiol. 62: 249-255.

Timpa, J.D. 1991. Application of universal calibration in gel permeation chromatography for molecular weight determinations of plant cell wall polymers: cotton fiber. J. Agric. Food Chem. 39: 270-275.

Tingwa, P.O. & Young, R.E. 1975. Studies on the inhibition of ripening in attached avocado (*Persea americana* Mill.) fruits. J. Amer. Soc. Hort. Sci. 100: 447-449.

Tong, C.B.S. & Gross, K.C. 1988. Glycosyl-linkage composition of tomato fruit cell wall hemicellulosic fractions during ripening. Physiol. Plant. 74: 365-370.

Tucker, G.A., Robertson, N.C. & Grierson, D. 1980. Changes in polygalacturonase isoenzymes during the 'ripening' of normal and mutant tomato fruit. Eur. J. Biochem. 112: 119-124.

Tucker, G.A., Robertson, N.G. & Grierson, D. 1982. Purification and changes in activities of tomato pectinesterase isoenzymes. J. Sci. Food Agr. 33: 396-400.

Tucker, M.L. & Laties, G.G. 1984. Interrelationships of gene expression, polysome prevalence and respiration during ripening of ethylene and/or cyanide treated avocado fruit. Plant Physiol. 74: 307-315.

Tucker, M.L. & Milligan, S.B. 1991. Sequence analysis and comparison of avocado fruit and bean abscission cellulases. Plant Physiol. 95: 928-933.

Tucker, M.L., Baird, S.L. & Sexton, R. 1991. Bean leaf abscission: tissue-specific accumulation of a cellulase mRNA. Planta 186: 52-57.

Tucker, M.L., Durbin, M.L., Clegg, M.T. & Lewis, L.N. 1987. Avocado cellulase: nucleotide sequence of a putative full length cDNA clone and evidence for a small gene family. Plant Mol. Biol. 9: 197-203.

Tucker, M.L., Sexton, R., del Campillo, E. & Lewis, L.N. 1988. Bean abscission cellulase: characterization of a cDNA and regulation of gene expression by ethylene and auxin. Plant Physiol. 88: 1257-1262.

United States Department of Agriculture. 1992. Horticultural products review. FHORT 6-92, June 1992. Foreign Agricultural Service, USDA, Washington, DC.

Updegraff, D.M. 1969. Semimicro determination of cellulose in biological materials. Anal. Biochem. 32: 420-424.

Valmayor, R.V. 1967. Cellular development of the avocado from blossom to maturity. Philippine Agr. 50: 907-975.

Varner, J.E. & Cassab, G.I. 1986. A new protein in petunia. Nature 323: 110.

Verma, D.P., Maclachlan, G.A., Byrne, H. & Ewings, D. 1975. Regulation and *in vitro* translation of messenger RNA for cellulase from auxin treated pea epicotyls. J. Biol. Chem. 250:1019-1026.

Vian, B., Nairn, J. & Reid, J.S.G. 1991. Enzyme-gold cytochemistry of seed xyloglucans using two xyloglucan-specific hydrolases. Importance of prior heat-deactivation of the enzymes. Histochem. J. 23: 116-124.

Walker, L.P. & Wilson, D.B. 1991. Enzymatic hydrolysis of cellulose: an overview. Bioresearch Technol. 36: 3-14.

Wang, C.Y., Sams, C.E. & Gross, K.C. 1985. Ethylene, ACC, soluble polyuronide, and cell wall noncellulosic neutral sugar content in 'Eldorado' pears during cold storage and ripening. J. Amer. Soc. Hort. Sci. 110: 687-691.

Warwicker, J.O., Jeffries, R., Colbran, R.L. & Robinson, R.N. 1966. A review of the literature on the effect of caustic soda and other swelling agents on the fine structure of cotton. Shirley Institute Pamphlet. 93: 57.

Woodward, M.P., Young, W.W. & Bloodgood, R.A. 1985. Detection of monoclonal antibodies specific for carbohydrate epitopes using periodate oxidation. J. Imm. Meth. 78: 143-153.

Wong, Y.S., Fincher, G.B. & Maclachlan, G.A. 1977. Kinetic properties and substrate specificities of two cellulases from auxin treated pea epicotyls. J. Biol. Chem. 525: 1402-1407.

Wood, T.M. 1971. The cellulase of *Fusarium solani*: purification and specificity of the β-(1,4)-glucanase and the β-D-glucosidase components. Biochem. J. 121: 353-362.

Wood, T.M. 1985. Properties of cellulolytic enzyme systems. Biochem. Soc. Trans. 13: 407-410.

Wood, T.M. & McCrae, S.I. 1979. Synergism between enzymes involved in the solubilization of native cellulose. In: Hydrolysis of Cellulose: Mechanisms of Enzymatic and Acid Catalysis. American Chemical Society. Ed. R.D. Brown Jr. & L. Jurasek. pp. 181-209.

Yamaki, S., Machida, Y. & Kakiuchi, N. 1979. Changes in cell wall polysaccharides and monosaccharides during development and ripening of Japanese pear fruit. Plant Cell Physiol. 20: 311-321.

York, W.S., Darvill, A.G. & Albersheim, P. 1984. Inhibition of 2,4-dichlorophenoxyacetic acid-stimulated elongation of pea stem segments by a xyloglucan oligosaccharide. Plant Physiol. 75: 295-297.

Zauberman, G. & Schiffmann-Nadel, M. 1972. Pectinmethylesterase and polygalacturonase in avocado fruit at various stages of development. Plant Physiol. 49: 864-865.

BIOGRAPHICAL SKETCH

Erin Margaret O'Donoghue is a New Zealander, born in Levin on December 26, 1961. She was raised in Shannon and attended Manawatu College, Foxton, from 1975 to 1979. She has a Bachelor of Science (First Class Hons.) degree in chemistry from Massey University, Palmerston North, where she studied from 1980 to 1983.

She was formerly employed as a postharvest scientist by the New Zealand Ministry of Agriculture and Fisheries from 1984 to 1992 and currently holds the same position in the New Zealand Institute for Crop and Food Research. Overseas study toward a doctoral degree at the University of Florida has been possible through a MAFTech Fellowship (NZ) and a Fulbright Travel Grant, both awarded in 1988.

I certify that I have read this study and that in my opinion it conforms to acceptable standards of scholarly presentation and is fully adequate, in scope and quality, as a dissertation for the degree of Doctor of Philosophy.

D.J. Huber, Chairman
Professor of Horticultural Science

I certify that I have read this study and that in my opinion it conforms to acceptable standards of scholarly presentation and is fully adequate, in scope and quality, as a dissertation for the degree of Doctor of Philosophy.

J.K. Brecht
Associate Professor of Horticultural Science

I certify that I have read this study and that in my opinion it conforms to acceptable standards of scholarly presentation and is fully adequate, in scope and quality, as a dissertation for the degree of Doctor of Philosophy.

G.W. Erdos
Assistant Scientist of Microbiology and Cell Science

I certify that I have read this study and that in my opinion it conforms to acceptable standards of scholarly presentation and is fully adequate, in scope and quality, as a dissertation for the degree of Doctor of Philosophy.

P.A. Klein
Professor of Pathology and Laboratory Medicine

This dissertation was submitted to the Graduate Faculty of the College of Agriculture and to the Graduate School and was accepted as partial fulfillment of the requirements for the degree of Doctor of Philosophy.

December 1992

Jack L. Fry

Dean, College of Agriculture

Dean, Graduate School